PB193029

Radian

Radian Corporation

8409 RESEARCH BLVD. • P.O. BOX 9948 • AUSTIN, TEXAS 78758 • TELEPHONE 512 - 454-9535

VOLUME I

FINAL REPORT FOR
CONTRACT NO. CPA-22-69-138

A THEORETICAL DESCRIPTION OF THE LIMESTONE INJECTION - WET SCRUBBING PROCESS

To:

NATIONAL AIR POLLUTION CONTROL ADMINISTRATION
DEPARTMENT OF HEALTH, EDUCATION, AND WELFARE
5710 Wooster Pike
Cincinnati, Ohio 45227
Attention Mr. J. L. Phillips

9 June 1970

Reproduced by the
CLEARINGHOUSE
for Federal Scientific & Technical
Information Springfield Va. 22151

CHEMICAL RESEARCH • SYSTEMS ANALYSIS • COMPUTER SCIENCE • CHEMICAL ENGINEERING

171

Radian

Radian Corporation

8409 RESEARCH BLVD. • AUSTIN, TEXAS 78758 • TELEPHONE 512 - 454-9535

VOLUME I

FINAL REPORT FOR
CONTRACT NO. CPA-22-69-138

A THEORETICAL DESCRIPTION OF THE LIMESTONE INJECTION - WET SCRUBBING PROCESS

To:

NATIONAL AIR POLLUTION CONTROL ADMINISTRATION
DEPARTMENT OF HEALTH, EDUCATION, AND WELFARE
5710 Wooster Pike
Cincinnati, Ohio 45227
Attention Mr. J. L. Phillips

9 June 1970

Prepared by:

Philip S. Lowell
Philip S. Lowell
Principal Scientist

Delbert M. Ottmers Jr.
Delbert M. Ottmers, Jr.
Senior Engineer

Klaus Schwitzgebel
Senior Scientist

Thomas I Strange
Thomas I. Strange
Senior Computer Scientist

David W. DeBerry
David W. DeBerry
Engineer/Scientist

CHEMICAL RESEARCH • SYSTEMS ANALYSIS • COMPUTER SCIENCE • CHEMICAL ENGINEERING

Radian Corporation 8409 RESEARCH BLVD. • AUSTIN, TEXAS 78758 • TELEPHONE 512 - 454-9535

ABSTRACT

A basis for a theoretical description of the limestone injection - wet scrubbing process for removal of SO_2 from power plant flue gases is given. A literature survey yielded the pertinent chemical data for the aqueous system. A computer program to calculate the partial pressures of SO_2 and CO_2 above aqueous solutions containing Ca^{++}, Mg^{++}, Na^+, NO_3^-, CO_2, SO_2, $SO_4^=$, and Cl^- was written and checked against experimental data. Turbulent contact absorbers and marble bed absorbers were described mathematically. Thermodynamic data for the dissociation constants of $CaSO_3$ and $MgSO_3$ and the solubility product constant for $CaSO_3 \cdot \frac{1}{2}H_2O$ were determined experimentally.

Sulfur dioxide sorption systems were simulated that approximate the process used at Kansas Power and Light and the process to be used in the NAPCA prototype system at TVA's Shawnee Power Plant. Flow rates, stream compositions, and important process variables are given.

This program was conducted under the sponsorship of the National Air Pollution Control Administration, Process Control Engineering Division, Contract No. CPA 22-69-138.

ACKNOWLEDGEMENTS

The authors wish to acknowledge the helpful guidance of the many NAPCA personnel with whom this work was discussed and in particular Messrs. J. L. Phillips (Project Officer) and R. E. Harrington. We also wish to thank Mrs. Betty Danner and Mrs. Cheryl Goad for their part in the preparation of this manuscript.

TABLE OF CONTENTS

Page

I. INTRODUCTION 1
II. MODEL DEVELOPMENT 3
  A. LITERATURE 4
  B. OTHER DATA FOR PROCESS MODEL 12
  C. CONCLUSIONS AND MODELS 15
    1. Unit Models 15
    2. Process Model 19
      a. Process Model Description 20
      b. Model Basis 24
      c. Mathematical Solution 24
III. PROCESS SIMULATIONS 29
  A. MODEL ASSUMPTIONS AND PARAMETERS 29
  B. PROTOTYPE SIMULATION 32
  C. KP&L SIMULATIONS 44
  D. NAPCA VENTURI SIMULATION 50
IV. PHYSICAL CHEMICAL DATA 60
  A. LITERATURE 61
    1. Definition of Important Species in the Scrubbing Solution 62
    2. Chemical Equilibrium Constants 65
      a. Survey of Experimental Methods 65
      b. Accepted Constants 67
      c. Temperature Dependence of the Equilibrium Constants 67
    3. Activity Coefficients 73
      a. Equation Form 73
      b. Temperature Dependence of Activity Coefficients 76
    4. Oxidation Rate of Sulfite 78
  B. IMPLEMENTATION 80
  C. EXPERIMENTAL WORK 86
    1. Theory 87

TABLE OF CONTENTS (continued) Page

2. Activity Measurements 90
3. Experimental Procedure 92
    a. Dissociation Constants 92
    b. Solubility Product Constants 94

D. RESULTS OF THE EXPERIMENTAL PROGRAM. 95
1. $CaSO_4$ Equilibria 97
2. $CaNO_3^+$ Equilibria 98
3. $CaSO_3$ Equilibria 100
4. $MgSO_3$ Equilibria 105
5. Temperature Dependence of the Dissociation Constants of $CaSO_3^\circ$ and $MgSO_3^\circ$ 110

V. CHEMICAL EQUILIBRIUM COMPUTER PROGRAM. 111
A. PROBLEM FORMULATION. 111
B. PROGRAM IMPLEMENTATION 117
C. OBSERVATIONS REGARDING CONVERGENCE 121
D. VERIFICATION 122
1. Solubility of SO_2 in Water and in Aqueous H_2SO_4 123
2. Ca-CO_2-H_2O System. 123
3. Ca-SO_2-H_2O System. 123
4. Mg-SO_2-SO_4-H_2O System. 125
5. Simulation of Laboratory Experiment. 125
6. Sea Water Model. 130
7. Other Systems. 130

VI. INHOUSE TEST PROGRAM 136
VII. SUMMARY AND CONCLUSIONS. 138
VIII. NOMENCLATURE 142
IX. LITERATURE CITED 151

LIST OF ILLUSTRATIONS

Page
FIGURE II-1 - RESIDENCE-TIME DISTRIBUTION CURVE. 7
FIGURE II-2 - WET SCRUBBING SCHEME 21
FIGURE III-1 - PROTOTYPE SIMULATION 33
FIGURE III-2 - KP&L SIMULATION. 45
FIGURE III-3 - NAPCA VENTURI SIMULATION 51
FIGURE III-4 - NAPCA VENTURI SIMULATION NV#6. 56
FIGURE IV-1 - EFFECT OF INHIBITORS AND NO_x ON THE OXIDATION RATE OF SO_2. 79
FIGURE IV-2 - CATALYTIC EFFECT OF Co^{++} ON THE OXIDATION RATE OF SO_2. 79
FIGURE IV-3 - DIVALENT ELECTRODE pH INFLUENCE. 91
FIGURE IV-4 - X-RAY DIFFRACTION PATTERN OF CALCIUM SULFITE 96
FIGURE IV-5 - RELATIVE DEVIATION OF CALCULATED Ca^{++} ACTIVITY VS TRIAL DISSOCIATION CONSTANT. . . 102
FIGURE V-1 - pH CORRELATION 128
FIGURE V-2 - P_{SO_2} CORRELATION 129
FIGURE V-3 - COMPARISON OF CALCULATED AND EXPERIMENTAL PARTIAL PRESSURES OF SO_2 AND CO_2 FOR THE SYSTEM STUDIED 135

LIST OF TABLES

Page

TABLE II-1 SCRUBBER MODEL-BACKMIXED-LIQUID CONTACTING . . 16

TABLE II-2 BASIS OF PROCESS MODEL. 25

TABLE III-1 FILTER BOTTOMS COMPOSITIONS IN PROTOTYPE SIMULATION. 38

TABLE III-2 SCRUBBER BOTTOMS COMPOSITIONS IN PROTOTYPE SIMULATIONS 39

TABLE III-3 KP&L SIMULATIONS. 48

TABLE III-4 SIMULATIONS OF NAPCA VENTURI SYSTEM 54

TABLE III-5 COMPOSITION OF SCRUBBER BOTTOMS NV#6. 57

TABLE III-6 COMPOSITION OF CLARIFIER BOTTOMS NV#6 58

TABLE IV-1 CHEMICAL SPECIES ORIGINALLY CONSIDERED. . . . 63

TABLE IV-2 EQUILIBRIUM CONSTANTS AND TEMPERATURE DEPENDENCE. 68

TABLE IV-3 ACTIVITY COEFFICIENT PARAMETERS 77

TABLE IV-4 REACTIONS CONSIDERED. 82

TABLE IV-5 SPECIES CONSIDERED. 84

TABLE IV-6 DIVALENT ELECTRODE INTERFERENCES. 91

TABLE IV-7 SATURATED $CaSO_4 \cdot 2H_2O$ SOLUTION AT 25°C. . . . 99

TABLE IV-8 CALCIUM ACTIVITY IN CALCIUM NITRATE SOLUTIONS 101

TABLE IV-9 RESULTS OF THE $CaSO_3^\circ$ DISSOCIATION CONSTANT DETERMINATION 103

TABLE IV-10 CHEMICAL EQUILIBRIA FOR CASE 3 OF $CaSO_3^\circ$ EQUILIBRIUM CONSTANT DETERMINATION USING $K_D = 4.0x10^{-4}$ 104

TABLE IV-11 RESULTS OF THE $CaSO_3 \cdot \frac{1}{2}H_2O$ SOLUBILITY PRODUCT DETERMINATION 106

TABLE IV-12 RESULTS OF THE $MgSO_3^\circ$ DISSOCIATION CONSTANT DETERMINATION 107

TABLE IV-13 CHEMICAL EQUILIBRIA FOR CASE 2 OF $MgSO_3^\circ$ K_D DETERMINATION USING $K_D = 1.2x10^{-3}$ AND ASSUMING SULFITE OXIDIZED IN SOLUTION. 108

TABLE IV-14 CHEMICAL EQUILIBRIA FOR CASE 2 OF $MgSO_3$ DETERMINATION USING $K_D = 1.2x10^{-3}$ AND ASSUMING NO OXIDATION IN SOLUTION 109

LIST OF TABLES (continued) Page

TABLE V-1 SOLUBILITY OF SO_2 IN H_2O AND AQUEOUS H_2SO_4 AT 25°C. 124

TABLE V-2 COMPARISON OF EXPERIMENTAL AND CALCULATED P_{CO_2} FOR THE Ca-CO_2-H_2O SYSTEM 124

TABLE V-3 COMPARISON OF EXPERIMENTAL AND CALCULATED P_{SO_2} FOR CaO-SO_2-H_2O SYSTEM. 126

TABLE V-4 COMPARISON OF THE EXPERIMENTAL AND CALCULATED P_{SO_2} AND pH FOR THE Mg-SO_2-SO_4-H_2O SYSTEM . . . 126

TABLE V-5 SEA WATER MODEL RESULTS. 131

TABLE V-6 SOLUBILITY OF $CaSO_4$- $2H_2O$ IN A $MgCl_2$, NaCl SOLUTION AT 25°C 133

TABLE V-7 SOLUBILITY OF $Ca(OH)_2$ IN A $NaNO_3$ SOLUTION AT 50°C. 134

I. INTRODUCTION

The object of the work described in this report (performed under NAPCA contract CPA 22-69-138) was to develop a theoretical description of the limestone injection - wet scrubbing process for SO_2 control. This process employs injection of limestone into an operating fossil fuel-burning boiler, with subsequent removal of both particulate and sulfur oxide pollutants by a wet scrubber. SO_2 reacts partially with calcined limestone carried into the scrubber with the flue gas and to a greater extent with the aqueous slurry that is recycled to the scrubber after removal of waste solids (mostly $CaSO_3/SO_4$ + flyash). Major investigators of the process have noted a serious lack of data with respect to the complex chemical and vapor-liquid equilibria and rate expressions needed to predict and extrapolate process performance reliably. The primary effort in this work was directed at equilibria in the aqueous scrubbing system. It is expected that information developed under the present contract will be valuable during the test program and test facility design effort now underway at Bechtel Corporation for NAPCA's limestone injection - wet scrubbing test facility.

The approach taken covered three aspects of the problem. The first aspect was a description of the types of scrubbers of interest, i.e., a turbulent contact absorber (TCA) (UOP, Air Correction Division) and a marble bed absorber (Hydro-Filter by National Dust Collectors). This consisted of a literature survey followed by derivations of various mathematical descriptions. A "best" description is put forth for this process with appropriate justification. This first aspect is described in Section II of this report.

Preceding page blank

The second aspect of this effort was that of computing order-of-magnitude results for various process schemes. These calculations were based upon the scrubber models described above and various process assumptions. This is described in Section III of this report. Process simulations were made for a system similar to that operated by Kansas Power and Light (KP&L) in Lawrence, Kansas and for the NAPCA prototype system to be operated by TVA at Paducah, Kentucky.

The third aspect of this work was a quantitative description of the chemistry of the scrubbing system as required by the process model. This was comprised of a vapor-liquid-solid(s) system. The species included in this system were CO_2 and SO_2 in the vapor phase, thirty-one ionic and non-ionic species in the aqueous phase, and six solid species. This task was accomplished by performing a literature survey to determine the possible reactions and the equilibrium and kinetic data available. These data were screened and only the pertinent reactions and chemical species retained. Missing thermodynamic data were determined experimentally. This is described in Section IV.

Equilibrium data were calculated by solving the set of equilibrium and mass balance equations that describe the system. Individual ion activities were calculated as the product of an activity coefficient and the molarity. The rather complex numerical solution of these equations is described in Section V.

II. MODEL DEVELOPMENT

To describe mass transfer in a scrubber the species mass balances must be solved. These mass balances must account for the flow patterns within the equipment and for mass transfer resistances. The scrubber reaction system in the limestone injection - wet scrubbing process is different from the usual scrubber in that all three phases must be considered. The overall reactions are vapor to solid.

Most complex chemical processes have one step that determines the rate of the overall process. If this step can be identified and described then the overall rate can be described with relative ease. Preliminary equilibrium calculations indicated that not enough $Ca(OH)_2$ could be dissolved in the first pass through the scrubber so that a clear liquid feed to a scrubber would be feasible. A slurry would have to be used. Hence the rate might be controlled by either the vapor or liquid side of the vapor-liquid film, the liquid film of the liquid-solid interface, or the solid reaction rate.

The model development work was accomplished by surveying the literature and the state-of-the-art of the scrubbers of interest to try to learn the salient features of flow patterns and the rate limiting step for mass transfer. Based upon this information mathematical derivations were made to describe the system. These derivations should provide a means of estimating the behavior of the system. They should also provide a first model with which to correlate data.

A. LITERATURE

The primary guide for the literature search relating to the development of a process model was Chemical Abstracts. The major objectives of this part of the literature search included assembling and evaluating information concerning

- "State of the art" for the limestone injection - wet scrubbing process,
- Operating experiences for various limestone - wet scrubbing systems,
- Performance characteristics of pertinent contactors,
- Flow patterns in various process vessels,
- Gas-liquid mass transfer rates for this process,
- Liquid-phase reactions occurring in the process,
- Solid-liquid mass transfer rates for this process.

The objectives and results of the literature survey which relate to determining physical and chemical data and chemical equilibria formulation for the process are reported in Section IV.

A recent report by the Tennessee Valley Authority (TE-001) on a program to conduct conceptual design and cost studies of the limestone injection - wet scrubbing process describes the status of this process and reviews briefly other process studies. Strauss (ST-001) and Nonhebel (NO-002) discuss the field of industrial gas cleaning, including descriptions of processing schemes and equipment. Squires (SQ-002) reviews processes for the removal of SO_2 as a means of air pollution control from power plant stacks.

As part of the NAPCA program, Bechtel Corporation (BE-001) is designing and constructing a prototype system of the limestone injection - wet scrubbing process at TVA's Shawnee Power Plant near Paducah, Kentucky. Performance characteristics of various scrubber types will be studied as part of the test program planned for this prototype unit. In commercial application of the process, Combustion Engineering (PL-002) has installed limestone injection - wet scrubbing systems at two power stations. In one installation at Kansas Power and Light Company's Lawrence Station (GR-001, MI-002) relatively low ionic strength scrubbing solutions are employed due to the once-through nature of the process. In the second installation, the Combustion Engineering system at Union Electric's Meramec Station in St. Louis, Missouri (JO-002), scaling and plugging problems were experienced.

The primary type of gas-liquid contactor being considered by NAPCA for the limestone injection - wet scrubbing process is the mobile packed bed. Two variations were considered. The first is the turbulent contact absorber (TCA; moving bed of hollow plastic spheres), designed and manufactured by Universal Oil Products Company, Air Correction Division. The second, a marble bed absorber (Hydro-Filter; moving bed of glass marbles) is manufactured by National Dust Collector Corporation. Pilot unit studies at Wisconsin Electric's Oak Creek Station in 1965 (PO-001) were made jointly by Wisconsin Electric Power Company and Universal Oil Products. Dust and SO_2 removal efficiencies and equipment performance were evaluated using a slurry of pulverized limestone circulating through a 14-inch diameter TCA unit. Combustion Engineering and Detroit Edison have reported (PL-001) pilot unit studies at Detroit Edison's St. Clair Station in 1966-67 whereby limestone was injected into the boiler and collected in a marble bed scrubber. In general, these studies as reported provide dust and SO_2 efficiencies as well as general operating characteristics. However, data providing mass transfer coefficients and gas and liquid flow patterns are not reported.

Pressure drop and absorption data for a TCA scrubber have been reported by H. R. Douglas, et al., (DO-001) for the SO_2-NaOH system. Heat and mass transfer coefficients in a TCA scrubber were correlated by W. J. M. Douglas (DO-002) for the ammonia-boric acid system. The fluid dynamics characteristics of liquid holdup and minimum fluidization velocity in a TCA have been studied by B. H. Chen and W. J. M. Douglas (CH-001). In a second study (CH-003), they examined the axial mixing of liquid in a 12-inch diameter TCA unit.

Chen and Douglas reported that total holdup was relatively insensitive to liquid rate. Residence-time distribution curves were interpreted by means of the one dimensional dispersion model. Liquid flow patterns in these scrubbers seem to be well approximated by idealized backmix flow in certain instances.

Several of Chen's residence-time distribution curves are presented in Figure II-1. They are compared with idealized plug and backmixed flow cases. Although the theoretical disperpersion model fits Chen's results very well, one also can see that Chen's experimental curves approach idealized backmix case as the gas and liquid flows approach 2,700 and 11,000 lbs/hr-ft^2, respectively. In fact, the number of idealized backmix vessels in series (corresponding to the dispersion observed), M, is 1.12 for Run C. Pilot studies by Pollock, et al., with a TCA indicate that for efficient operation scrubber gas and liquid

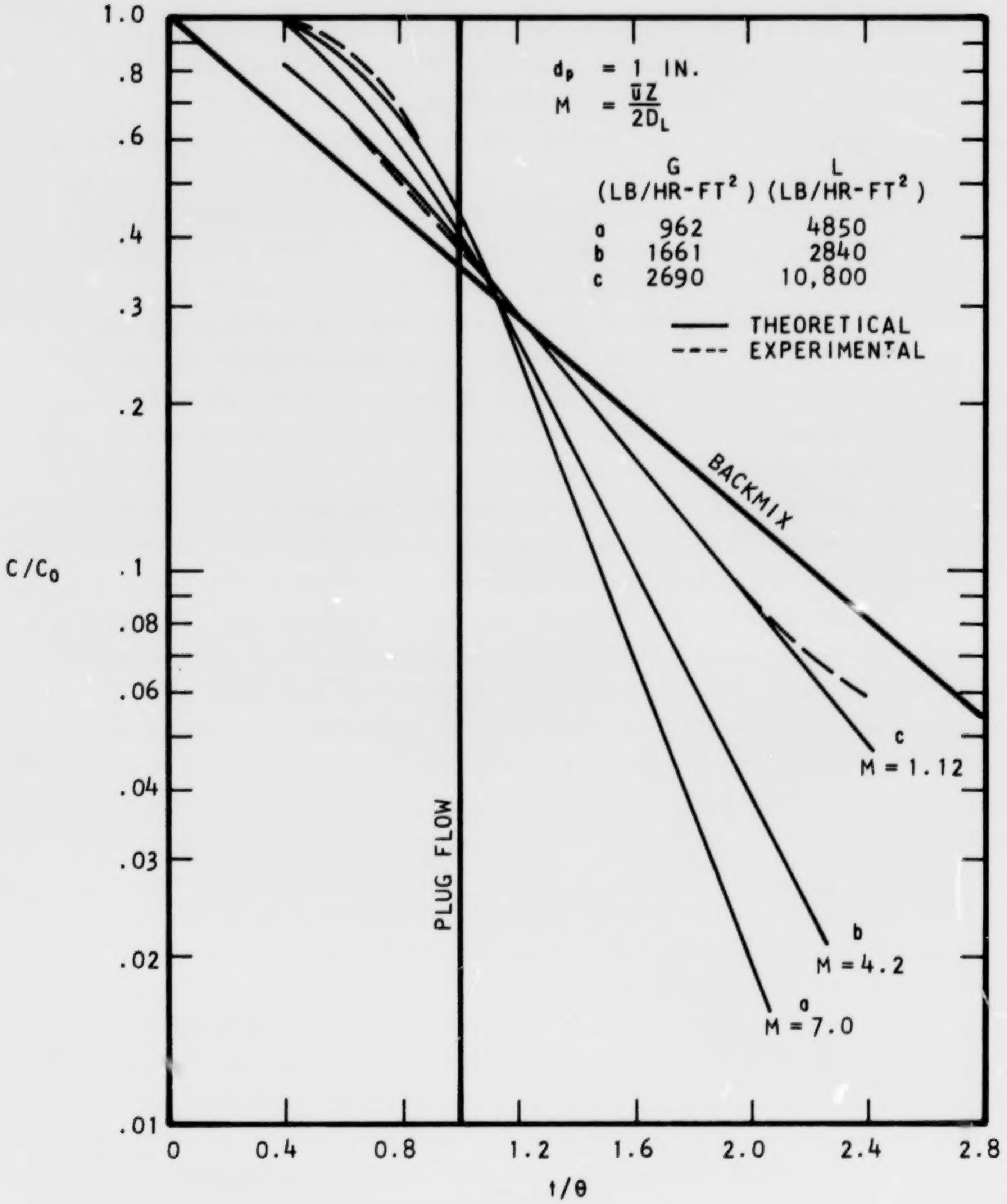

FIGURE II-1 RESIDENCE - TIME DISTRIBUTION CURVE
(SOURCE: CH-003)

flows should be in the ranges 2,500 to 3,500 and 15,000 to 25,000 lbs/hr-ft^2, respectively. Thus, for the normal operating conditions in wet scrubbers, the liquid phase in TCA units should be well approximated by one idealized backmix vessel.

The mass transfer coefficients for a TCA unit reported by H. R. Douglas, et al., for SO_2 absorption in NaOH solutions were based upon equilibrium partial pressures calculated from $MgO-SO_2-H_2O$ equilibrium data. That is to say, instead of using $NaOH-SO_2-H_2O$ equilibrium data, Douglas used equilibrium SO_2 partial pressures as determined from "readily available" data for "analogous magnesium bisulfite solutions" in the calculation of the absorption coefficient. Apparently, Douglas' calculations are also based upon countercurrent flow in the scrubber. Thus, the reported coefficients appear to be unreliable. Radian has recalculated the equilibrium SO_2 partial pressures above the scrubber liquor for the three runs reported by Douglas. Within the probable experimental accuracy, these equilibrium partial pressures approach the SO_2 partial pressures in the exit gas stream. Thus, if the liquid flow is approximately backmixed as indicated by Chen and Douglas, the SO_2-NaOH scrubbing system reported by Douglas would appear to be close to vapor-liquid equilibrium.

No similar studies have been reported in the literature with regard to the marble bed contactor. Venturi scrubbers are also to be tested in the prototype demonstration runs. Their primary function in this process was originally to be a means of getting limestone in a slurried condition and not as a vapor-liquid contacting device. Numerous studies (for example, BR-006, HA-006, SE-001, SE-002, TA-002) have been reported on the performance of Venturi scrubbers. Dust and SO_2 removal efficiencies have been reported but no correlations of mass transfer coefficients in the SO_2-lime or caustic system have been found. Volgin (VO-002) has studied the absorption of sulfur dioxides by ammonium sulfite-bisulfite solutions in a venturi scrubber.

Thus, no studies using the three types of contactors proposed for the prototype test program have been reported which investigate the gas-liquid mass transfer rates and relate the absorption efficiencies to the scrubber liquor composition.

Hobler (HO-001) and Sherwood (SH-001) discuss the theory of g-ℓ mass transfer and absorbers. The mass transfer rates within a piece of equipment can be described by a combination of a material balance and a kinetic equation. Classically, for a dilute species being absorbed from a gas in plug flow,

$$N_G = -\int_{y_1}^{y_2} \frac{dy}{y-y^*} = K_G aPSZ/V \qquad \text{(II-1)}$$

where N_G = number of transfer units,
y = mole fraction of dilute species in the gas phase,
y^* = mole fraction of dilute species which is in equilibrium with the liquid phase,
K_G = overall mass transfer coefficient based upon the gas film,
a = gas-liquid interfacial area,
P = total pressure of the gas phase,
S = cross sectional area of the contactor,
Z = height of the contacting section,
V = molar rate of the gas.

The value of K_G is itself a function of two individual film coefficients - one for the gas film and one for the liquid film. To predict absorber performance, these individual film coefficients are then correlated with 1) equipment dimensions and operating conditions and 2) chemical and physical properties of the gas and liquid phases. When chemical reaction occurs in the liquid phase, the liquid film coefficient should be modified (TE-003, BR-004, BR-005). The g-ℓ interfacial area "a" is also a strong function of equipment design and operation.

To predict absorption efficiency in a scrubber, the values of K_G, a, and y* and the gas-liquid contacting pattern must be known or determined from correlations. Chertkov (CH-002) has reported mass transfer coefficients for the absorption of SO_2 from gases by a lime slurry. However, these coefficients (K_G and a) were determined in a pilot-scale, grid-packed absorber and would not appear to be applicable to a mobile-bed contactor.

The chemical reactions that take place in the liquid phase are quite complex. For the most part these reactions are ionic and will be considered to be at equilibrium (see Table IV-4 in Section IV-B). The hydration rates of dissolved SO_2 and CO_2 to give H^+, HSO_3^-, and HCO_3^-, would appear to be at equilibrium also. Eigen (EI-001), et al., determined the forward rate constant for SO_2 hydration as $3.4x10^6 sec^{-1}$ at 20°C and found it to be several orders of magnitude greater than for CO_2 hydration. Campbell (CA-001) also reported the hydration rate of SO_2 to be several orders of magnitude greater than CO_2. However, Himmelblau and Wang (HI-001) determined a rate constant for SO_2 hydration of $2.2x10^{-2} sec^{-1}$ at 20°C, and they stated the CO_2 hydration constant is the same order of magnitude.

The rate of oxidation of sulfite ion is a liquid phase reaction which must be considered in the process model of the wet scrubbing process. This rate is strongly influenced by the metal catalysts which may be introduced into the liquid phase from the fly ash and by NO_x compounds from the flue gas. Literature concerning the oxidation rate of sulfite is reviewed in Section IV-A-4 of this report.

The solid-liquid mass transfer rates both in the scrubbing sections and the effluent hold tanks appear to be very important to the development of a meaningful process model. The hydration and dissolution rates of CaO and MgO are important steps in the scrubber and hold tank units. These rates could be strongly dependent upon the properties of the solid (particle size, surface area, etc.) and liquid (pH, Ca^{++}, etc.) phases. Prediction of the precipitation rates of various solid species, such as $CaSO_3$, $CaSO_4$, and $CaCO_3$, is also important and strongly dependent upon the scrubber and hold tank environments.

No rate data which are directly applicable to predicting s-ℓ mass transfer rates are available in the literature. Boynton (BO-002) gives a general treatment of the chemistry and technology of lime and limestones which may be helpful in characterizing these solids. Mullins (MU-001) and Nielsen (NI-001) present material on crystallization processes and the kinetics of precipitation. Glasson (GL-003, GL-004) and Kontorovich (KO-002, KO-003) have studied the hydration rate of CaO in water and various electrolytic solutions. A description of the crystallization rate of magnesium sulfate was given by Branscm and Trollope (BR-001). They claimed the driving force function for magnesium sulfate precipitation was the concentration difference between the solution and a saturated solution. Unfortunately the variation in driving force in the experiments was not sufficient to distinguish between a concentration difference driving force and an activity product difference driving force.

Ishii (IS-001) correlated the dissolution and growth rate of K_2SO_4 crystals in stirred tanks, whereas Larson and Randolph (LA-002) use the population balance in relating system parameters and crystallization kinetics with particle size distribution in a continuous, stirred tank crystallizer.

In summary, the literature reporting the status of the limestone injection - wet scrubbing process has been reviewed. However, data giving the g-ℓ mass transfer rates for this gas-liquid-solid system contacted in TCA, marble bed, or Venturi scrubbers have not been reported. Likewise, sufficient data to predict the liquid-phase oxidation of sulfite and the s-ℓ mass transfer rates as they occur in this system are not available. General correlation forms for these rates are suggested by the literature for various rate mechanisms. Chemical and physical data pertinent to chemical equilibria formulation and calculations are given later in this report.

B. OTHER DATA FOR PROCESS MODEL

Other information pertinent to the development of a process model was gathered via site visits to Kansas Power and Light's wet scrubbing installation at Lawrence Station and to the research laboratories of the Tennessee Valley Authority at Muscle Shoals, Alabama. Experimental results from tests conducted by NAPCA were also considered in the model development.

Kansas Power and Light (KP&L) has installed and operated a limestone injection - wet scrubbing unit on the flue gas stream from a 140-megawatt boiler. The system installed by Combustion Engineering initially had water sprays directing water upward to the base of the marble bed. It was found that not all of the spray penetrated the bed. About 30% of the water spray liquid went down to the bottom of the scrubber at 100% gas load and 70% went down at 70% gas load. This downward flow of spray water probably carried a major portion of the reactive material down to the hold tank and out of the scrubber system.

The system was modified so that the slurry in the scrubber effluent hold tank was recycled into the marble bed. The slurry was drained from the top of the marble bed and sent to the ash pond. This scheme (see Figure III-2 in Section III) is a deviation from the processing scheme envisioned for the prototype system in which a portion of the slurry would be sent to a clarifier, sludge sent to disposal, and clear liquid from the clarifier plus some slurry recycled to the scrubber.

A significant improvement in SO_2 removal was obtained in the KP&L system when the slurry was recycled. This could be the result of several factors. First, more limestone was actually getting into the marble bed. Secondly, the limestone had time to hydrate when retained in the hold tank below the scrubbing unit so that the recycled slurry contained hydrated CaO. Thus, the $Ca(OH)_2$ need only dissolve in the scrubber to attain its reactive scrubbing form. The improved SO_2 removal could be explained in terms of 1) rapid v-ℓ mass transfer rates (approaching equilibrium), 2) slow limestone hydration rates, and 3) moderate dissolution rates of hydrated limestone. The overall rate of 2 and/or 3 appeared to be the rate limiting step.

While the KP&L scrubber was not in service during the Radian visit, KP&L personnel did have pictures as well as verbal descriptions of the marble bed operation. Their pictures and descriptions depicted the liquid phase to be very uniform, i.e., no channeling of vapor through the bed (gas distribution baffles were used below the bed). They felt that the liquid phase was highly mixed. The water rates used within the scrubber are recommended at 8-10 gpm/ft^2. They have run at liquid rates as high as 15 gpm/ft^2.

The fly ash that is removed from the system apparently does not serve as nucleation sites for the calcium sulfate, sulfite, and carbonate. The material that comes out appears to be a heterogeneous mixture of fly ash and calcium solids. KP&L had no data available on the scrubber solutions other than that published in the literature.

Radian personnel also visited TVA. Their activities related to the limestone injection - wet scrubbing program were along two lines. First, Dr. John D. Hatfield had conducted some preliminary work on the development of a computer program to calculate chemical equilibrium in the CO_2-CaO-H_2O system. Secondly, TVA was conducting experimental programs to study rates associated with injecting crushed limestone into the scrubber as opposed to limestone injection into the boiler followed by wet scrubbing. They were studying solution rates of calcium carbonate as a function of particle size, temperature, solution composition, and impurities.

In bench-scale experiments conducted inhouse by NAPCA, a stirred, batch reactor containing limestone (high calcium and dolomitic) liquors was used to scrub SO_2 from a flue gas stream. The flue gas stream was bubbled through several inches of liquid, and the exit SO_2 concentration and the solution pH were monitored with time. In each case, all of the SO_2 in the flue gas was removed (i.e., below a measurable level) until the reactant limestone had been utilized. Although these "bubbler" results cannot be related to scrubber performance in a quantitative way, they certainly indicate that the gas absorption rate is a rapid step and suggest that v-ℓ equilibrium will be approached in the mobile-bed contactors.

C. CONCLUSIONS AND MODELS

In developing a process model for the limestone injection - wet scrubbing process, Radian first examined the process to determine the critical areas requiring description. The two process units which appear critical to obtaining a good process model are the scrubber and the scrubber effluent hold tank. Thus, Radian has formulated generalized equations for the scrubber and hold tank units which are consistent with our present knowledge of the flow patterns and rate steps in these units. A process model was then developed which combined these unit models with other unit operations. Due to the lack of pertinent rate data, rate forms were not specified or included in process model formulation. The "conversion" expected in each processing unit is presently specified as an input parameter in the Radian model or determined by an equilibrium assumption.

1. Unit Models

Depending upon the flow patterns occurring in the scrubber unit, several scrubber models can be formulated. Based upon the work reported by Chen and Douglas (CH-003) on a pilot-scale TCA and the observations made by KP&L with a marble-bed contactor, Radian has formulated a scrubber model in which the liquid phase is idealized backmix flow and the gas phase is idealized plug flow (designated here as backmixed liquid contacting). Rate and balance equations for this scrubber model are presented in Table II-1. Definitions of the symbols used are given in the nomenclature list in Section VIII. Four other model formulations representing various combinations of idealized plug, idealized backmix, and dispersed flow for the gas and liquid streams are given in Appendix A.

TABLE II-1
SCRUBBER MODEL - BACKMIXED-LIQUID CONTACTING

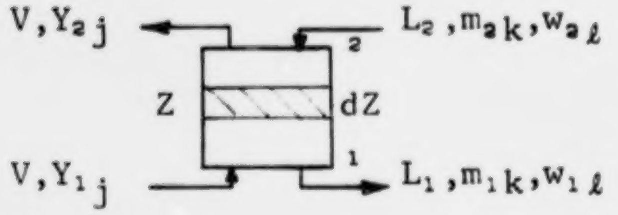

Gas Flow: Plug
Liquid Flow: Backmixed
Solid Flow: Same as liquid
Assume: V is constant

A. GAS-LIQUID RATES:

$$-VdY_j = k_{G_j}aSP(y-y_i)_j dZ \tag{1a}$$

or

$$-VdY_j = K_{G_j}aSP(y-y^*)_j dZ \tag{1b}$$

Since y* is constant and for $Y_j \simeq y_j$,

$$\ln\left(\frac{y_1-y^*}{y_2-y^*}\right)_j = \frac{K_{G_j}aSPZ}{V} \tag{1b'}$$

B. LIQUID RATES:

$$L_1 m_{1k} - L_2 m_{2k} = \left(\sum_n r_{nk}\right)Z \tag{2}$$

C. SOLID-LIQUID RATES:

$$L_1 w_{1\ell} - L_2 w_{2\ell} = \left(\sum_n \bar{r}_{n\ell}\right)Z \tag{3}$$

D. MATERIAL BALANCE:

$$V(Y_1 - Y_2)_j = \sum_k (L_1 m_{1k} - L_2 m_{2k}) + \sum_\ell (L_1 w_{1\ell} - L_2 w_{2\ell}) \tag{4}$$

NOTE: In general,

$$r_n = k_n\left[f_{n1}(a_m's) - f_{n2}(a_m's)/K_n\right] \tag{5}$$

$$\bar{r}_n = \int_0^{t_s} r_n R(t/\tau)dt \tag{6}$$

The backmixed-liquid model was selected for two reasons. The first reason was that its representation of the physical situation was adequate. The second reason was that the additional mathematical complexity involved in the dispersion model did not justify its improved predictive capabilities. Recall that Chen and Douglas report that the liquid phase dispersion corresponds to approximately 1.1 idealized backmix vessels placed in series. Although no experimental results with marble-bed scrubbers have been found in the literature, the turbulent bed agitation observed by Kansas Power and Light would indicate that a backmixed-liquid model would also fit for a marble-bed scrubber. The Venturi scrubber was not considered in the model formulations for the scrubber.

No experimental results predicting the degree of gas mixing in these scrubbers were found in the literature. Studies (KU-001) in fluidized beds indicate that the gas approximates idealized plug flow at scrubber gas velocities. The solids in the scrubber slurry are assumed to be carried along with the liquid phase. This assumption seems reasonable and should give an adequate prediction.

In general, the scrubber model listed in Table II-1 contain four types of equations. The first type expresses the rates of gas absorption of species such as SO_2, CO_2, and NO_x. The left-hand sides of Equations 1a and 1b express the absorption rate of the $j^{\underline{th}}$ species in terms of the molar flow rate of inert gas (V) and the differential change in mole ratio of the $j^{\underline{th}}$ species (dY_i) across the differential height element (dZ). The right-hand side expresses this rate in terms of the mass transfer coefficients [k_G in (1a) and K_G in (1b)], the gas-liquid interfacial area (a), scrubber cross-sectional area (S), absolute pressure in the scrubber (P), and the mole fraction driving force [$(y-y_i)_j$ in (1a) and $(y-y^*)_j$ in (1b)]. In Equation 1a the individual gas film coefficient (k_G) is used in conjunction with the gas-phase driving force $(y-y_i)_j$, where $(y_i)_j$ is the gas-phase mole fraction of the $j^{\underline{th}}$ species at the g-ℓ interface. In Equation 1b the overall coefficient based upon the gas-phase (K_G) is used in conjunction with the overall driving force $(y-y^*)_j$, where $(y^*)_j$ is the gas-phase mole fraction of the $j^{\underline{th}}$ species which is in equilibrium with the scrubber bulk liquid.

The second type of equation considers the chemical reactions occurring in the liquid phase, such as sulfite oxidation. The left-hand side expresses the rate of change of the $k^{\underline{th}}$ liquid species (e.g., sulfite) in terms of 1) the liquid flow rates in and out of the scrubber (L_2 and L_1) and 2) the molalities of the $k^{\underline{th}}$ liquid species in and out of the scrubber (m_{2k} and m_{1k}). The right-hand side expresses this rate in terms of the sum of all rate steps (n) which either form or consume species k and the scrubber height (Z). Each rate r_{nk} is written in terms of the formation of the $k^{\underline{th}}$ species by the $n^{\underline{th}}$ step. A generalized formulation of the rate is given by Equation 5. Here, k_n and K_n are temperature dependent constants and f_{n1} and f_{n2} represent driving force functions. These functions are possibly dependent upon the activities of several species ($a_{m's}$).

The third type of equation considers the solid-liquid mass transfer rates occurring in the process, such as $Ca(OH)_2$ dissolution and $CaSO_3$ precipitation. The left-hand side of Equation 3 expresses the formation rate of the $\ell^{\underline{th}}$ species in terms of the liquid flow rates and the molalities of the $\ell^{\underline{th}}$ solid species going in and out of the scrubber ($w_{2\ell}$ and $w_{1\ell}$). The right-hand side expresses this rate in terms of the sum of all rate steps which either form or consume the $\ell^{\underline{th}}$ species. Here again, the rate r_n is given in generalized form in Equation 5. In this case, the constants k_n and K_n will be dependent upon other factors such as s-ℓ interfacial area in addition to temperature. Also, the rates given in Equation 3 are rates averaged over the residence time-distribution of the solid species in the scrubber. Equation 6 expresses this averaged rate in terms of the residence time-distribution function $R(t/\tau)$, the mean residence time of the scrubber solids (τ), and the time required for complete solid reaction (t_s). For a completely backmixed system as postulated here, the residence time-distribution function is an exponential decay.

The last type of equation involves species material balances. Here the subscripts j, k, and ℓ refer to gas, liquid, and solid species containing a common chemical entity, such as Ca.

The unit model for the effluent hold tank also involves a specification of the flow pattern and a formulation of the rate and balance equations. In this vessel, the stirring required to obtain reasonable s-ℓ mass transfer rates will undoubtedly produce flow patterns closely approximated by an idealized backmixed vessel. The rate steps involved here are s-ℓ rates: 1) limestone hydration and dissolution and 2) precipitation of calcium (and/or magnesium) sulfite, sulfate, and carbonate. Thus, the equations for the s-ℓ rates and the component material balances which were formulated for the scrubber also apply to the hold tank model.

2. Process Model

Due to the absence of rate data for this process, Radian formulated a process model based upon conversions for these rate steps as specified by model inputs or by equilibrium assumptions. In this section, the Radian process model will be described by 1) presenting a qualitative description of how the Radian model relates to process operation, 2) listing the model assumptions and input specifications, and 3) briefly outlining the mathematical solution to the model.

a. Process Model Description

The process model description will be given in terms of the wet scrubbing scheme which represents the essential features of the prototype system to be used for the forthcoming NAPCA test program. The process model description for other processing schemes should follow by analogy from this one. Figure II-2 is a schematic diagram showing the various process vessels and streams.

The scrubber serves as a gas-liquid contacting device with some dissolution of limestone solids. In the present model, the scrubber (S) is assumed to trap all of the solids in the flue gas stream so that no solids leave with the stack gas. For material balance calculations the inlet gas stream to the scrubber has been divided into two fractions, a flue gas stream (FG) containing only gaseous components and a limestone-fly ash stream (LA) containing only solid components. In some instances, it may be convenient to divide the solids stream into a limestone (LS) and fly ash (FA) stream. The liquid flow through the scrubber is taken as idealized backmix flow so that the scrubber liquor composition is uniform and the same as the composition of the scrubber bottoms (SB). In this model the stack gas (SG) leaving the scrubber is assumed to be in equilibrium with the scrubber liquor (and thus with the scrubber bottoms).

The scrubber effluent hold tank (E) serves mainly as a solids dissolution and precipitation vessel. This stirred tank should approximate idealized backmix flow and in practice should be designed to provide enough residence time and agitation to hydrate and dissolve the major portion of the CaO and MgO that dissolves in the system. In this model all CaO and MgO entering the E tank is assumed to be available for reaction. The liquid

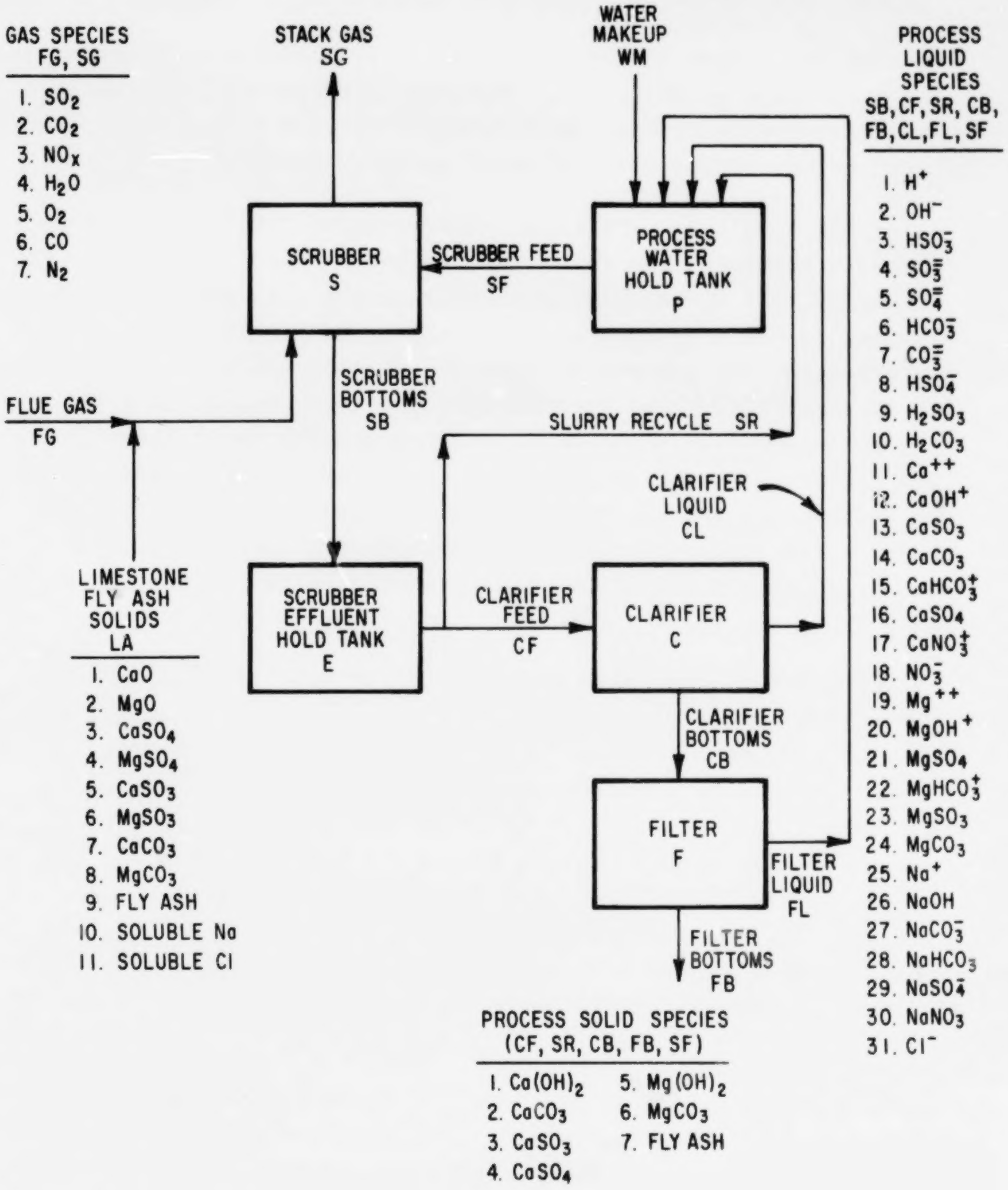

FIGURE II-2 WET SCRUBBING SCHEME

leaving the E tank is assumed to be in equilibrium with respect to the liquid and solid phases. This assumes that several species will dissolve or precipitate. A major portion of the precipitation in an actual process should occur in the E tank.

The clarifier and filter vessels serve mainly as solid-liquid separators. In the model presented, the clarifier liquid (CL) was assumed to be in equilibrium with the solids leaving in the clarifier bottoms (CB). The liquid in the clarifier bottoms was assumed to have the same composition as the CL stream. This model also assumes that the compositions of the solid and liquid phases in streams leaving the filter (FB and FL) are the same as the compositions of the solid and liquid in equilibrium in the clarifier and the filter. This situation would exist if the clarifier and filter were operated at the same temperature, or if the solid-liquid "shift" in the filter were insignificant.

Although some solid dissolution and precipitation could take place in the clarifier due to its long retention time, the stagnant nature of the liquid in this vessel should retard significant solid-liquid transfer. Actually the present model would be altered only slightly if it were assumed that not all dissolution and precipitation took place in the E tank and the remainder of this solid-liquid redistribution took place in the clarifier and/or the process water hold tank. As long as the clarifier liquid could still be taken to be in equilibrium with the clarifier solids, only the composition of the SR and CF stream would be altered.

The process water hold tank (P) is a stirred tank which serves as a liquid mixer. Here the clarifier and filter liquids (CL and FL) and slurry recycle (SR) are diluted with water makeup (WM) to produce the scrubber feed (SF) for the scrubber.

Figure II-2 also shows the chemical species possibly present in various process streams. Seven gaseous species are listed for the flue and stack gases. The nitrogen oxides in the gas phase are designated NO_x since not enough information concerning 1) NO_x composition in the gas phase, 2) oxidation rates, and 3) chemical reactions in liquid phase has been found in the literature. Due to this uncertainty, a realistic fraction of the NO_x in the flue gas will be taken as absorbing and this NO_x will show up in the process liquids as "equivalent" nitrates. A refinement of this approximation can be made if enough information concerning the NO_x system becomes available.

The limestone-fly ash stream (LA) could contain eleven solid species, CaO and MgO being the major ones. The fly ash component is not specified in further detail because fly ash compositions vary to some extent and because the soluble nature of the fly ash is not fully known at this point. For the purposes of this model, the fly ash will be assumed to contain a certain fraction of soluble Na^+, K^+, Cl^-. The soluble K^+ will be treated as "equivalent" Na^+. Both the "modified" Na^+ and the Cl^- are considered in the equilibrium calculations, although the Cl^- only affects the pH and ionic strength of the electrolytic solutions.

The thirty-one species listed under process liquids are the liquid species currently considered significant in Radian's equilibrium calculations. These species will be present in all process streams containing a liquid phase (except the water makeup stream, of course). The process streams CL and FL are clear liquid streams containing no solids, whereas SB, SR, CF, and CB are slurries. The filter bottoms stream (FB) is a "cake" containing a minor portion of liquid. Seven solid species are listed as possible species leaving in the FB stream. For the model formulation in this report, no CaO and MgO are lost with the filter solids since all of this material is assumed to be hydrated to $Ca(OH)_2$ and $Mg(OH)_2$ in the E tank. In the actual process, these two species could appear in this exit stream and their amounts must be predicted by hydration rates in the various process vessels.

b. Model Basis

A categorized list of the (A) process and equipment assumptions, (B) equilibrium assumptions, and (C) items to be specified for the system model is given in Table II-2. In addition to the items listed under Part C, two more model parameters must be specified. These represent case options. For example, the amount of slurry recycle (SR) and scrubber feed (SF) can be specified and the resulting SO_2 removal will be determined by the model. An alternate case would involve specifying the scrubber feed rate and the desired SO_2 removal and calculating the required slurry recycle rate.

c. Mathematical Solution

A fairly detailed description of the system to be modeled and a list of the basic model assumptions has just been given. At this point, a brief outline of the mathematical solution to model will be presented. The steps listed below correspond to a computerized case in which the scrubber feed rate (SF) and the desired SO_2 removal have been specified.

1. Input data are assembled and converted to a consistent basis. These inputs are those necessary for model specification. The input and output units were chosen as those frequently used in industry.

TABLE II-2
BASIS OF PROCESS MODEL

A. PROCESS AND EQUIPMENT ASSUMPTIONS:

1. Liquid flow in scrubber is idealized backmix flow.
2. Scrubber effluent hold tank operates as follows:
    a. Liquid and solid flows are completely backmixed.
    b. No solids are withdrawn as a separate stream.
3. Flue gas stream behaves as an ideal gas.
4. No solids or mist leave the scrubber with the stack gas.

B. EQUILIBRIUM ASSUMPTIONS:

1. The SO_2, CO_2, and H_2O in the stack gas leaving the scrubber are in equilibrium with the scrubber liquid (solid-liquid equilibrium not necessarily assumed).

2. All of the CaO and MgO hydrates in the scrubber and effluent hold tanks.

3. Equilibrium amounts of the hydroxides dissolve in the effluent hold tank.

4. Solids precipitate to their equilibrium value in the scrubber and/or the effluent hold tank.

5. Ionic reactions taking place in the liquid phase are rapid and thus at equilibrium.

6. The clarifier and filter are solid-liquid separators only.

7. The s-ℓ equilibrium is unchanged in going from the clarifier to the filter.

(continued)

TABLE II-2 (continued)

C. ITEMS TO BE SPECIFIED:

1. Amount and composition of the flue gas.
2. Amount and composition of the limestone and fly ash streams.
3. Fraction of limestone species dissolved in the scrubber.
4. Fraction of sulfite oxidized to sulfate in the scrubber.
5. Fraction of liquid leaving with the clarifier and filter bottoms.
6. Fraction of NO_x absorbed in the scrubber.

2. An overall material balance is used to determine the concentrations of the eight key species (total Ca^{++}, total Mg^{++}, total Na^{+}, total SO_2, total CO_2, total $SO_4^{=}$, total NO_3^{-}, and total Cl^{-}) leaving in the filter bottoms (FB). For this calculation, an initial guess for the amount of CO_2 absorbed is required. Later, this calculation must be repeated to obtain a fraction of CO_2 absorbed that is consistent with equilibrium CO_2 absorption.

3. With the amounts of these eight species known, the chemical equilibrium program (discussed in Section V) can be used to calculate the solid and liquid compositions of the FB stream. The composition of the liquid in the clarifier and filter overflow will be the same as the liquid in equilibrium with the solids leaving in the filter bottoms.

4. An initial guess for slurry recycle (SR) is used in conjunction with material balances around the clarifier (C), filter (F), and process water hold tank (P) to determine the composition of the SR stream. For this calculation the composition of the liquid and solid phases in the SR stream are taken to be the same as those of the FB stream. Only the relative amounts of these two phases are different in the two streams.

5. Species material balances around the process water hold tank (P) are used to determine the composition of the scrubber feed stream (SF).

6. A material balance around the scrubber (S) and the equilibrium program are now used to determine the amount and composition of the scrubber bottoms (SB). In this calculation the partial pressure of CO_2 in the stack gas as determined by the initial estimate for CO_2 absorption is used as one of the eight key species inputs.

7. The equilibrium partial pressure of SO_2 above the scrubber liquor is determined from the equilibrium program to see if the system has scrubbed the required amount of SO_2. If this partial pressure does not agree with the outlet flue gas partial pressure of SO_2 which was specified initially, an iterative procedure is adopted whereby the slurry recycle rate is varied until convergence is obtained.

8. After SO_2 convergence is obtained, the molality of total CO_2 in the scrubber bottoms as determined by the equilibrium calculation for the scrubber and the material balance around the scrubber with a given SF composition are compared to determine if CO_2 convergence is attained. If not, the fraction of CO_2 absorbed is revised and the calculation scheme is repeated beginning with Step 2.

9. The calculation cycle is repeated until the system converges with respect to SO_2 and CO_2.

10. The desired information is printed.

Although the process model presented here is based upon equilibrium assumptions, it should be very useful in estimating the SO_2 removal possible for a given set of operating conditions. This formulation can then be modified to mirror more closely the actual behavior of the process when rate data become available. For example, instead of assuming solid-liquid equilibrium in the effluent hold tank, hydration and dissolution rates of CaO and MgO could be taken as a rate-determining step. Then, the fraction of CaO and MgO hydrated and dissolved for a given tank size and operating condition could be calculated in a hold-tank model subroutine. Extensions of this kind will be necessary to determine equipment sizing.

III. PROCESS SIMULATIONS

Process simulations for three limestone wet scrubbing systems have been made using Radian's chemical equilibrium program and several process assumptions. The three systems are the prototype system being designed by Bechtel for NAPCA (prototype), the Kansas Power and Light System at Lawrence Station (KP&L), and the NAPCA pilot unit system employing a Venturi scrubber (NAPCA Venturi). These simulations estimate the technical feasibility of various processing schemes, the compositions in process units, and the effect of various model parameters on process operation. Prior to presenting the simulations of these three systems, the model assumptions and parameters will be discussed briefly.

A. MODEL ASSUMPTIONS AND PARAMETERS

Each of the simulations described here are based upon two key assumptions:

1. The partial pressures of SO_2, CO_2, and H_2O in the stack gas leaving the scrubber are in equilibrium with the scrubber liquid at the scrubber temperature (vapor-liquid equilibrium is achieved and the scrubber liquid in the bed is ideally backmixed).

2. Solid-liquid equilibrium is achieved in the scrubber effluent hold tank.

The first assumption is based on the premise that the gas-liquid absorption step is not rate controlling, whereas the second assumes the effluent hold tank is large enough to permit solid-liquid equilibrium. Chemical equilibrium is also assumed for the ionic species in solution. This last condition is most probably satisfied and is not considered restrictive. In each simulation, "typical" inlet compositions and operating conditions were assumed which were thought to best approximate field conditions.

Chemical equilibria for the scrubber and hold tank were calculated using a computer program developed by Radian and described in a later section of this report. Given the molalities of the eight species (Ca^{++}, Mg^{++}, Na^{+}, SO_2, CO_2, $SO_4^{=}$, NO_3^{-}, Cl^{-}), this program solves the set of 39 (or less) nonlinear equations describing chemical equilibrium for the wet scrubbing solutions. The program is capable of predicting equilibrium compositions as a function of temperature. Six equations involve the solubility product relationship so that the program is capable of predicting solids formation for saturated solutions when these solubility products are exceeded. These six equations can be suppressed in the calculation if supersaturated conditions are to be simulated. The equilibrium program is also capable of predicting the partial pressures of SO_2 and CO_2 above the scrubbing liquid. If desired, the partial pressures of SO_2 and CO_2 above the solution can be specified as inputs and the total molalities of SO_2 and CO_2 in solution will be calculated.

The compositions for the system inlet and exit streams [limestone (LS), flyash (FA), flue gas (FG), stack gas (SG), and water makeup (WM)] and operating conditions for the process are specified by model parameters. Other model parameters are used to set the "conversion" in the process due to various rate steps. That is to say, the fraction of precipitating solids, limestone in the flue gas entering the scrubber and dissolving, sulfite oxidizing, and NO_x absorbed in the scrubber are set by the model parameters. Later, as rate data become available, the Radian model can be revised to include computation of conversion from rate correlations. A list of the model parameters (along with typical units) is given below.

1. Theoretical limestone $\left(\frac{\text{moles CaO + MgO in LS}}{\text{moles } SO_2 \text{ in FG}}\right)$
2. Limestone composition $\left(\frac{\text{moles MgO in LS}}{\text{moles CaO + MgO in LS}}\right)$
3. Solids precipitated in scrubber (Yes or No)
4. Limestone hydrated and available for reaction in scrubber $\left(\frac{\text{LS available in S}}{\text{LS total}}\right)$
5. Liquid in filter bottoms $\left(\frac{\text{wt. liquid } H_2O}{\text{wt. non-water}}\right)$
6. Scrubber feed rate (gpm)
7. Slurry recycle rate (gpm)
8. SO_2 level in flue gas (mole% SO_2)
9. SO_2 absorbed $\left(\frac{SO_2 \text{ absorbed}}{SO_2 \text{ in FG}}\right)$
10. Sulfite oxidized $\left(\frac{\text{sulfite oxidized}}{SO_2 \text{ absorbed}}\right)$
11. CO_2 level in flue gas (mole% CO_2)
12. NO_x level in flue gas (mole% NO_x)
13. NO_x absorbed $\left(\frac{NO_x \text{ absorbed}}{NO_x \text{ in FG}}\right)$
14. Soluble Na^+ and Cl^- in coal
    a. Soluble Na^+ (wt. fraction Na^+ in LS + FA)
    b. Soluble Cl^- (wt. fraction Cl^- in LS + FA)

15. Fly ash level (wt. fraction FA in LS + FA)

16. Temperatures in the scrubber, effluent hold tank, clarifier, filter, and process water hold tank (°F)

To simulate a process, approximate material balance calculations about the process must be made to obtain the eight input species required for an equilibrium calculation. An iterative calculation is usually required to satisfy the material balance equations.

B. PROTOTYPE SIMULATION

The first process simulated was one of the operational modes proposed by Bechtel Corporation (BE-001) for the forthcoming test program on a prototype unit. A schematic diagram for the prototype simulation is presented in Figure III-1. In this process, the scrubber bottoms (SB) are discharged into an effluent hold tank (E) where lime particles are given time to hydrate and dissolve. Precipitation of such solids as $CaSO_3$, $CaSO_4$, and $CaCO_3$ also takes place in this hold tank. The exit stream from the effluent hold tank can either be recycled as a slurry (SR) to the scrubber (S) by way of the process water hold tank (P), or this exit stream can be clarified (C) and filtered (F) with only clear liquid (RL) being recycled to the scrubber via the process water hold tank.

In general, the amounts and compositions of all peripheral streams except the filter bottoms are known (or easily calculated by an overall material balance if the fraction of water in the filter bottoms is specified). In addition to the two key assumptions stated earlier, the clarifier (C) and filter (F) were taken to function as solid-lqiuid separators only and the process water

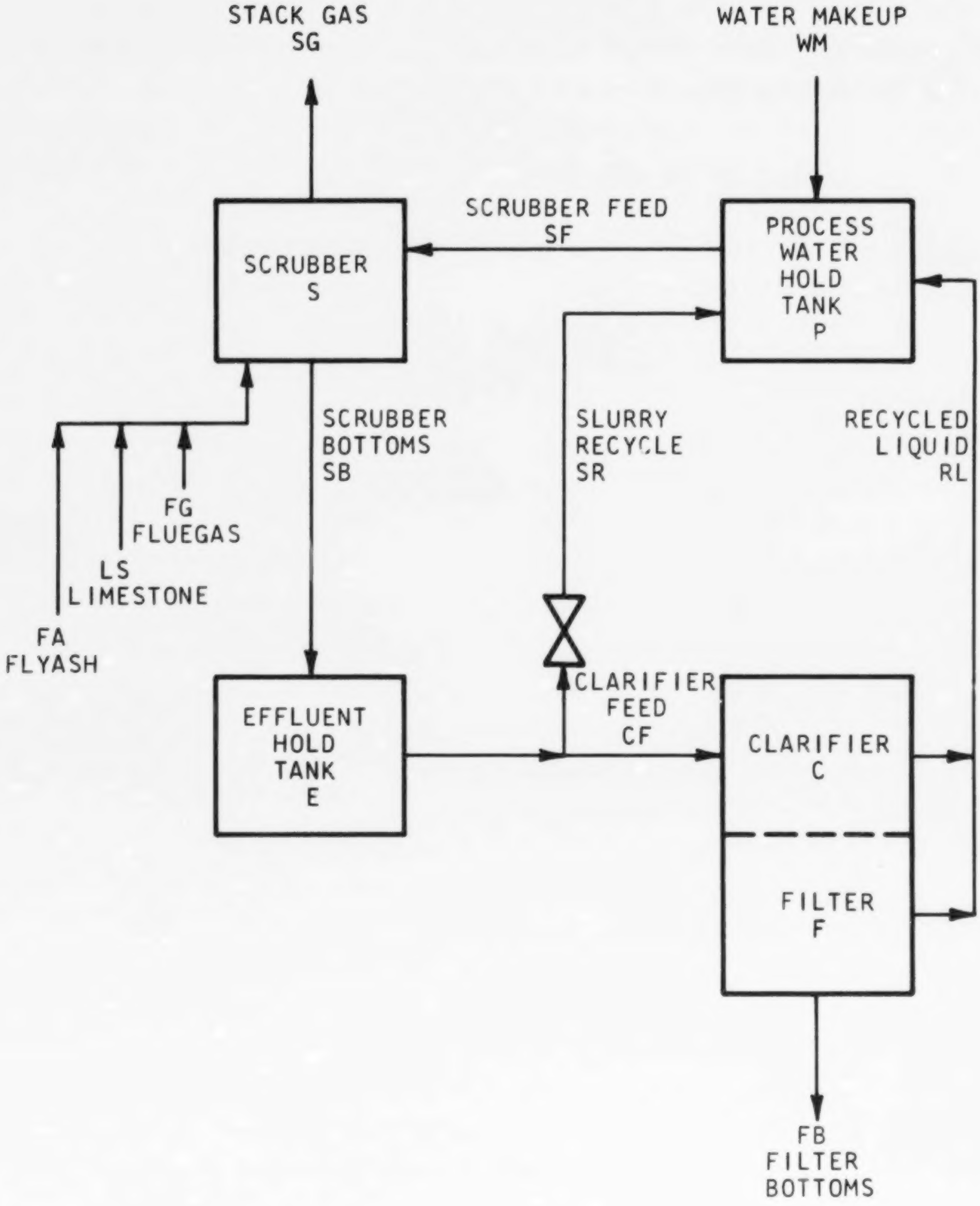

FIGURE III-1 PROTOTYPE SIMULATION

hold tank (P) was taken to be merely a mixing vessel for combining the recycled liquid (RL), slurry recycle (SR), and water makeup (WM) streams. If the second key assumption holds and the process approaches isothermal operation, the two assumptions listed above are valid.

A partial analysis of the typical flue gas chosen for this simulation is given below:

Component	Mole%
SO_2	0.30
NO_x	0.05
CO_2	15.00
H_2O	8.00
O_2	3.00
N_2	balance

Three limestone types were selected for study. Type I contained no MgO, Type II contained 20 mole% MgO, and Type III contained 50 mole% MgO. The following processing conditions were chosen as base conditions:

1. 130% theoretical limestone for 100% SO_2 removal,
2. 90% SO_2 removal in the scrubber,
3. 50% sulfite oxidation,
4. 20% NO_x removal in the scrubber,
5. stack gas was saturated with water at the scrubber temperature,
6. the scrubber liquid did not become supersaturated,
7. 80 wt.% solids in the filter bottoms stream,
8. temperature in each of the processing units was 122°F (50°C).

The remaining model parameters such as slurry recycle rate, limestone dissolving in the scrubber, and scrubber feed rate were varied from one case to the next to determine their effect or to obtain convergence in the iteration scheme.

With the necessary processing conditions specified and with the compositions of the flue gas (FG), limestone (LS), and fly ash (FA) streams known the total molalities of the eight key species (SO_2, CO_2, $SO_4^=$, NO_3^-, Ca^{++}, Mg^{++}, Na^+, and Cl^-) were calculated for the filter bottoms (FB) stream by a total material balance around the process. These molalities were then used as inputs to the chemical equilibrium program to determine the composition and amount of the liquid and solid phases leaving the filter. With the process assumptions given above, it follows that the composition of the liquid and solid phases in the RL and SR streams are the same as for the corresponding phases in the FB stream. Once the amount of the slurry recycle (SR) stream has been fixed, the fraction of solids in this stream can be determined by material balances about the clarifier (C) and filter (F) network. The amount of the SR stream can be varied until the desired SO_2 removal is achieved in the scrubber, i.e., SR is varied until the equilibrium partial pressure of SO_2 over the scrubber liquid (SB) stream is equal to the desired SO_2 partial pressure in the stack gas.

Actually, an iteration on the amount of CO_2 absorbed is also required. However, this iteration is of secondary importance in these simulations since the scrubber composition can be set relatively close by taking CO_2 partial pressure above the scrubber liquid as equal to the CO_2 partial pressure in the flue gas. Thus, in the CO_2 iteration, an initial guess for CO_2 absorbed is made and the overall material balance around the process is made to determine the eight total molalities for the filter bottoms. The equilibrium calculation for the filtering system is made and then the eight total molalities for the scrubber bottoms (SB) stream are determined for a given SR rate. The equilibrium calculation for the scrubber is now made using these total molalities for all species except CO_2. Instead of using the CO_2 molalities as an input, the CO_2 partial pressure of the stack gas (SG) is used. Since there is little difference between the CO_2 partial pressures in the flue gas and stack gas (relatively high CO_2 mole fractions and low CO_2 solubility), very little error is introduced into the equilibrium calculation of the scrubber bottoms composition. The amount of CO_2 absorbed can be adjusted until convergence is obtained. However, this quantity has little effect upon SO_2 convergence if CO_2 partial pressure is specified in the scrubber equilibrium calculation and if excess limestone is still leaving the system as $Ca(OH)_2$ or $Mg(OH)_2$ in FB. The major effect of varying CO_2 absorption is that of removing the excess limestone as $CaCO_3$ (or possibly $MgCO_3$) instead of $Ca(OH)_2$ in the FB stream.

As described above, SO_2 convergence is obtained for each simulation by adjusting the fraction of slurry recycle used in the scrubber feed stream. Recycling slurry increases the concentration of hydrated CaO in the scrubber (as long as excess limestone is used) and thus increases SO_2 absorption. On the other hand, high recycle rates of slurry produce process streams with a high solids content which can cause problems in scrubber operation. In these simulations, all of the hydrated CaO was taken to be available for dissolution, i.e., all of the $Ca(OH)_2$ was assumed to be available for reaction. In actual operation the amount of slurry reacting might be only a portion of the solids actually recycled.

Sulfur dioxide convergence could be obtained in a number of ways (i.e., iterate with other model parameters) and each of these represent programming options for scrubber simulation.

Two of the simulations reported here recycled only clear liquid (SR=0) and used limestone dissolution and recycle liquid rate (RL) as the iterative parameters.

Results from the prototype simulations are summarized in Tables III-1 and III-2. Table III-1 presents condensed results from equilibrium calculations on the filter bottoms stream, whereas Table III-2 presents condensed results from equilibrium and iterative calculations on the scrubber bottoms stream. Computer printouts giving complete analyses for selected cases are given in Appendix B. The items listed under "process operation" combined with the six processing conditions listed earlier and those required to specify a given state of operation. It should be noted here that molality (g-moles per kg of water in solution) is the convenient unit of concentration in making process engineering calculations.*

---

* In conducting experimental studies to determine equilibrium data, molarity (g-moles per liter) is the more common unit. Radian has assumed that the densities of process liquids in these wet scrubbing systems can be expressed by

$$\rho_{solution} = 1000 + \sum_i m_i MW_i$$

where

$\rho_{solution}$ = solution density in grams of solution per liter of solution

m_i = molality of the $i^{\underline{th}}$ species (g-moles of the $i^{\underline{th}}$ species per kg of water in solution)

MW_i = molecular weight of the $i^{\underline{th}}$ species.

This is the only practical assumption available and should give a fairly accurate prediction of the solution density. When this relation is valid, molalities and molarities become (cont. p.40)

TABLE III-1
FILTER BOTTOMS COMPOSITIONS IN PROTOTYPE SIMULATIONS

QUANTITY	UNITS	CASE NUMBER				
		PS#1	PS#2	PS#4	PS#5	PS#6
Process Operation:						
Theoretical Limestone	%	130	130	130	130	130
Limestone Composition	Mole% MgO in LS	0	0	0	20	50
Soluble Na^+ in Fly Ash	Wt.fr. in LS+FA	0	0	0.0023	0.0025	0.0024
Soluble Cl^- in Coal	Wt.fr. in LS+FA	0	0	0.0024	0.0026	0.0025
Fly Ash Level	Wt.fr. in LS+FA	0	0.6122	0.6122	0.6256	0.6470
FB Characteristics:						
pH	----------------	11.21	11.31	11.35	11.35	7.76
Ionic Strength	----------------	1.05	0.66	0.82	0.84	2.37
Solid Molalities:						
$CaCO_3$	g-moles/kg H_2O	0.98	0.57	0.38	0.36	0.59
$CaSO_4$	g-moles/kg H_2O	11.03	6.42	6.41	6.51	2.39
$CaSO_3$	g-moles/kg H_2O	11.04	6.44	6.43	6.53	6.63
$Ca(OH)_2$	g-moles/kg H_2O	0.83	4.90	5.13	1.46	0.00
$Mg(OH)_2$	g-moles/kg H_2O	0.00	0.00	0.00	3.77	5.13
$MgCO_3$	g-moles/kg H_2O	0.00	0.00	0.00	0.00	0.00
Liquid Key-Species Molalities:						
SO_2	g-moles/kg H_2O	$2.4x10^{-4}$	$2.6x10^{-4}$	$2.5x10^{-4}$	$2.5x10^{-4}$	$3.2x10^{-2}$
CO_2	g-moles/kg H_2O	$3.2x10^{-8}$	$3.6x10^{-8}$	$3.8x10^{-8}$	$3.7x10^{-8}$	$4.8x10^{-3}$
$SO_4^=$	g-moles/kg H_2O	$1.4x10^{-2}$	$1.5x10^{-2}$	$1.9x10^{-2}$	$1.9x10^{-2}$	4.26
NO_3^-	g-moles/kg H_2O	0.82	0.48	0.48	0.48	0.49
Ca^{++}	g-moles/kg H_2O	0.44	0.27	0.23	0.23	$1.3x10^{-2}$
Mg^{++}	g-moles/kg H_2O	0.00	0.00	0.00	$7.3x10^{-7}$	4.49
Na^+	g-moles/kg H_2O	0.00	0.00	0.28	0.28	0.29
Cl^-	g-moles/kg H_2O	0.00	0.00	0.18	0.19	0.19
Total Key-Species Molalities (Input Values):						
SO_2	g-moles/kg H_2O	11.04	6.44	6.43	6.53	6.66
CO_2	g-moles/kg H_2O	0.98	0.57	0.38	0.36	0.59
$SO_4^=$	g-moles/kg H_2O	11.04	6.43	6.43	6.53	6.66
NO_3^-	g-moles/kg H_2O	0.82	0.48	0.48	0.48	0.49
Ca^{++}	g-moles/kg H_2O	31.87	18.60	18.58	15.08	9.62
Mg^{++}	g-moles/kg H_2O	0.00	0.00	0.00	3.77	9.62
Na^+	g-moles/kg H_2O	0.00	0.00	0.28	0.28	0.29
Cl^-	g-moles/kg H_2O	0.00	0.00	0.18	0.19	0.19

TABLE III-2

SCRUBBER BOTTOMS COMPOSITIONS IN PROTOTYPE SIMULATIONS

QUANTITY	UNITS	CASE NUMBER						
		PS#1	PS#2	PS#4A	PS#4B	PS#4C	PS#5	PS#6
Process Operation:								
Theoretical Limestone	%	130	130	130	130	130	130	130
Limestone Composition	Mole% MgO in LS	0	0	0	0	0	20	50
Soluble Na^+ in Fly Ash	Wt.fr. in LS+FA	0	0	0.0023	0.0023	0.0023	0.0024	0.0025
Soluble Cl^- in Coal	Wt.fr. in LS+FA	0	0	0.0024	0.0024	0.0024	0.0025	0.0026
Fly Ash Level	Wt.fr. in LS+FA	0	0.6122	0.6122	0.6122	0.6122	0.0026	0.6470
Limestone Dissolving in S	%	15	15	15	30	15	15	15
Scrubber Feed	gpm/ft^2*	10	10	10	10	13.75	10	10
Slurry Recycle	gpm/ft^2*	3.74	3.30	3.27	0	0	3.27	3.94
SB Characteristics:								
pH	---------------	3.67	3.78	3.82	3.83	3.81	3.82	4.47
Ionic Strength	---------------	1.05	0.66	0.82	0.82	0.83	0.83	2.38
SO_2 Partial Pressure**	atm	$2.87x10^{-4}$	$2.87x10^{-4}$	$2.87x10^{-4}$	$2.69x10^{-4}$	$2.81x10^{-4}$	$2.87x10^{-4}$	$2.87x10^{-4}$
CO_2 Partial Pressure***	atm	0.143	0.143	0.143	0.143	0.143	0.143	0.143
Ca^{++} Molality	g-moles/kg H_2O	0.315	0.199	0.170	0.170	0.174	0.167	0.006
Mg^{++} Molality	g-moles/kg H_2O	0.000	0.000	0.000	0.000	0.000	0.007	0.583
Solids in SF	g/100 g H_2O	0.36	0.54	0.54	0.000	0.000	0.51	0.57
Solids in SR	g/100 g H_2O	0.98	1.65	1.65	1.10	0.82	1.56	1.44
COMMENTS:								
SO_2 Convergence		yes	yes	yes	close	close	yes	yes
SO_2 Removal		---	---	---	too much	too much	---	---
CO_2 Convergence		close	close	close	close	close	close	close

---

* Ft^2 refers to scrubber cross sectional area; scrubber sized to yield superficial gas velocity of 10 ft/sec.

** Equilibrium partial pressure should be $2.87x10^{-4}$ atm for 90% SO_2 removal.

*** Equilibrium partial pressure should be approximately 0.143 atm for equilibrium CO_2 absorption.

The amounts of soluble Na^+, soluble Cl^-, and fly ash used in each simulation are based upon a 3.8 wt.% S coal containing 13.8 wt.% fly ash. The soluble Na^+ used in the "Na^+ equivalent" of the fly ash containing 0.2 wt.% (based on FA) soluble Na^+ and 0.3 wt.% soluble K^+. The soluble Cl^- shown corresponds to a coal which produces 0.054 wt.% (based on coal) water soluble chlorides. In the first simulation (PS#1), no fly ash was included, whereas fly ash but no soluble Na^+ or Cl^- was included, in the second one. In all subsequent simulations (PS#4, 5, and 6) the equivalent of a 13.8 wt.% fly ash coal was used.

Comparison of simulations PS#1 and PS#2 indicates that the effect of fly ash inclusion is to increase solids loading and thereby to reduce ionic strength. Since these two simulations were made using a fixed value (0.80) for the weight fraction of solids leaving in the filter bottoms, fly ash inclusion increases the liquid flow out with the filter bottoms and thus tends to reduce the ionic strength. For this instance the reduction in ionic strength (from 1.05 in PS#1 to 0.66 in PS#2) improves process operation in that less slurry recycle is required (3.74 gpm/ft^2 in PS#1 and 3.30 gpm/ft^2 in PS#2). Undoubtedly, there is an optimum ionic strength (I) for process operation since the activity coefficient versus ionic strength curve goes through a minimum for several ionic species (Ca^{++}, for one). Inclusion of the soluble Na^+ and Cl^- (compare PS#4A with

---

* (continued from page 37) numerically equal. In this report, molalities have been used as the unit of concentration in the process model and simulation sections, whereas molarities have been used in the sections describing the chemical equilibrium data and computer program.

PS#2 in Table III-2) tends to increase the ionic strength and improve process operation slightly (SR=3.27 gpm/ft^2). Simulations of the NAPCA venturi system, which are presented later in this section, show that a system with a very low ionic strength (0.07) is not as efficient as a system with an intermediate ionic strength (0.33). This indicates that the maximum amount of basic species (e.g., OH^-, $CaOH^+$, $CO_3^=$, etc.) are in solution when the ionic strength is $0.07 < I < 1.05$.

The solid molalities given in Table III-1 show that most of the $CO_3^=$, $SO_4^=$, and $SO_3^=$ are removed as Ca solids for both the 0 and 20 mole% MgO limestones. This condition exists because enough CaO is available (which depends upon the amount of limestone used) to precipitate $CaCO_3$, $CaSO_3$, and $CaSO_4$. For the 50 mole% MgO limestone, only 36% of the $SO_4^=$ leaves as $CaSO_4$. In this case, 64% leaves as $MgSO_4$ in solution.

Comparison of simulations PS#4, 5, and 6 as reported in Table III-1 also shows the effect of MgO content in the limestone on the pH of the filter bottoms. As long as enough CaO is present to combine with the acidic SO_2, CO_2, and $SO_4^=$ species, most of the MgO leaves the system as $Mg(OH)_2$ solid. The pH remains the same as the pure CaO case (compare PS#5 with PS#4). With the 50% MgO limestone and 130% theoretical limestone added, not enough CaO is present to combine with the acid species and some MgO is used for this purpose. Since no $Ca(OH)_2$ remains, the pH drops to 7.76. Also, since more Mg^{++} goes into solution, the ionic strength increases. Actually, the correlations for activity coefficients used by Radian in their equilibrium program are questionable for this high MgO case (PS#6) since an ionic strength of 2.38 is predicted.

The results presented in Table III-1 approximate the composition of the filter bottoms stream if equilibrium is approached in the effluent hold tank. If this is not the case in actual field units, rate expressions must be combined with the equilibrium and stoichiometric considerations presented here.

A comparison of simulations PS#4A, 5, and 6 in Table III-2 shows the effect of MgO content in the limestone on process operation. The scrubber liquid for PS#5 is very similar to that of PS#4A in that only a relatively minor amount of Mg-species is present. Process operation is essentially the same for PS#4A and PS#5. This situation exists because in this equilibrium simulation practically all of the Mg is precipitated as $Mg(OH)_2$ in the bottoms. On the other hand, as the MgO content in the limestone in increased to 50 mole% (PS#6), more Mg remains in solution in the effluent hold tank (and thus in the clarifier and filter). This results in 1) a scrubber solution containing high concentrations of Mg compounds, 2) more soluble salts removed with the solids which might contribute to water pollution problems, 3) a high ionic strength liquid system, and 4) poorer process operation as evidence by the higher slurry recycle rate required. On the basis of these simulations the use of a dolomitic limestone would not be recommended where a significant portion of the magnesium content would be utilized.

Although these simulations correspond to 130% theoretical limestone and solid-liquid equilibrium in the effluent hold tank, they should closely approximate the cases of higher percentages of theoretical limestone added and lower limestone utilizations. For example, these simulations should approximate the case of 260% theoretical limestone, 50% limestone utilization (with 50% of the limestone remaining as CaO, uncalcined $CaCO_3$, MgO, or uncalcined $MgCO_3$), and a higher percentage solids leaving with the filter bottoms. The simulation of the Type II limestone should correspond to the use of a dolomitic limestone in which a smaller fraction of the MgO (slower hydrating) is utilized than CaO.

Comparison of simulations PS#4A, 4B, and 4C in Table III-2 shows the effect of three model parameters on process operation. PS#4A was made as usual with SR adjusted to obtain SO_2 convergence. However, in PS#4B and 4C, only clear liquid was recycled (SR=0). Limestone dissolution in the scrubber was adjusted to obtain SO_2 convergence in PS#4B, whereas the scrubber feed rate (SF) was adjusted in PS#4C. The results from the simulations show that 30% of the limestone (when 130% theoretical LS is used) in the flue gas must be entrained into the scrubber and dissolve if a clear liquid rate of 10 gpm per ft^2 of scrubber cross section is fed to the scrubber. If only 15% of the limestone dissolves in the scrubber (PS#4C), 13.75 gpm/ft^2 of clear liquid feed are required. Thus, the scrubber feed rate must be increased by 37.5% if clear liquid feed containing dissolved $Ca(OH)_2$, etc., is used as compared to using a scrubber feed of 10 gpm/ft^2 including 3.27 gpm/ft^2 of slurry recycle. It should be noted here again that these figures are based upon the simulation assumption that all of the hydrated CaO in the slurry recycle stream dissolves and reacts in the scrubber.

Table III-2 also lists the solids content in the SF and SR streams. In each case where slurry is recycled, the SF stream contains about 0.5 wt.% solids and the SR stream contains about 1.5 wt% solids. When no slurry is recycled, the solids content of the CF stream is approximately 1.0 wt.% solids.

The prototype simulations reported here are rather limited, but they are useful in predicting the technical feasibility of various process schemes and the compositions in process units. For example, the simulations predict the amount of limestone that must dissolve in the scrubber to achieve a desired level of SO_2 removal if only clear liquid at a fixed rate is recycled to the scrubber (refer to PS#4B in Table III-2). That is to say, the scrubbing capacity of the recycled liquid is determined by the equilibrium relations in the effluent hold tank. The maximum recycle rate is governed by pumping costs and flooding characteristics of the scrubber. Thus, this simulation can predict the fraction of limestone that must react in the scrubber for a given clear liquid feed. If this fraction is not reasonable, a slurried recycle should be used.

The composition for the various process streams as predicted by these simulations are also useful in determining the analytical procedures to be used in test programs on the limestone injection - wet scrubbing process. For example, certain analytical methods are not valid in high concentration regions and in the presence of interfering substances.

The model in its present form should accurately predict the technical feasibility of process schemes and the composition in process units. These simulations are also useful in determining the relative importance of various model parameters. For example, several levels of MgO content in the limestone were studied in these simulations, but the effect of SO_2 oxidation was not examined. This model parameter and others require additional study.

C. KP&L SIMULATIONS

The second process simulated was typical of the one operated by Kansas Power and Light at their Lawrence Station. This once-through operation is diagrammed in Figure III-2. Several of the same stream designations used for the prototype simulations have been used in this system. Due to basic differences in the prototype and KP&L systems, these streams are not necessarily analogous. The limestone (LS), fly ash (FA), flue gas (FG), and stack gas (SG) streams are analogous. However, the scrubber bottoms (SB) stream in the KP&L system does not represent the slurry coming out of the scrubber bed as the

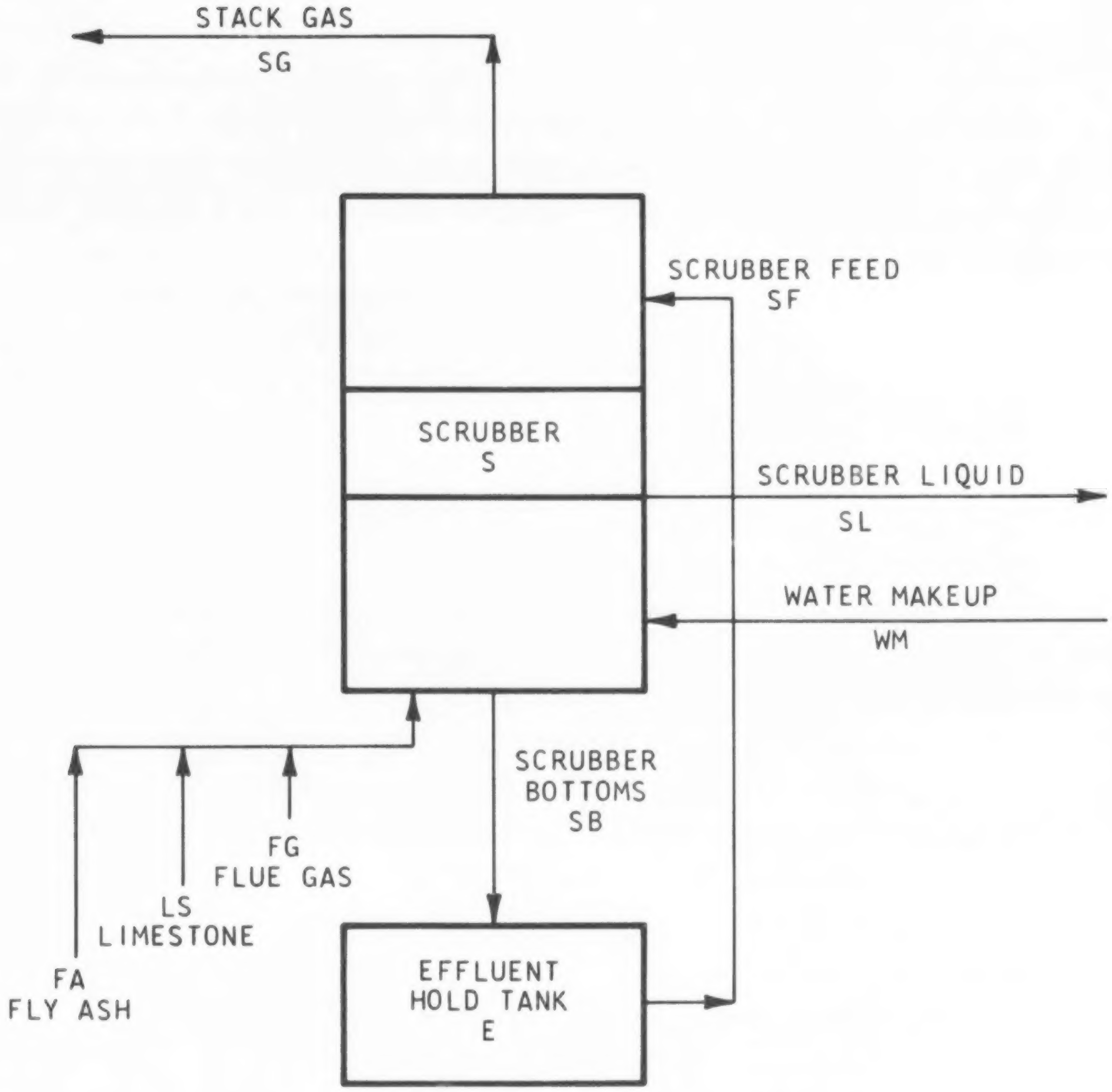

FIGURE III-2 KP & L SIMULATION

SB stream did in the prototype system. In this instance, the scrubber liquid (SL) stream is the slurry in the scrubber bed. The SB stream represents a combination of the water makeup (WM) not getting up into the bed, liquid coming down out of the bed, and solids which are "knocked-down" by the liquid raining down from the sprays and marble bed. The scrubber feed (SF) stream in the KP&L system is also not analogous to the SF stream in the prototype study. In the KP&L system, the spray water going into the bed (a portion of the WM stream) plus the scrubber feed (SF) stream represent the liquid feeds to the scrubber, whereas the SF stream in the prototype system is the only liquid feed stream.

In the KP&L simulations the scrubber liquid (SL) stream is taken to have the composition of the liquid on the scrubber bed (S) and the scrubber feed (SF) stream has the composition of the liquid in the effluent hold tank (E).

The same "typical" flue gas used in the prototype simulation was used for the KP&L simulation. Two limestone types were selected for study. Type I contains no MgO, whereas Type IV contains 10 mole% MgO. Estimates of the soluble sodium and chloride from the fly ash were made, although this estimate was relatively insignificant since the process is essentially once-through and no build up of these ions would be anticipated.

The following processing conditions were chosen for the KP&L simulation:

1. scrubber liquid rate (SL) of 10 gpm/ft^2 cross section,
2. 90% SO_2 removal in the scrubber,
3. 20% NO_x removal in the scrubber,
4. 0.2% CO_2 removal in the scrubber,
5. stack gas is saturated with water at the scrubber temperature,

6. the scrubber solution does not become supersaturated,
7. 20% of the water makeup goes into the scrubber bed,
8. temperature in each unit is 122°F.

These eight conditions are similar to the eight listed for the prototype simulation with the exceptions that the percent theoretical limestone was adjusted to converge on the SO_2 removal and that two levels of SO_2 oxidation were studied. In addition, a 0.2% CO_2 removal was specified. The dissolved salts in the water makeup were neglected even though this water is ash pond water. This assumption should not affect the results significantly since the ionic strength change will be small.

An overall material balance was used to determine the eight key species in the SL stream. The percent theoretical limestone added was adjusted until the equilibrium partial pressure of SO_2 corresponding to 90% SO_2 removal ($P^*_{SO_2} = 2.87 \times 10^{-4}$ atm) was obtained. The results of four SL simulations are summarized in Table III-3. (Computer printouts for selected cases shown in Table III-3 are in Appendix B.) The results show that 90% SO_2 removal can be achieved using 75% theoretical limestone for each of the four SL cases presented. Thus, the differences in pH, ionic strength, and SO_2 partial pressure for a 0 to 10% variation in percent MgO, zero and estimated soluble Na and Cl, and 40 to 50% variation in percent SO_2 oxidized are very small. These simulations predict a pH of approximately 4.1 for the KP&L scrubber.

The material balance calculations for the results presented here were made by hand and thus some iterative calculations do not represent "completely converged" cases. No iteration was made to obtain convergence on CO_2 absorption. However, convergence was considered adequate for the purposes of these simulations.

TABLE III-3

KP&L SIMULATIONS*

CASE NUMBER	SCRUBBER LIQUID (SL)				HOLD TANK LIQUID (SF)
	KPL#7A	KPL#7B	KPL#7C	KPL#7D	KPL#7B**
Process Conditions:					
Theoretical Limestone, %	75	75	75	75	110
MgO in Limestone, %	0	10	10	10	10
SO_2 Removal, %	90	90	90	90	90
SO_2 Oxidized, %	50	50	50	40	50
Scrubber Liquid, gpm/ft^2	10	10	10	10	10
Soluble Na and Cl	Est.	Est.	0	Est.	Est.
Results:					
pH	4.06	4.10	4.09	4.10	11.7
Ionic Strength	0.078	0.084	0.083	0.080	0.073
SO_2 Partial Pressure, atm.	3.2×10^{-4}	2.93×10^{-4}	3.03×10^{-4}	2.97×10^{-4}	2×10^{-19}

---

* Cases are not converged with respect to CO_2.

** Case No. KPL#7B-SL was used as a basis and 30% of the SO_2, CO_2, and NO_x removed was assumed to occur before the FG stream contacts the marble bed (in the boiler or scrubber entrance chamber). This 30% was taken as going with the LS and FA streams and a portion of the WM stream into the E tank. The remaining 70% is removed in the scrubber.

The 75% theoretical limestone figure may seem unrealistic at first. However, for equilibrium simulations, this figure represents limestone utilization in the scrubber. Thus, to achieve 90% SO_2 removal (from a 3000 ppm SO_2 flue gas), 0.75 times the stoichiometric amount for 100% SO_2 removal must be utilized. If only .75 stoichiometric were utilized however, the exit stream in the KP&L process would be an acidic stream with a high proportion (approximately 60%) of sulfur in the form of $SO_3^=$, HSO_3^-, $SO_4^=$, and HSO_4^- ions and with the limestone in excess of 75% theoretical in the form of undissolved CaO, $Ca(OH)_2$, MgO, and $Mg(OH)_2$. If the limestone does not dissolve further and neutralize these acidic species in the exit lines and in the pond, the pond liquid would release some SO_2 to the atmosphere due to its high SO_2 vapor pressure. Data from KP&L show that the pH of the exit stream does indeed increase between the scrubber and the ash pond.

The KP&L cases shown in Table III-3 were made based on the assumption that these mixtures were saturated with respect to the solid and liquid phases. Actually, the precipitation rate in the scrubber will likely not be fast enough to permit this approximation and these solutions will actually be supersaturated to some extent. The equilibrium program was run on case KPL #7B-SB whereby solids formation was not allowed. This case (not shown) represents the other extreme, i.e., complete supersaturation. To achieve 90% SO_2 removal for the supersaturated case, only 69% theoretical limestone (as compared to 75% theoretical for the saturated case) must be utilized in the scrubber. The pH of the scrubber liquid was essentially the same (4.1) for the saturated and supersaturated cases. As the supersaturation subsides (e.g., in the exit lines), more limestone dissolution will be required to maintain the pH level around 4 and the vapor pressure near 300 ppm.

One calculation was made to estimate the composition of the effluent hold tank material (SF). These results are shown in the last column of Table III-3 and predict a pH of 11.7. In this case, 30% of the SO_2, CO_2, and NO_x removed in the process was assumed to take place before the flue gas stream contacts the marble bed and be carried out through the SB stream.

D. NAPCA VENTURI SIMULATION

The third process simulated was NAPCA's pilot unit system using a venturi scrubber. These simulations are based upon the current Radian model of the wet scrubbing process and were used by Radian to estimate process flow rates and compositions for the NAPCA inhouse test program.

A schematic diagram depicting the process simulated is given in Figure III-3. For these simulations, three pieces of equipment - the venturi scrubber, a knockout drum, and a cyclone separator - are grouped together and termed the scrubber section. These three pieces perform the functions of gas-liquid contacting and disengaging which are also the functions of the turbulent contact absorber and the marble bed contactors. Thus, the key "scrubber" assumption for these simulations is that the stack gas leaving the cyclone (SG) is in vapor-liquid equilibrium with the scrubbing liquid leaving the knockout drum (SB). This assumption is probably less valid here then in the case of TCA and marble bed scrubbers. In the NAPCA pilot unit system, the effluent holding system (E) is composed of a surge tank and two stirred 55-gallon durms.

In the NAPCA system, the flue gas is generated by a natural gas furnace. The volumetric flow rate is increased and the temperature decreased by adding air. The SO_2 and NO_x species are added downstream of the furnace. Limestone samples which have been calcined in commercial boiler units are dispersed into the system by a venturi located upstream of the scrubbing venturi. The following flue gas composition should be typical for this system:

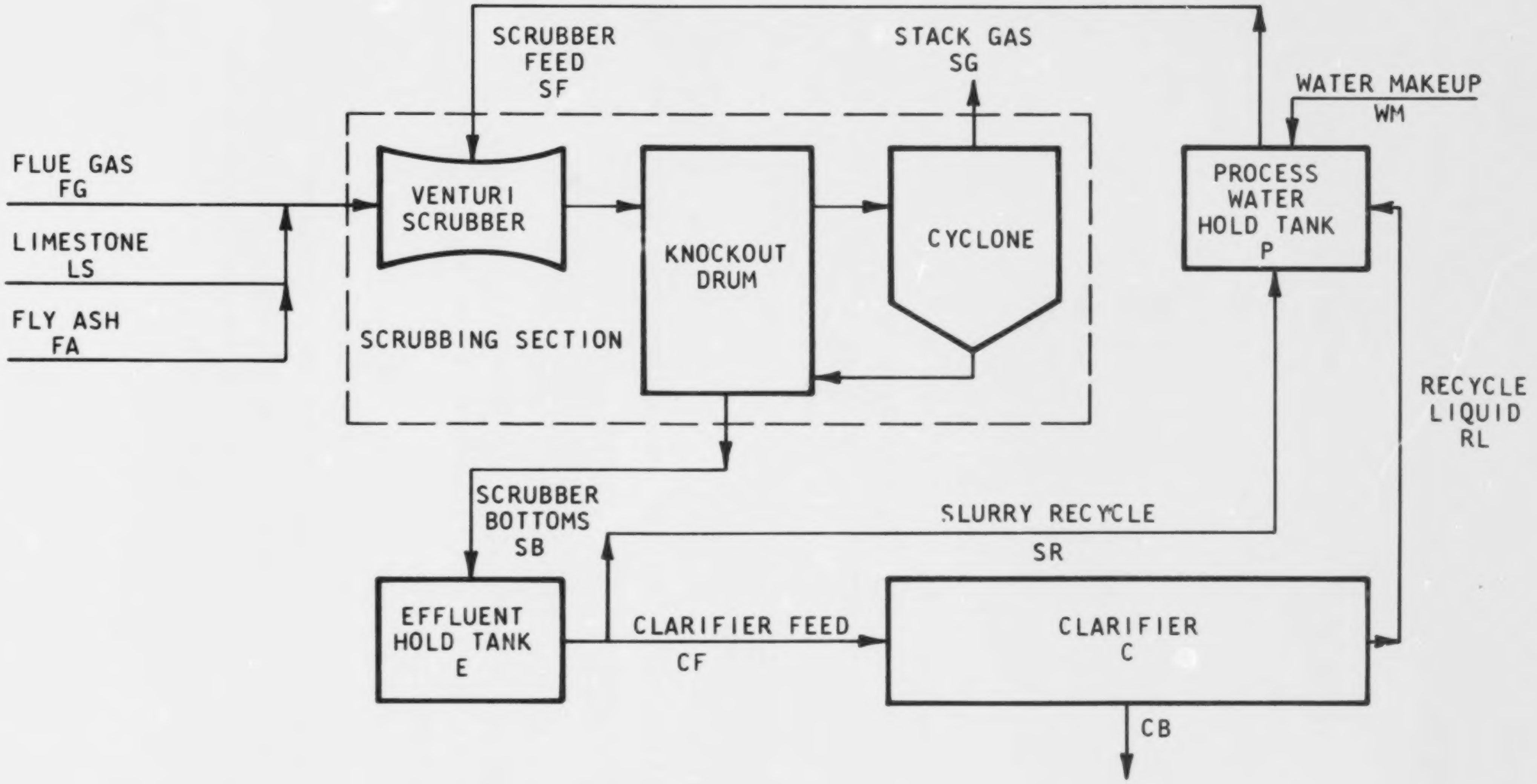

FIGURE III-3 NAPCA VENTURI SIMULATION

Component	Mole%
SO_2	0.20
CO_2	2.50
NO_x	0.05
H_2O	5.00
O_2	15.00
CO	0.00
N_2	77.25

In three preliminary simulations, an SO_2 concentration of 0.15 mole% and a flue gas rate of 1250 ACFM at 250°F and 14.7 psia were used. Later, an SO_2 concentration of 0.20 mole% and a flue gas rate of 1000 ACFM were selected as "base" conditions. In each case reported here, the limestone was taken to be 100% CaO (no MgO) and varying amounts of fly ash, soluble Na^+, and soluble Cl^- were studied.

The following processing conditions were chosen for the NAPCA venturi simulations:

1. 70% SO_2 removal by the process,
2. 50% SO_2 oxidation in the scrubbing section,
3. stack gas is saturated with water at the scrubber temperature,
4. the feed to the scrubber (SF) is 10 gpm,
5. no CaO hydrates in the scrubbing section,
6. hydrated CaO in the slurry recycle stream (SR) dissolves in the scrubbing section,
7. the scrubber liquid does not become supersaturated,
8. the temperature in each of the process units is 122°F.

The remaining model parameters such as theoretical limestone, soluble Na^+ and Cl^-, and NO_x absorbed were varied from one case to the next. As in the case of the prototype simulations, the amount of slurry recycle was adjusted to obtain SO_2 convergence.

The results from the NAPCA venturi simulations are presented in Table III-4. Computer printouts for selected cases of the scrubber liquid (SB) and clarifier effluent (CB) compositions are given in Appendix B. The first simulation reported in Table III-4 (NV#2) represents a process containing no fly ash, soluble Na^+, soluble Cl^-, or NO_x compounds. For this system, the ionic strength is very low (0.07) and 1.08 gpm of slurry recycle are required for 70% SO_2 removal from a 1250 ACFM flue gas stream containing 0.15 mole% SO_2. In simulation NV#3, soluble Na^+ and Cl^- [equivalent to a 3.0 wt.% sulfur coal containing 10.8 wt.% of fly ash, 0.043 wt.% of water soluble chloride in the coal, and 0.26 wt.% soluble "equivalent" sodium ($Na^+ + K^+$) in the fly ash] are added to the system. For this case, the ionic strength is 0.32 and only 0.50 gpm of slurry recycle are required for 70% SO_2 removal. Thus, the effect of adding Na^+ and Cl^- to a relatively low ionic strength scrubbing mixture is to improve process operation.

Simulation NV#4 represents the same processing conditions as NV#3 except that the assumptions of 20% NO_x absorption from a flue gas containing 500 ppm NO_x and enough CaO to neutralize this NO_x (the theoretical limestone increased from 110% to 113.7%) are included in the NV#4 case. The addition of the NO_x to the process increased the ionic strength to 1.47 and the required slurry recycle to 4.12 gpm for this "equilibrium-type" simulation. The "optimum" ionic strength has been exceeded for this case. The high ionic strength of NV#4 is a result of the high NO_3^- concentration of 0.861 g-moles/kg of H_2O.

TABLE III-4

SIMULATIONS OF NAPCA VENTURI SYSTEM

QUANTITY	UNITS	CASE NUMBERS NV#2	NV#3	NV#4	NV#6
Process Operation:					
Theoretical Limestone	%	110	110	113.7	113.7
Soluble Na^+ in Fly Ash	Wt.fr. in LS+FA	0	5.0×10^{-3}	5.0×10^{-3}	1.7×10^{-3}
Soluble Cl^- in Coal	Wt.fr. in LS+FA	0	7.5×10^{-3}	7.5×10^{-3}	2.5×10^{-3}
Fly Ash Level	Wt.fr. in LS+FA	0	0	0	0.646
SO_2 in FG	Mole fraction	1.5×10^{-3}	1.5×10^{-3}	1.5×10^{-3}	2.0×10^{-3}
NO_x Absorbed	%	0	0	20	20
Flue Gas Rate	ACFM	1250	1250	1250	1000
Liquid to Solid Ratio in CB	lbs liq H_2O/lb non-H_2O	0.5	0.5	0.5*	1.0**
Slurry Recycle Rate	gpm	1.08	0.50	4.12	2.9
Solids in SF	g/100 g H_2O	---------	---------	---------	0.47
Solids in SR	---------------------	---------	---------	---------	1.61
SB Characteristics:					
pH	---------------------	3.90	3.83	3.49	3.72
Ionic Strength	---------------------	0.07	0.32	1.47	0.38
SO_2 Partial Pressure	atm	4.16×10^{-4}	4.16×10^{-4}	4.16×10^{-4}	5.56×10^{-4}
CO_2 Partial Pressure	atm	0.0231	0.0231	0.0231	0.0231
NO_3^- Molality	g-moles/kg H_2O	0.00	0.00	0.861	0.182
Ca^{++} Molality	g-moles/kg H_2O	0.021	0.034	0.381	0.101
Na^+ Molality	g-moles/kg H_2O	0.00	0.204	0.197	0.050
Cl^- Molality	g-moles/kg H_2O	0.00	0.203	0.203	0.050
FB Characteristics:					
pH	---------------------	11.66	11.65	11.16	11.45
Ionic Strength	---------------------	0.09	0.35	1.46	0.38
Solid Molalities					
$CaCO_3$	g-moles/kg H_2O	0.067	0.025	0.025	0.025
$CaSO_4$	g-moles/kg H_2O	5.34	5.19	5.21	1.36
$CaSO_3$	g-moles/kg H_2O	5.36	5.22	5.22	1.38
$Ca(OH)_2$	g-moles/kg H_2O	6.02	6.45	5.96	1.54

---

* Corresponds to approximately 67 wt.% solids when no fly ash is included and 80 wt.% solids when fly ash is included.

** Corresponds to approximately 50 wt.% solids.

In each of these first three simulations (NV#2, 3, and 4), the liquid to solid ratio in the clarifier effluent stream (CB) was taken to be 0.5 lbs of liquid H_2O per pound of non-H_2O species. This liquid to solid ratio is equivalent to approximately 67 wt.% solids leaving with the CB stream. For these three cases no fly ash solids were included in the simulations. If fly ash equivalent to a 3.0 wt.% sulfur coal containing 10.8 wt.% of fly ash were to be included in these simulations as solids loading, the liquid draw-off (CB liquid) rates used in NV#2, 3, and 4 would correspond to a CB stream containing 80 wt.% solids. Thus, these simulations correspond to a system operating with an efficient solid-liquid separation system and to cases which allow a large build-up of dissolved solids.

Simulation NV#6 represents processing conditions which should best typify the NAPCA system operating with a high CaO limestone. In this case, fly ash, soluble Na^+, soluble Cl^-, and NO_x absorption have all been included. The liquid draw-off rate corresponds to having 1.0 lb of liquid H_2O per pound non-H_2O species (approximately 50 wt.% solids) leaving in the clarifier effluent. As determined by NV#6, liquid flow rates, pH values, and ionic strengths are shown in Figure III-4 for the various process streams. The compositions of the scrubber bottoms (SB) and clarifier bottoms (CB) are given in Table III-5 and III-6.

Although these flow rates and compositions are only approximate, they allow several useful observations to be made about the system which are helpful in designing a test program. First of all, pumps can be sized to give the proper flow rates. Secondly, time constants for various parts of the system can be approximated so that some idea of the time required to achieve steady-state operation is obtained. Of course, a knowledge of the approximate compositions is most helpful in determining the analytical procedures to be used in the test program.

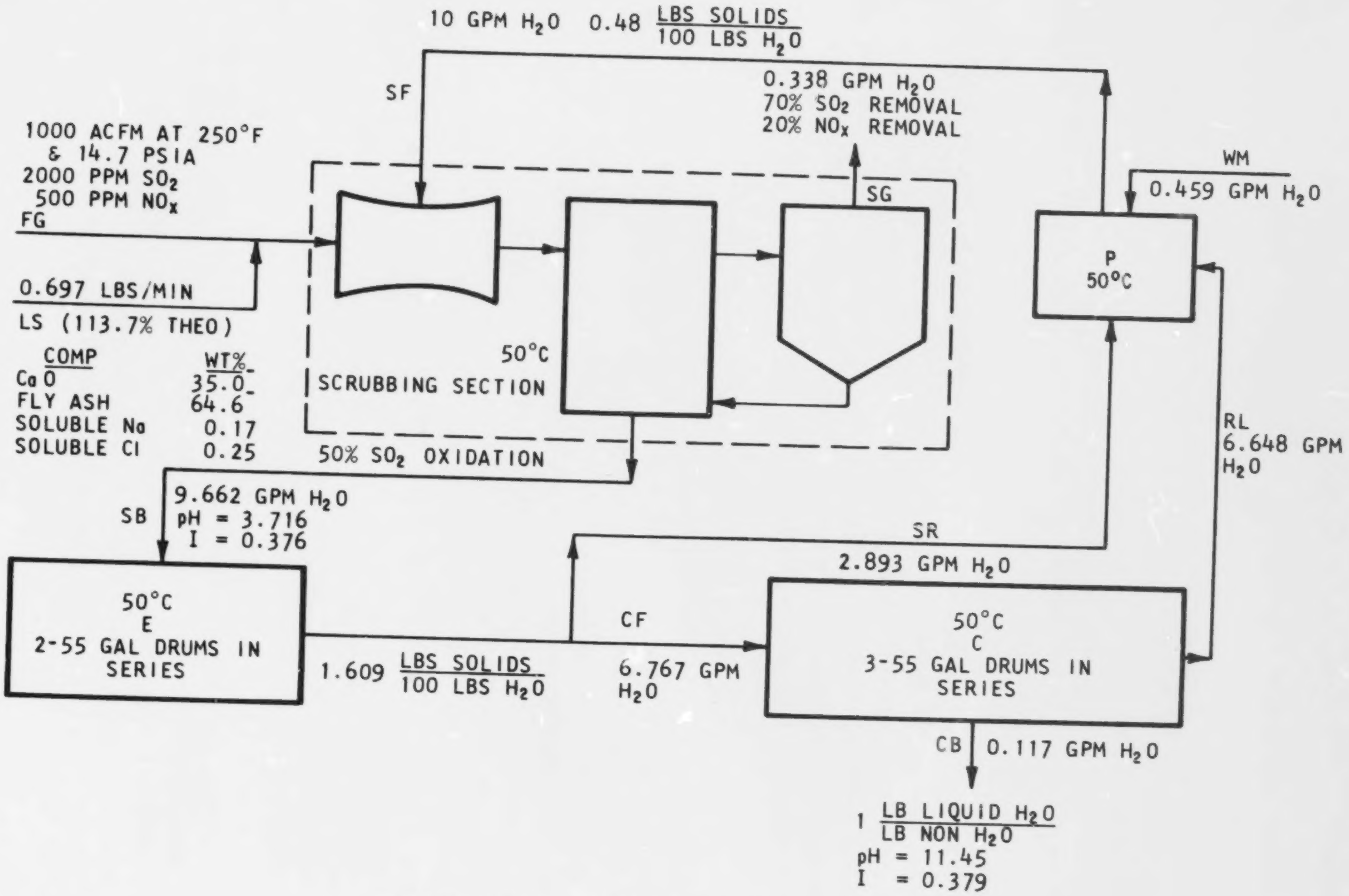

FIGURE III-4 NAPCA VENTURI SIMULATION NV#6

TABLE III-5 - COMPOSITION OF SCRUBBER BOTTOMS NV#6

DMO
22 Dec.69

```
                           INPUT CONCENTRATIONS (MOLES/LITER)

SO4--=4.20566-02     NO3- =1.97403-01     CA++ =1.55161-01     MG++ =0.00000
NA+  =5.12709-02     CL-  =4.98332-02
SO2  =2.39990-02
PCO2 =2.31179-02   ATM.
                              AQUEOUS SOLUTION EQUILIBRIA

          COMPONENT         CONCENTRATION        ACTIVITY         ACTIVITY COEFFICIENT
          H+                  2.241-04           1.921-04              8.573-01
          OH-                 3.965-10           2.850-10              7.189-01
          HSO3-               1.690-02           1.215-02              7.189-01
          SO3--               1.009-05           2.695-06              2.671-01
          SO4--               8.745-03           1.337-03              1.520-01
          HCO3-               1.617-06           1.159-06              7.189-01
          CO3--               1.523-12           4.067-13              2.671-01
          NO3-                1.815-01           9.658-02              5.321-01
          HSO4-               7.379-05           5.305-05              7.189-01
          H2SO3               2.791-04           2.981-04              1.068+00
          H2CO3               4.041-04           4.316-04              1.068+00
          CA++                1.009-01           2.509-02              2.487-01
          CAOH+               2.772-10           1.993-10              7.189-01
          CASO3               6.331-05           6.761-05              1.068+00
          CACO3               2.014-11           2.151-11              1.068+00
          CAHCO3+             8.809-07           6.332-07              7.189-01
          CASO4               8.892-03           9.497-03              1.068+00
          CANO3+              1.462-02           1.051-02              7.189-01
          CACO3(S)            1.216-37           1.216-37              1.000+00
          CASO4(S)            2.394-02           2.394-02              1.000+00
          CASO3(S)            6.746-03           6.746-03              1.000+00
          CA(OH)2(S)          1.216-37           1.216-37              1.000+00
          NA+                 4.958-02           3.572-02              7.204-01
          NAOH                2.566-12           2.740-12              1.068+00
          NACO3-              4.484-13           3.224-13              7.189-01
          NAHCO3              2.180-03           2.329-03              1.068+00
          NASO4-              4.031-04           2.898-04              7.189-01
          NANO3               1.286-03           1.373-03              1.068+00
          CL-                 4.983-02           3.285-02              6.593-01
PSO2 =5.55407-04   ATM.
CO2  =4.06628-04

          PH =       3.716          IONIC STRENGTH = 3.75880-01          RES. E.N. =   6.977-10
```

NOT REPRODUCIBLE

TABLE III-6 - COMPOSITION OF CLARIFIER BOTTOMS NV#6

DMO
22 Dec.69

```
                              INPUT CONCENTRATIONS (MOLES/LITER)

SO4--=1.38232+00     NO3- =1.97475-01     CA++ =4.44940+00     MG++ =0.00000
NA+  =5.19132-02     CL-  =5.04634-02
SO2  =1.38232+00
CO2  =2.46848-02

                                AQUEOUS SOLUTION EQUILIBRIA

        COMPONENT          CONCENTRATION         ACTIVITY          ACTIVITY COEFFICIENT
        H+                   4.156-12            3.566-12              8.580-01
        OH-                  2.137-02            1.536-02              7.189-01
        HSO3-                3.265-10            2.347-10              7.189-01
        SO3--                1.050-05            2.805-06              2.670-01
        SO4--                9.145-03            1.391-03              1.521-01
        HCO3-                5.520-09            3.968-09              7.189-01
        CO3--                2.809-07            7.501-08              2.670-01
        NO3-                 1.821-01            9.669-02              5.308-01
        HSO4-                1.426-12            1.025-12              7.189-01
        H2SO3                1.000-19            1.069-19              1.069+00
        H2CO3                2.566-14            2.742-14              1.069+00
        CA++                 9.711-02            2.410-02              2.482-01
        CAOH+                1.435-02            1.032-02              7.189-01
        CASO3                6.327-05            6.761-05              1.069+00
        CACO3                3.567-06            3.812-06              1.069+00
        CAHCO3+              2.897-09            2.082-09              7.189-01
        CASO4                8.887-03            9.497-03              1.069+00
        CANO3+               1.406-02            1.011-02              7.189-01
        CACO3(S)             2.468-02            2.468-02              1.000+00
        CASO4(S)             1.364+00            1.364+00              1.000+00
        CASO3(S)             1.382+00            1.382+00              1.000+00
        CA(OH)2(S)           1.544+00            1.544+00              1.000+00
        NA+                  5.006-02            3.605-02              7.201-01
        NAOH                 1.395-04            1.490-04              1.069+00
        NACO3-               8.348-03            6.001-03              7.189-01
        NAHCO3               7.528-11            8.045-11              1.069+00
        NASO4-               4.235-04            3.044-04              7.189-01
        NANO3                1.299-03            1.388-03              1.069+00
        CL-                  5.046-02            3.324-02              6.586-01
PSO2 =1.99118-19   ATM.
PCO2 =1.46870-12   ATM.

        PH =       11.448          IONIC STRENGTH = 3.78944-01            RES. E.N. =  -7.948-09
```

In summary, the simulations reported here demonstrate the utility of the current Radian model to estimate 1) the technical feasibility of various processing schemes, 2) process flow rates and compositions, and 3) the effect of various model parameters on process operation. The simulations showed that solutions with ionic strengths in the neighborhood 0.7 contained a maximum amount of basic species. Ionic strengths in this range are feasible by controlling filter efficiency. Magnesium had little influence on solution strength so long as there was enough calcium present to precipitate $Mg(OH)_2$. For dolomite stones, however, dissolved salt strength is highly increased. When not enough calcium was present, i.e., a significant portion of the magnesium was utilized, the magnesium content of the circulating solution increases. This can cause the ionic strength to approach values of 2.5. These high values have a detrimental effect on the process.

Ionic strength is controlled by the rate at which soluble components enter and the rate at which solution is removed from solution. Soluble components enter in the fly ash, flue gas (NO_x), make up water and limestone. The removal rate of dissolved solids is a function of filter efficiency, total solids removal, and clear liquid removal (if desired).

IV. PHYSICAL CHEMICAL DATA

The description of the liquid phase of the lime/limestone wet scrubbing process was based upon an investigation of the literature to determine what the possible chemical species in the reacting system might be. Equilibrium constants were selected from the literature. Calculations were made so that the list of possible reactions was reduced to a set of significant reactions needed to thermodynamically describe the system. It was also possible to combine certain species (e.g., sodium and potassium) for computational efficiency. As is usually the case, some important physical/chemical data were missing. These values were determined experimentally.

The ionic strengths of the solutions involved were in a range where the assumption of ideality was not valid. A significant effort was devoted to developing an accurate activity coefficient correlation.

In this section the results of the literature search and the selection of the significant species, reactions, and equilibrium constants are described. The activity coefficient correlation, formulation of equilibrium and mass balance equations, temperature dependence of the various quantities, and experimental determinations are discussed.

A. LITERATURE

The primary guides for the literature search were Chemical Abstracts and Gmelin's Handbuch der Anorganischen Chemie. Compilations of pertinent thermochemical values were also used. Sillén's compilation of stability constants and solubility products for metal-inorganic ligands published through 1960 proved to be extremely useful (SI-001).

The major objectives of the literature search concerning physical chemical data were:

- The definition of important complexes in the aqueous phase.
- The selection of the most reliable dissociation constants.
- The definition of important solid-liquid equilibria.
- The selection of the most reliable solubility products.
- The quantitative description of the liquid-gas equilibria.
- The selection of pertinent activity coefficient correlations.
- Correlations to describe the temperature dependency of the dissociation constants, solubility products, gas-liquid equilibria and activity coefficients.

- The definition of missing parameters.
- Side reactions.

1. Definition of Important Species in the Scrubbing Solution

The key species in the aqueous phase originate from lime (Mg, Ca), flue gas (CO_2, SO_2, SO_3, O_2, NO_x) and the fly ash (Na, K, Cl, plus others). In interacting with water the neutral and ionic species formed are given in Table IV-1.

H_2SO_3 and H_2CO_3 stand for the sum of the hydrated and unhydrated SO_2 and CO_2 in the aqueous phase. $S_2O_5^=$ is formed by the reaction: $SO_2 + SO_3^= \rightleftarrows S_2O_5^=$. "Others" stands for complexes formed by trace elements and for complexes which were not mentioned in the literature. The compilation by Sillén was used as the basis for the establishment of Table IV-1.

The aqueous phase is related to the gas phase by the equilibria:

$$SO_{2\,gas} \rightleftarrows SO_{2\,aq} \qquad \text{(IV-1)}$$

$$SO_{2\,aq} + H_2O \rightleftarrows H_2SO_3 \qquad \text{(IV-2)}$$

$$CO_{2\,gas} \rightleftarrows CO_{2\,aq} \qquad \text{(IV-3)}$$

$$CO_{2\,aq} + H_2O \rightleftarrows H_2CO_3 \qquad \text{(IV-4)}$$

$$O_{2\,gas} \rightleftarrows O_{2\,aq} \qquad \text{(IV-5)}$$

$$NO_{x\,gas} \rightleftarrows NO_{x\,aq} \qquad \text{(IV-6)}$$

TABLE IV-1

CHEMICAL SPECIES ORIGINALLY CONSIDERED

Soluble Species

1. H_2O
2. H^+
3. OH^-
4. H_2SO_3
5. HSO_3^-
6. $SO_3^{=}$
7. HSO_4^-
8. $SO_4^{=}$
9. H_2CO_3
10. HCO_3^-
11. $CO_3^{=}$
12. Ca^{++}
13. $CaOH^+$
14. $CaSO_3$
15. $CaSO_4$
16. $CaCO_3$
17. $CaHCO_3^+$
18. $CaNO_3^+$
19. NO_3^-
20. $MgOH^+$
21. Mg^{++}
22. $MgSO_3$
23. $MgSO_4$
24. $MgCO_3$
25. $MgHCO_3^+$
26. $NaOH$
27. Na^+
28. $NaSO_4^-$
29. $NaCO_3^-$
30. $NaHCO_3$
31. $NaNO_3$
32. Cl^-
33. K^+
34. KSO_4^-
35. KNO_3
36. $S_2O_5^{=}$
37. O_2
38. HNO_3
39. HNO_2
40. HCl
41. Others

Insoluble Species

42. $CaCO_3(S)$
43. $CaSO_4(S)$
44. $CaSO_3(S)$
45. $Ca(OH)_2(S)$
46. $Mg(OH)_2(S)$
47. $MgCO_3(S)$
48. $MgSO_3(S)$

$CaCO_3$ precipitates in two modifications, calcite and aragonite. Both phases have no water of hydration. In the temperature range of interest the calcite is the stable phase (GM-001).

Several modifications are reported for $CaSO_4$, namely α - $CaSO_4$, β - $CaSO_4$, and γ - $CaSO_4$. In addition, two modifications with water of hydration are given in the literature, $CaSO_4 \cdot 2H_2O$ and $CaSO_4 \cdot \frac{1}{2}H_2O$. In the temperature range of interest in the wet scrubbing process only $CaSO_4 \cdot 2H_2O$ and β - $CaSO_4$ are stable. The transition temperature is ~ 40°C (GM-001). At 50°C β - $CaSO_4$ (anhydrite) is the stable phase.

The literature describing the $CaSO_3$- hydrates is very contradictory. The older literature reports $CaSO_3 \cdot 2H_2O$ as being the stable phase. Matthews and McIntosh (MA-001), however, found $CaSO_3 \cdot \frac{1}{2}H_2O$ only. This phase was always found by these authors independent of the preparation methods. The identification was based on chemical analysis and X-ray diffraction. $CaSO_3 \cdot \frac{1}{2}H_2O$ was therefore assumed to be the stable solid phase in the present study.

For $MgCO_3$ three hydrates are reported: $MgCO_3 \cdot 5H_2O$, $MgCO_3 \cdot 3H_2O$, and $MgCO_3 \cdot H_2O$. The pentahydrate is stable at lower temperatures up to about room temperature. Between room temperature and about 100°C, $MgCO_3 \cdot 3H_2O$ is the stable compound.

$MgSO_3$ forms two hydrates. $MgSO_3 \cdot 6H_2O$ is stable up to 38°C. Above this temperature $MgSO_3 \cdot 3H_2O$ is the stable modification.

2. Chemical Equilibrium Constants

a. Survey of Experimental Methods

Many of the experimental methods for determining the equilibrium constants for ion-pair or complex formation are indirect. A given property of the system is measured and compared to that calculated from some assumed ideal behavior, such as the Debye-Hückel Law. Part of the deviation from ideal behavior can then be ascribed to the extent of ion-pair formation. This involves the assumption that the ions remaining free will obey the assumed activity law.

The conductivity of an electrolyte solution, for instance, may be modified by the formation of ion pairs which are uncharged or have a different equivalent conductance than the free ions. The fraction of ion-pair formation and the equilibrium constant can be calculated assuming that the free ions obey the limiting equation of Onsager or extensions thereof. Dilute solutions must be used to satisfy the latter requirement, but then the degree of association is usually small and therefore more difficult to determine.

Potentiometric methods have also been applied to the determination of equilibrium constants. Measurements on a single pure electrolyte solution yield precise values for the apparent mean activity coefficient. For dilute solutions a negative deviation of the measured activity coefficient from that calculated for the completely dissociated electrolyte can be related to the degree of ion association. The method may be extended to treat the ion-pairing that results when two electrolytes are mixed. Potentiometric measurements have provided accurate values for the ionization of weak acids.

The measurement of the solubility of a slightly soluble salt in the presence of another electrolyte may in some cases be used to derive equilibrium constants. The solubility is increased in the presence of an electrolyte containing ions which can form ion-pairs with the ions of the saturating salt. This increase in solubility can be used to calculate the concentrations of the ion-pair species in solution.

Other methods used less frequently than those given above include measurements with ion selective electrodes, ultrasonic absorption, freezing point depression, and kinetic studies. Ion selective electrodes are a fairly recent development and have not as yet been put to extensive use. These electrodes measure directly the activity of the uncomplexed ion in solution. The degree of ion association can be calculated from this measurement along with the total amount of species in solution and suitable activity coefficients.

Ultrasonic absorption spectra of an electrolyte in solution may yield peaks corresponding to the rapid dissociation and recombination of the ion pair. The relaxation times can be related to the forward and reverse reaction rates which are combined to give an equilibrium constant.

The freezing points of dilute solutions of electrolytes are closely related to the number of particles in solution. Measurement of the freezing point depression of such solutions may be used to investigate ion-pair formation. The temperature range at which such measurements may be made is limited.

Relatively straightforward analytical techniques may be employed to determine the solubilities of gases or sparingly soluble salts. Correction to zero ionic strength must be made to obtain usable equilibrium constants. This involves either an extrapolation and/or the calculation of activity coefficients.

b. Accepted Constants

Most of the techniques described above require careful measurements. The assumptions involved in their interpretation must also be examined. For these reasons there is often disagreement between the published values describing the same ion association constant. Most of the original papers were studied to determine the experimental and computational methods used, difficulties encountered, and stated limits of accuracy, if any. The agreement of values obtained by several different methods was usually considered a good criterion for the acceptance of that value. When there were only a few published values, the choice was more subjective. The accepted values are summarized in Table IV-2. No values were found for the dissociation constants of the ion-pairs $CaSO_3^0$ or $MgSO_3^0$.

In order to keep the numerical problem within reasonable limits, not all complexes listed previously (IV-A-1) are considered in Table IV-2. The reason for this will be given in Section IV-B.

c. Temperature Dependence of the Equilibrium Constants

The temperature dependence of the equilibrium constants is usually determined by either measuring K at different temperatures or by calorimetry. If K is known at various temperatures, the equation

$$\frac{\partial \ell n K_T}{\partial T} = \frac{\Delta H_T}{RT^2} \qquad \text{(IV-7)}$$

TABLE IV-2

EQUILIBRIUM CONSTANTS AND TEMPERATURE DEPENDENCE

	COMPOUND	REFERENCE	METHOD	T(°C)	K	DERIVED VALUES	REMARKS
1)	H_2O	HA-002	Potentiometric	25	1.008×10^{-14}	A = 4470.99 C = 0.017060 D = 6.0875	These values are for the activity product constant of water (K_w). They are well established.
2)	H_2SO_3	JO-001	Conductivity, Chem. Analysis	25 50	1.30×10^{-2} 7.6×10^{-3}	ΔH°_{298} = -3.86 kcal/mole	The K_{298} value agrees with that obtained by (YU-001) from potentiometric measurements. H_2SO_3 is the sum of SO_2(aq) and actual H_2SO_3.
3)	HSO_3^-	YU-001	Potentiometric	25	6.24×10^{-8}		This value agrees with that obtained by (TA-001).
		AR-001	Potentiometric Titration			ΔH°_{298} = -2.9 kcal/mole	This ΔH°_{298} value will be used in conjunction with the above K_{298}.
4)	HSO_4^-	RO-001	Spectrophotometric	25 55	1.04×10^{-2} 4.13×10^{-3}	A = 475.14 C = 0.018222 D = 5.0435	These are considered the most reliable values. Potentiometric values agree well.
5)	H_2CO_3	HA-003	Potentiometric	25 50	4.45×10^{-7} 5.19×10^{-7}	A = 3404.71 C = 0.032786 D = 14.8435	H_2CO_3 is the sum of CO_2(aq) and actual H_2CO_3.
6)	HCO_3^-	HA-004	Potentiometric	25 50	4.69×10^{-11} 6.73×10^{-11}	A = 2902.39 C = 0.02379 D = 6.4980	
7)	$CaOH^+$	GI-001	Potentiometric	25 35	4.3×10^{-2} 4.0×10^{-2}	ΔH_{298} = -1.25 kcal/mole	Other values for K_{298} range from 0.03-0.054.
8)	$CaSO_3^0$	Radian Detr. Radian Calc.	See Text Fuoss Equation	25 40	4.0×10^{-4} 3.2×10^{-4}	A = -504.8 D = -5.091	No values were found in the lit.
9)	$CaCO_3^0$	GA-001	Potentiometric Titration (pH)	25	6.3×10^{-4}		This is the only value reported.
		Radian Calc.	Fuoss Equation	55	4.1×10^{-4}	A = -475.5 D = -4.795 ΔH°_{298} = -2.17 kcal/mole	See text.

TABLE IV-2 (continued)

COMPOUND	REFERENCE	METHOD	T(°C)	K	DERIVED VALUES	REMARKS
10) $CaHCO_3^+$	GR-002	Potentiometric Titration (pH)	25	5.5×10^{-2}		This value was obtained by correction to 0 ionic strength by (GA-001). It is the only value reported.
	Radian Calc.	Fuoss Equation	55	4.2×10^{-2}	A = -301.8 D = -2.272 ΔH°_{298} = -1.38 kcal/mole	See text.
11) $CaSO_4^\circ$	BE-002	Solubility	25 40	4.9×10^{-3} 4.1×10^{-3}		The K_{298} value agrees well with those obtained from conductivity, potentiometric, and Ca++ electrode measurements.
	HE-001	Calculated			ΔH°_{298} = -1.94 kcal/mole ΔC°_p = -46 cal/mole°K	These were calculated from (BE-002 data by theoretical considerations.
12) $CaNO_3^+$	CA-002	Conductivity	25	4.9×10^{-1}	ΔH°_{298} = -1.7 kcal/mole	The K_{298} value is in good agreement with that found by (DA-002). The ΔH°_{298} is an estimation since the only other measurement was at 18°C.
13) $CaCO_3$(S)	FR-001	Solubility	25	4.8×10^{-9}	A = -1660 D = -13.88	The values of A and D were calculated from the data given by FR-001 for the ratio of the solubility at T to that at 25°C.
14) $CaSO_4 \cdot 2H_2O$(S)	LA-001 MA-002	See Section IV-D-1	25	2.4×10^{-5}	A = 4944.0 B = 37.745 D = 105.36	$CaSO_4 \cdot 2H_2O$ is the stable phase up to ~ 42°C. Above this $CaSO_4$ is the stable species.
$CaSO_4$(S)	MA-002	Solubility Chem. Analysis			A = 1200.9 B = -6.6489 C = 0.032057 D = -7.084	
15) $CaSO_3 \cdot \frac{1}{2}H_2O$(S)	Radian Detr.	Solubility Chem. Analysis	25	8.4×10^{-8}		See text. The literature results are contradictory. There is little change in solubility with temperature.

TABLE IV-2 (continued)

COMPOUND	REFERENCE	METHOD	T(°C)	K	DERIVED VALUES	REMARKS
16) $Ca(OH)_2(S)$	MA-003	Solubility Chem. Analysis	25 50	9.37×10^{-6} 5.68×10^{-6}	A = 530.49 B = -12.9722 C = 0.032331 D = -25.7085	The temperature range is 0-350°C.
17) $MgOH^+$	DA-003	Potentiometric Titration	25	2.6×10^{-3}		
	Radian Calc.	Fuoss Equation	55	1.64×10^{-3}	A = -518.0 D = -4.322 ΔH°_{298} = -2.37 kcal/mole	See text.
18) $MgSO_3^\circ$	Radian Detr.	See Text	25	1.2×10^{-3}	A = -432.5 D = -4.3715	No values found in literature.
	Radian Calc.	Fuoss Equation	40	1.0×10^{-3}		
19) $MgHCO_3^+$	HO-002	Potentiometric (pH)	25	1.1×10^{-1}		Agrees fairly well with the value calculated from data of (GR-002).
	Radian Calc.	Fuoss Equation	55	8.9×10^{-2}	A = -235.1 D = -1.747 ΔH°_{298} = -1.08 kcal/mole	See text.
20) $MgSO_4^\circ$	NA-001	Potentiometric	25 45	5.69×10^{-3} 3.20×10^{-3}	ΔH°_{298} = -4.84 kcal/mole	These values agree with those obtained from conductivity, ultrasonic, and solubility measurements.
21) $MgCO_3^\circ$	GA-002	Potentiometric Titration (pH)	25	4.0×10^{-4}		This is the only value corrected to zero ionic strength.
	Radian Calc.	Fuoss Equation	55	2.56×10^{-4}	A = -504.8 D = -5.091 ΔH°_{298} = -2.31 kcal/mole	See text.
22) $Mg(OH)_2(S)$	FE-001	Review of Literature	25	1.26×10^{-11}		These values are for the "stable" form of $Mg(OH)_2(S)$.
	GJ-001	Potentiometric			ΔH°_{298} = -2.2 kcal/mole	
23) $MgCO_3 \cdot 3H_2O(S)$	HA-001	Solubility	25 55	2.16×10^{-5} 1.10×10^{-5}	ΔH°_{298} = -4.37 kcal/mole	

TABLE IV-2 (continued)

COMPOUND	REFERENCE	METHOD	T(°C)	K	DERIVED VALUES	REMARKS
24) $NaOH^\circ$	GI-001	Potentiometric	25-45	3.7	$\Delta H^\circ_{298} \sim 0$	The K values given from 25-40°C are constant within experimental error.
25) $NaCO_3^-$	GA-002	Potentiometric Titration (pH)	25	5.4×10^{-2}		This is the only value found.
	Radian Calc.	Fuoss Equation	55	4.13×10^{-2}	A = -303.4 D = -2.285 ΔH°_{298} = -1.39 kcal/mole	See text.
26) $NaHCO_3^\circ$	GA-002	Potentiometric Titration (pH)	25	1.78		This value will be assumed temperature independent.
27) $NaSO_4^-$	JE-001	Conductivity	25	0.19		This value agrees with the earlier conductivity work of (DA-002).
	AU-001	Calorimetry	25		ΔH°_{298} = -1.1 kcal/mole A = -241 D = -1.529	
28) $NaNO_3^\circ$	RO-002	Conductivity	25	2.6		This is an average value. The range is 2.0-3.2. This value will be assumed temperature independent.
29) $SO_2(g) + H_2O \rightleftarrows H_2SO_3$	JO-001	Conductivity Chem. Analysis	25 50	1.23 0.56	ΔH°_{298} = -6.26 kcal/mole	The constants given are for P_{SO_2} in atm. The results show a Henry's law relationship from 2.7×10^{-4} - 1.3 atm SO_2.
30) $CO_2(g) + H_2O \rightleftarrows H_2CO_3$	HA-005	Solubility	25 50	3.44×10^{-2} 1.97×10^{-2}	ΔH°_{298} = -4.65 kcal/mole	The constants given are for P_{CO_2} in atm.

BLANK PAGE

TABLE IV-2 (continued) TEMPERATURE 25.000 DEGREES C

REACTANT	K(25 C)	K(TEMP)	EQUILIBRIUM CONSTANTS A	B	C	D
H2O	1.0129-14	1.0129-14	4.4710+03	0.0000	1.7060-02	6.0875+00
H2SO3	1.2957-02	1.2957-02	-8.4367+02	0.0000	0.0000	-4.7171+00
HSO3	6.2207-08	6.2207-08	-6.3384+02	0.0000	0.0000	-9.3320+00
HSO4	1.0396-02	1.0396-02	4.7514+02	0.0000	1.8222-02	5.0435+00
H2CO3	4.4513-07	4.4513-07	3.4047+03	0.0000	3.2786-02	1.4843+01
HCO3	4.6817-11	4.6817-11	2.9024+03	0.0000	2.3790-02	6.4980+00
CAOH+	4.2229-02	4.2229-02	-2.7300+02	0.0000	0.0000	-2.2900+00
CASO3	3.9999-04	3.9999-04	-5.0480+02	0.0000	0.0000	-5.0910+00
CACO3	6.2996-04	6.2996-04	-4.7548+02	0.0000	0.0000	-4.7954+00
CAHCO3+	5.5002-02	5.5002-02	-3.0185+02	0.0000	0.0000	-2.2720+00
CASO4	4.8969-03	4.8969-03	2.5721+03	2.3150+01	0.0000	6.3600+01
CANO3+	4.8485-01	4.8485-01	-1.2450+03	0.0000	0.0000	-4.4900+00
CACO3(S)	4.8695-09	4.8695-09	-1.6600+03	0.0000	0.0000	-1.3880+01
CASO4(S)	2.4000-05	2.4000-05	4.9440+03	3.7745+01	0.0000	1.0536+02
CASO3(S)	8.4004-08	8.4004-08	0.0000	0.0000	0.0000	-7.0757+00
CA(OH)2(S)	9.3440-06	9.3440-06	5.3049+02	-1.2972+01	3.2331-02	-2.5709+01
MGOH+	2.6001-03	2.6001-03	-5.1799+02	0.0000	0.0000	-4.3223+00
MGSO3	1.1997-03	1.1997-03	-4.3250+02	0.0000	0.0000	-4.3715+00
MGHCO3+	1.1001-01	1.1001-01	-2.3508+02	0.0000	0.0000	-1.7470+00
MGSO4	5.6636-03	5.6636-03	-1.0579+03	0.0000	0.0000	-5.7950+00
MGCO3	3.9999-04	3.9999-04	-5.0480+02	0.0000	0.0000	-5.0910+00
MG(OH)2(S)	1.2552-11	1.2552-11	-4.8085+02	0.0000	0.0000	-1.2514+01
MGCO3(S)	2.1500-05	2.1500-05	-9.5514+02	0.0000	0.0000	-7.8710+00
NAOH	3.7154+00	3.7154+00	0.0000	0.0000	0.0000	5.7000-01
NACO3-	5.4002-02	5.4002-02	-3.0341+02	0.0000	0.0000	-2.2852+00
NAHCO3	1.7783+00	1.7783+00	0.0000	0.0000	0.0000	2.5000-01
NASO4-	1.9024-01	1.9024-01	-2.4100+02	0.0000	0.0000	-1.5290+00
NANO3	2.5119+00	2.5119+00	0.0000	0.0000	0.0000	4.0000-01
PP(SO2)	1.2158+00	1.2158+00	-1.3700+03	0.0000	0.0000	-4.5100+00
PP(CO2)	3.4215-02	3.4215-02	-1.0150+03	0.0000	0.0000	-4.8700+00

HYDRATES IF PRECIPITATED ARE MGCO3•5H2O, MGSO3•6H2O, CASO3•(1/2)H2O, CASO4•2H2O

Preceding page blank

can be used to describe the temperature dependence. Calorimetry offers a more direct measurement, but the heat effects are generally small and care must be taken to isolate the heat of reaction from other possible sources.

The quality and form of data available for the temperature dependence of the equilibrium constants varied widely with the specific reaction concerned. For some reactions a four parameter equation was available, while for others there was no temperature dependence data available. The available and estimated data were all converted to a common form which could be used in computer calculations. This is given in Equation IV-8.

$$\log K_T = -A/T - B \log T - CT + D \qquad \text{(IV-8)}$$

This form results from the integration of Equation IV-7 with the assumption that the heat capacity of the solution is a linear function of T. The most common case was that only ΔH°_{298} was known, for which B = C = 0, and

$$A = \frac{\Delta H_{298}}{2.3026R} \qquad \text{(IV-9)}$$

$$D = \log K_{298} + A/298 \qquad \text{(IV-10)}$$

This form should be useful over a limited range of temperature (25-60°C).

The temperature dependence for ion-pairs or complexes for which an equilibrium constant was available at only one temperature was estimated using the Fuoss equation (FU-001) for the dissociation constant.

$$K = \frac{3000}{4\pi Na^3} \exp\left[\frac{-|z_1 z_2|\varepsilon^2}{aD^*kT}\right] \qquad \text{(IV-11)}$$

This equation was solved for "a", the center-to-center distance of the ions in a pair using the experimental value of K, the temperature T and dielectric constant D^*, at which it was measured. This equation has three roots, but only the intermediate value of "a" has any physical significance. This value of "a" was then used to calculate ΔH_T°.

$$\Delta H_T^\circ = R \frac{|z_1 z_2|\varepsilon^2}{akD^*}\left[1 + \frac{T}{D^*}\frac{\partial D^*}{\partial T}\right] \qquad \text{(IV-12)}$$

ΔH_{298}° was calculated and then used to calculate A and D from Equations IV-9 and IV-10. For $CaSO_4^\circ$ the calculated value of ΔH_{298}° was within 10% of the literature value.

The pertinent information for each compound is summarized in Table IV-2. The thermodynamic values listed are for the reactions as written in Table IV-4.

3. Activity Coefficients

a. Equation Form

For the chemical reaction of the form

$$eE + fF + \cdots \rightleftarrows xX + yY + \cdots \qquad \text{(IV-13)}$$

the equilibrium constant at constant temperature and pressure may be written

$$K = \frac{a_X^x a_Y^y \cdots}{a_E^e a_F^f \cdots} \qquad \text{(IV-14)}$$

where a_i is the activity of the $i^{\underline{th}}$ component. The activity may be related to the concentration of a component by the appropriate activity coefficient, γ_i.

$$a_i = \gamma_i M_i \qquad \text{(IV-15)}$$

In aqueous solutions it is convenient to adopt the convention that the activity coefficients of all components are unity at infinite dilution (standard state).

$$\lim_{M_i \to 0} \frac{a_i}{M_i} = 1 \qquad \text{(IV-16)}$$

A quantity which can be measured experimentally is the mean activity coefficient which can be written

$$\gamma_\pm = \left(\gamma_+^{v_+} \gamma_-^{v_-}\right)^{\frac{1}{v_+ + v_-}} \qquad \text{(IV-17)}$$

for an electrolyte which dissociates into v_+ cations and v_- anions per molecule of solute. In ionic equilibria, however, it is the individual ions which participate in chemical reactions and not the electrolyte as a compound. The multicomponent nature of the aqueous scrubbing solution also prohibits the use of mean activity coefficients.

Individual ion activity coefficients can be calculated from equations based on the Debye-Hückel theory. The derivation can be found in Harned and Owen (HA-002). The original Debye-Hückel limiting law is

$$\log \gamma_i = -Az_i^2 I^{\frac{1}{2}} \qquad \text{(IV-18)}$$

where A is a constant at a given temperature, z_i is the charge on the $i^{\underline{th}}$ ion, and I is the ionic strength.

$$I = \frac{1}{2} \sum_j M_j z_j^2 \qquad \text{(IV-19)}$$

The sum in Equation IV-19 is over all charged species. Equation III-18 is limited to very dilute solutions, I < 0.01. For more concentrated solutions, Equation IV-18 has been extended to

$$\log \gamma_i = \frac{-Az_i^2 I^{\frac{1}{2}}}{1 + B\mathring{a}_i I^{\frac{1}{2}}} \qquad \text{(IV-20)}$$

where B is a constant at a specified temperature and $\mathring{a}_i$ can be interpreted as the mean distance of closest approach of the ions in solution. The values of $\mathring{a}_i$ for many ions are tabulated by Klotz (KL-001). Another equation for γ_i takes a fixed value of 3Å for $\mathring{a}$ (so that $B\mathring{a}_i$ is unity) and contains a deviation parameter, b_i.

$$\log \gamma_i = Az_i^2 \left[\frac{-I^{\frac{1}{2}}}{1 + I^{\frac{1}{2}}} + b_i I\right] \qquad \text{(IV-21)}$$

Davies (DA-001) found empirically that b_i was 0.3 for many electrolytes. The additional linear term in Equation IV-21 provides a means of representing the experimentally observed reversal of slope and increase of the activity coefficient at relatively high ionic strengths. Equations III-20 and III-21 give good representation of γ_i up to I ~ 0.2 and may be used for practical calculations at higher values of I. In order to include the temperature variation of the B term and maintain generality, Equation IV-22 will be used for wet scrubber calculations.

$$\log \gamma_i = Az_i^2\left[\frac{-I^{\frac{1}{2}}}{1 + B\overset{\circ}{a}_i I^{\frac{1}{2}}} + b_i I\right] \qquad \text{(IV-22)}$$

Depending on the input values of $\overset{\circ}{a}_i$ and b_i, Equation IV-22 can represent either Equations IV-20 or IV-21 or an extension of the two.

The activity coefficients of the uncharged species are given to a good first approximation by the equation (HA-002)

$$\log \gamma_i = U_i I \qquad \text{(IV-23)}$$

in which U_i is an empirical constant. Values of $\overset{\circ}{a}_i$, b_i, and U_i are given in Table IV-3. The $\overset{\circ}{a}_i$ and b_i values were obtained either from Davies (DA-001), Klotz (KL-001), or Garrels' plots of γ_i vs. I (GA-003). Garrels calculated γ_i from experimental mean activity coefficients and the mean salt procedure which assumes $\gamma_{K+} = \gamma_{Cl-} = \gamma_{\pm KCl}$. This method is reported to give better results at high ionic strengths than the normal Debye-Hückel equations. The $\overset{\circ}{a}_i$ and b_i values were chosen so as to give a close fit to Garrels' results. There is little data available for the calculation of U_i. All uncharged species were assumed to behave like H_2CO_3 for which $U_i = 0.076$ (GA-003).

b. Temperature Dependence of Activity Coefficients

The temperature variations of activity coefficients is given by the equation

$$\frac{\partial \ln\gamma_i}{\partial T} = \frac{-\Delta H_i}{RT^2} \qquad \text{(IV-24)}$$

The enthalpy term is the difference between the partial molal enthalpy of the species at the ionic strength of interest and the partial molal enthalpy at infinite dilution. In view of

TABLE IV-3

ACTIVITY COEFFICIENT PARAMETERS

Species	$\mathring{a}_i$	b_i
H^+	6.0	0.4
Na^+	5.0	0.1
Ca^{++}	4.5	0.1
$SO_4^=$	3.0	0.0
Cl^-	4.0	0.0
NO_3^-	2.0	-0.2
$SO_3^=$	4.5	0.0
HSO_3^-	4.5	0.0
CO_3^-	4.5	0.0
HCO_3	4.5	0.0

All other charged species: $\mathring{a}_i = 3.0$; $b_i = 0.3$

All uncharged species: $U_i = 0.076$

All charged species: $U_i = 0.0$

the difficulty in determining these enthalpies, especially for single ions, the temperature variation predicted by the Debye-Hückel theory was used. For concentrations on a molar basis the constants A and B in Equation IV-22 are given by (HA-007)

$$A = \frac{1.8248\text{x}10^{6}}{\left(D^{*}T\right)^{3/2}} \left(\frac{\ell^{\frac{1}{2}}}{\text{mole}^{\frac{1}{2}}}\right) \qquad \text{(IV-25)}$$

$$B = \frac{50.292}{\left(D^{*}T\right)^{\frac{1}{2}}} \left(\frac{\ell^{\frac{1}{2}}}{\text{mole}^{\frac{1}{2}}\text{Å}}\right) \qquad \text{(IV-26)}$$

where D^{*} is the dielectric constant of water which decreases with temperature.

4. Oxidation Rate of Sulfite

The rate of oxidation of the sulfite ion in this system can strongly affect scaling problems because calcium sulfate is approximately 100 times more soluble than calcium sulfite. In addition the partial pressure of SO_2 over the solution is also affected. The oxidation of sulfite has been studied by several investigators. The reaction rate has been found to be dependent on pH, inhibitors, and catalysts such as Fe^{++}, Cu^{++}, Co^{++}, Ni^{++}, Mn^{++}, and nitrogen oxides. Figure IV-1 shows the results of Manvelyan (MA-005) and Figure IV-2 shows the catalytic effect of Co^{++} as published by Snavely and Blount (SN-001). Both groups of catalysts may be present in the scrubber solution. The heavy metal ions originate from soluble trace elements in the fly ash and the NO_x originates in the flue gas.

In spite of the great importance of the sulfite oxidation for the wet scrubbing process no experiments in the laboratory have been performed to establish the exact rate equations. The main reason for this is the fact that the nature and amount of catalysts present cannot be predicted without field experiments.

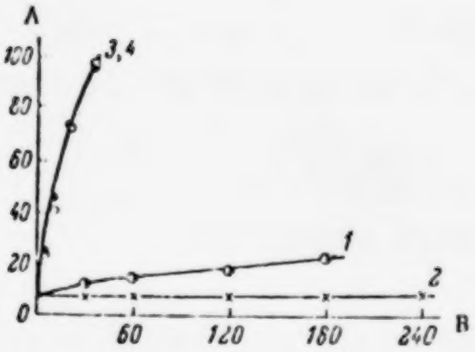

Effect of phenol on the degree of oxidation of magnesium sulfite to sulfate by atmospheric oxygen. A) Degree of oxidation (%); B) time (min). 1) Pure solution; 2) in presence of phenol; 3) in presence of NO and NO_2; 4) in presence of NO, NO_2, and phenol.

FIGURE IV-1

EFFECT OF INHIBITORS AND NO_x ON THE OXIDATION RATE OF SO_2

(MA-005)

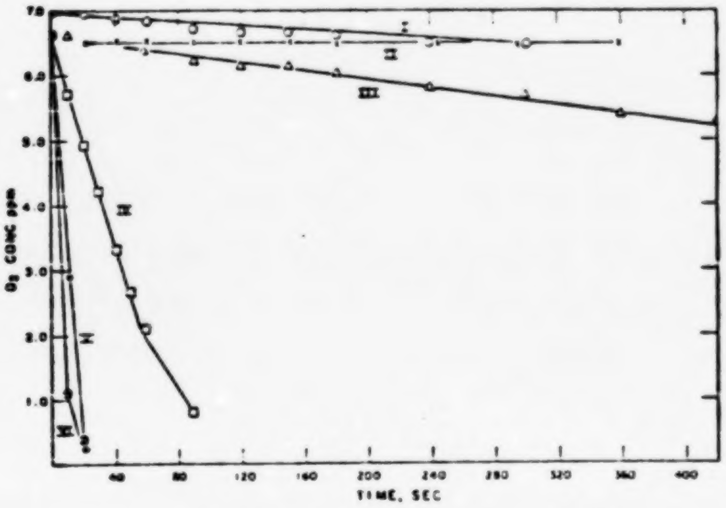

Reaction of dissolved oxygen with hydrogen sulfide and sodium sulfite in aqueous 3.5% sodium chloride solution at pH 6.2.

Curve	Scavenger	Catalyst
I	200 ppm H_2S	None
II	50 ppm Na_2SO_3	None
III	200 ppm H_2S + 50 ppm Na_2SO_3	None
IV	200 ppm H_2S + 50 ppm Na_2SO_3	5.0 ppm Co^{++}
V	200 ppm H_2S	5.0 ppm Co^{++}
VI	50 ppm Na_2SO_3	0.5 ppm Co^{++}

FIGURE IV-2

CATALYTIC EFFECT OF Co^{++} ON THE OXIDATION RATE OF SO_2

(SN-001)

B. IMPLEMENTATION

As mentioned earlier not all species listed in Table IV-1 were considered in the equilibrium program described in Section V.

The following simplifications were made.

1. Potassium and sodium were combined. Potassium present in actual cases can be converted into the equivalent amount of sodium. The error introduced by this is not too great. From the reactions:

$$NaSO_4^- \rightleftarrows Na^+ + SO_4^= \qquad \log K = -.72 \qquad (IV-27)$$

$$KSO_4^- \rightleftarrows K^+ + SO_4^= \qquad \log K = -.96 \qquad (IV-28)$$

$$NaNO_3 \rightleftarrows Na^+ + NO_3^- \qquad \log K = +0.4 \qquad (IV-29)$$

$$KNO_3 \rightleftarrows K^+ + NO_3^- \qquad \log K = +.24 \qquad (IV-30)$$

it can be seen that the complexes of the potassium and sodium compounds are moderately weak and of the same order of magnitude. Since the actual amounts of sodium and potassium will most probably not be accurately known, these two species were combined.

2. Nitrates and nitrites were combined. No dissociation constants for $CaNO_2^+$, $MgNO_2^+$, $NaNO_2$, and KNO_2 were found in the literature. Nitrite and sulfite are not stable in the presence of each other, at least not in acidic solutions (SE-004). Therefore the NO_x absorbed in the process was assumed to exist as NO_3^- or nitrate complexes.

3. Some complexes were disregarded. The K values for

$$HNO_3 \rightleftarrows H^+ + NO_3^- \qquad \log K = +1.38 \qquad \text{(IV-31)}$$

$$HCl \rightleftarrows H^+ + Cl^- \qquad \log K = +7 \qquad \text{(IV-32)}$$

indicated that HCl and HNO_3 would not appear in significant concentrations in the wet scrubbing process. The formation of $S_2O_5^=$ complex was very weak and would not be significant for this process. It was assumed that the solubility product for $MgSO_3$ would never be exceeded due to the extreme insolubility of $Mg(OH)_2$. Therefore the formation of solid magnesium sulfite was not considered.

4. Only the SO_2 and CO_2 gas-liquid equilibria were considered. The absorption of O_2 and NO_x involves non-equilibrium reactions.

These restrictions yielded the set of equations given in Table IV-4. The species considered are given in Table IV-5.

Equilibrium equations can be written for each of the reactions given in Table IV-4. In addition to the 30 equilibrium equations eight material balances were known.

$$\text{Total } Cl^- = (Cl^-) \qquad \text{(IV-33)}$$

$$\text{Total } SO_2 = (HSO_3^-) + (SO_3^=) + (H_2SO_3) + (CaSO_3) + (CaSO_{3\,solid}) + (MgSO_3) \qquad \text{(IV-34)}$$

$$\text{Total } CO_2 = (HCO_3^-) + (CO_3^=) + (H_2CO_3) + (CaCO_3) + (CaHCO_3^+) + (CaCO_{3\,solid}) + (MgHCO_3^+) + (MgCO_3) + (MgCO_{3\,solid}) + (NaCO_3^-) + (NaHCO_3) \qquad \text{(IV-35)}$$

TABLE IV-4

REACTIONS CONSIDERED

1) $H_2O \rightleftarrows H^+ + OH^-$

2) $HSO_3^- \rightleftarrows H^+ + SO_3^=$

3) $H_2SO_3 \rightleftarrows H^+ + HSO_3^-$

4) $HSO_4^- \rightleftarrows H^+ + SO_4^=$

5) $HCO_3^- \rightleftarrows H^+ + CO_3^=$

6) $H_2CO_3 \rightleftarrows H^+ + HCO_3^-$

7) $CaOH^+ \rightleftarrows Ca^{++} + OH^-$

8) $CaSO_3 \rightleftarrows Ca^{++} + SO_3^=$

9) $CaSO_4 \rightleftarrows Ca^{++} + SO_4^=$

10) $CaCO_3 \rightleftarrows Ca^{++} + CO_3^=$

11) $CaHCO_3^+ \rightleftarrows Ca^{++} + HCO_3^-$

12) $CaNO_3^+ \rightleftarrows Ca^{++} + NO_3^-$

13) $MgOH^+ \rightleftarrows Mg^{++} + OH^-$

14) $MgSO_3 \rightleftarrows Mg^{++} + SO_3^=$

15) $MgSO_4 \rightleftarrows Mg^{++} + SO_4^=$

16) $MgCO_3 \rightleftarrows Mg^{++} + CO_3^=$

17) $MgHCO_3^+ \rightleftarrows Mg^{++} + HCO_3^-$

18) $NaOH \rightleftarrows Na^+ + OH^-$

19) $NaSO_4^- \rightleftarrows Na^+ + SO_4^=$

20) $NaCO_3^- \rightleftarrows Na^+ + CO_3^=$

21) $NaHCO_3 \rightleftarrows Na^+ + HCO_3^-$

22) $NaNO_3 \rightleftarrows Na^+ + NO_3^-$

(continued)

TABLE IV-4 (continued)

LIQUID-SOLID EQUILIBRIA:

23) $CaCO_3(S) \rightleftarrows Ca^{++} + CO_3^{=}$

24) $CaSO_4(S) \rightleftarrows Ca^{++} + SO_4^{=}$

25) $CaSO_3(S) \rightleftarrows Ca^{++} + SO_3^{=}$

26) $Ca(OH)_2(S) \rightleftarrows Ca^{++} + 2OH^-$

27) $Mg(OH)_2(S) \rightleftarrows Mg^{++} + 2OH^-$

28) $MgCO_3(S) \rightleftarrows Mg^{++} + CO_3^{=}$

GAS-LIQUID EQUILIBRIA

29) $SO_2(g) + H_2O \rightleftarrows H_2SO_3$

30) $CO_2(g) + H_2O \rightleftarrows H_2CO_3$

TABLE IV-5

SPECIES CONSIDERED

1. H^+
2. OH^-
3. HSO_3^-
4. $SO_3^=$
5. H_2SO_3
6. HSO_4^-
7. $SO_4^=$
8. HCO_3^-
9. $CO_3^=$
10. H_2CO_3
11. $CaOH^+$
12. Ca^{++}
13. $CaSO_3$
14. $CaSO_4$
15. $CaCO_3$
16. $CaHCO_3^+$
17. $CaNO_3^+$
18. NO_3^-
19. $MgOH^+$
20. Mg^{++}
21. $MgSO_3$
22. $MgSO_4$
23. $MgCO_3$
24. $MgHCO_3^+$
25. $NaOH$
26. Na^+
27. $NaSO_4^-$
28. $NaCO_3^-$
29. $NaHCO_3$
30. $NaNO_3$
31. Cl^- (forms no complex)
32. $CaCO_3$ solid
33. $CaSO_4$ solid
34. $CaSO_3$ solid
35. $Ca(OH)_2$ solid
36. $Mg(OH)_2$ solid
37. $MgCO_3$ solid
38. SO_2 gas
39. CO_2 gas

$$\text{Total } SO_4^= = (SO_4^=) + (HSO_4^-) + (CaSO_4) + (CaSO_{4\,solid}) + (NaSO_4^-) + (MgSO_4) \qquad \text{(IV-36)}$$

$$\text{Total } NO_3^- = (NO_3^=) + (CaNO_3^+) + (NaNO_3) \qquad \text{(IV-37)}$$

$$\begin{aligned}\text{Total } Ca^{++} = {} & (Ca^{++}) + (CaOH^+) + (CaSO_3) + (CaCO_3) \\ & + (CaHCO_3^+) + (CaSO_4) + (CaNO_3^+) \\ & + (CaCO_{3\,solid}) + (CaSO_{4\,solid}) \\ & + (CaSO_{3\,solid}) + (Ca(OH)_{2\,solid}) \qquad \text{(IV-38)}\end{aligned}$$

$$\begin{aligned}\text{Total } Mg^{++} = {} & (Mg^{++}) + (MgOH^+) + (MgSO_3) + (MgHCO_3^+) \\ & + (MgSO_4) + (MgCO_3) + (Mg(OH)_{2\,solid}) \\ & + (MgCO_{3\,solid}) \qquad \text{(IV-39)}\end{aligned}$$

$$\begin{aligned}\text{Total } Na^+ = {} & (Na^+) + (NaOH) + (NaCO_3^-) + (NaHCO_3) \\ & + (NaSO_4^-) + (NaNO_3) \qquad \text{(IV-40)}\end{aligned}$$

Equation III-41 can be derived from the electroneutrality condition.

$$\begin{aligned}0 = {} & (H^+) + 2(Ca^{++}) + (CaOH^+) + (CaHCO_3^+) + (CaNO_3^+) \\ & + 2(Mg^{++}) + (MgHCO_3^+) + (Na^+) - (OH^-) - (HSO_3^-) - 2(SO_3^=) \\ & - 2(SO_4^=) - (HCO_3^-) - 2(CO_3^=) - (NO_3^-) - (HSO_4^-) \\ & - (NaCO_3^-) - (NaSO_4^-) - (Cl^-) \qquad \text{(IV-41)}\end{aligned}$$

This set of 39 equations with 39 unknowns can be solved by the computer program given a temperature and given the following eight key species in solution.

Total Cl^-
Total $SO_4^=$
Total NO_3^-
Total Ca^{++}
Total Mg^{++}
Total Na^+
Total SO_2
Total CO_2

As an alternate input, the partial pressures of SO_2 and/or CO_2 may be specified instead of the total amount(s) of SO_2 and/or CO_2 in solution. This utilizes the gas-liquid equilibria of Equations IV-42 and 43.

$$CO_{2\,gas} + H_2O \rightleftarrows H_2CO_3 \qquad \text{(IV-42)}$$

$$SO_{2\,gas} + H_2O \rightleftarrows H_2SO_3 \qquad \text{(IV-43)}$$

In wet scrubbing units using recycled fluids or slurries as sorbent, the content of soluble salts may build up. The activities of the species present in solution must be considered in solving the above set of equations. Individual activity coefficients based upon total ionic strength were calculated using Equation IV-44.

$$\log \gamma_i = Az_i^2 \frac{-I^{\frac{1}{2}}}{1 + B\mathring{a}_i I^{\frac{1}{2}}} + b_i I + U_i I \qquad \text{(IV-44)}$$

Table IV-3 summarizes the $\mathring{a}_i$, b_i, and U_i values for the species in solution. U_i is zero for charged species thus yielding Equation IV-22 and z_i is zero for uncharged species yielding Equation IV-23. These equations are solved using the equilibrium constants and activity coefficients at the temperature in question.

C. EXPERIMENTAL WORK

The dissociation constants and the solubility products of $CaSO_3$ and $MgSO_3$ are key parameters for the theoretical description of the wet scrubbing process. The literature search revealed, however, that no values for the dissociation constants were published. From the methods described in Section IV-A-2-a, the use of ion sensitive electrodes was selected for their determination. One difficulty encountered in the determination of these constants was the oxidation of sulfite to sulfate.

1. Theory

The data reported here are based on two assumptions.

1. The divalent electrode model 92-32 (ORION) shows no sulfite interference.

2. The strongest complex between Mg^{++} and $SO_3^=$ ions is $MgSO_3$. The strongest complex between Ca^{++} and $SO_3^=$ is $CaSO_3$.

The second assumption is supported by the analogy with the behavior of $MgSO_4$, $CaSO_4$, $MgCO_3$, and $CaCO_3$. The dissociation constants for the carbonate complexes at 25°C are:

$$K = \frac{a_{Mg^{++}} \cdot a_{CO_3^=}}{a_{MgCO_3}} = 4.0 \times 10^{-4} \qquad \text{(IV-45)}$$

$$K = \frac{a_{Mg^{++}} \cdot a_{HCO_3^-}}{a_{MgHCO_3^+}} = 1.1 \times 10^{-1} \qquad \text{(IV-46)}$$

$$K = \frac{a_{Ca^{++}} \cdot a_{CO_3^=}}{a_{CaCO_3}} = 6.3 \times 10^{-4} \qquad \text{(IV-47)}$$

$$K = \frac{a_{Ca^{++}} \cdot a_{HCO_3^-}}{a_{CaHCO_3^+}} = 5.5 \times 10^{-2} \qquad \text{(IV-48)}$$

The dissociation constants for the neutral complexes $MeCO_3$ are two to three orders of magnitude smaller than those for the $MeHCO_3^+$ complexes. For calcium and magnesium sulfate the only complexes reported are $CaSO_4$ and $MgSO_4$. It was therefore assumed that in the calcium and magnesium sulfite system the strongest complexes formed are $MgSO_3$ and $CaSO_3$.

In some of the tests the sulfites were prepared by adding Ca (or Mg) chloride solutions to a potassium sulfite solution. Considering potential sulfite oxidation, we have the following key species in the system: SO_2, $SO_4^=$, Cl^-, K^+, and Ca^{++} (or Mg^{++}).

The description of the aqueous phase must therefore consider the following equilibria.

$$K_1 = \frac{a_{Me^{++}} \cdot a_{SO_3^=}}{a_{MeSO_3}} \quad (Me = Ca \text{ or } Mg) \qquad (IV\text{-}49)$$

$$K_2 = \frac{a_{H^+} \cdot a_{HSO_3^-}}{a_{H_2SO_3}} \qquad (IV\text{-}50)$$

$$K_3 = \frac{a_{H^+} \cdot a_{SO_3^=}}{HSO_3^-} \qquad (IV\text{-}51)$$

$$K_4 = \frac{a_{Me^{++}} \cdot a_{SO_4^=}}{a_{MeSO_4}} \qquad (IV\text{-}52)$$

$$K_5 = \frac{a_{K^+} \cdot a_{SO_4^=}}{a_{KSO_4^-}} \qquad (IV\text{-}53)$$

$$K_6 = \frac{a_{H^+} \cdot a_{SO_4^=}}{a_{HSO_4^-}} \qquad (IV\text{-}54)$$

$$K_w = a_{H^+} \cdot a_{OH^-} \qquad \text{(IV-55)}$$

Chloride was assumed to form no complexes.

In case $a_{Me^{++}}$ is measured with a cation electrode the system comprises the following unknowns.

1. K_1
2. $a_{SO_3^=}$
3. a_{MeSO_3}
4. $a_{HSO_3^-}$
5. $a_{H_2SO_3}$
6. $a_{SO_4^=}$
7. $a_{HSO_4^-}$
8. a_{MeSO_4} (Me = Ca or Mg)
9. a_{OH^-}
10. $a_{KSO_4^-}$
11. a_{K^+}
12. Cl^-
13. a_{H^+}

The additional six equations needed to determine these unknowns can be established by the material balances for the five key species in solution and the electroneutrality condition.

The means of determining the unknown dissociation constants consisted of the following steps.

a. Determine $a_{Me^{++}}$ with a cation sensitive electrode.

b. Determine by chemical analysis total SO_2 and total Ca^{++}(Mg^{++}) in the solution.

c. Total $K^+$and Cl^- are known from the solution preparation. Total sulfate was calculated as the difference between total Ca^{++}(Mg^{++}) and total SO_2.

d. K_1 was taken as the value that minimized the relative deviation of measured and calculated values of $a_{Me^{++}}$

2. Activity Measurements

In most of the experiments the divalent cation electrode model 92-32 from ORION was used. In some cases the calcium ion electrode model 92-20 was applied.

The divalent cation electrode measures only the activity of the ionized and unbound divalent cations in solution. Errors can be caused by monovalent cations, if they are present in high concentration. The potential of the electrode in a solution containing Ca, Mg, and sodium is given by:

$$E = E_o + 2.3 \frac{RT}{2F} \log a_{Ca^{++}} + a_{Mg^{++}} + .15\, a^2_{Na^+} \qquad \text{(IV-56)}$$

Table IV-6 shows the errors introduced by the presence of sodium ions. The selectivity for potassium is slightly lower. The pH of the solution was in the range where the electrode potential was independent of pH (see Figure IV-3).

Perchlorate and iodide salts are reported to show interference when the calcium ion electrode is used. No anion interference is reported for the divalent electrode.

The potential of the ion sensitive electrodes was measured with a Beckman Century SS pH meter using a saturated calomel electrode as a reference. For the calibration of the electrode system $CaCl_2$ solutions of known $CaCl_2$ content were used. Calcium activities were calculated using Equation IV-22 with $\overset{\circ}{a}_i = 4.5$ and $b_i = 0.1$.

TABLE IV-6

DIVALENT ELECTRODE INTERFERENCES (OR-001)

levels of sodium ion producing 1% and 10% errors in the electrode response to calcium and magnesium ions

Activity of Ca^{++} and Mg^{++} (M)	Na^{+} (M) for 1% Error	Na^{+} (M) for 10% Error
10^{-1}	8.1×10^{-2}	0.26
10^{-2}	2.6×10^{-2}	8.1×10^{-2}
10^{-3}	8.1×10^{-3}	2.6×10^{-2}
10^{-4}	2.6×10^{-3}	8.1×10^{-3}
10^{-5}	8.1×10^{-4}	2.6×10^{-3}
10^{-6}	2.6×10^{-4}	8.1×10^{-4}
10^{-7}	8.1×10^{-5}	2.6×10^{-4}
10^{-8}	2.6×10^{-5}	8.1×10^{-5}

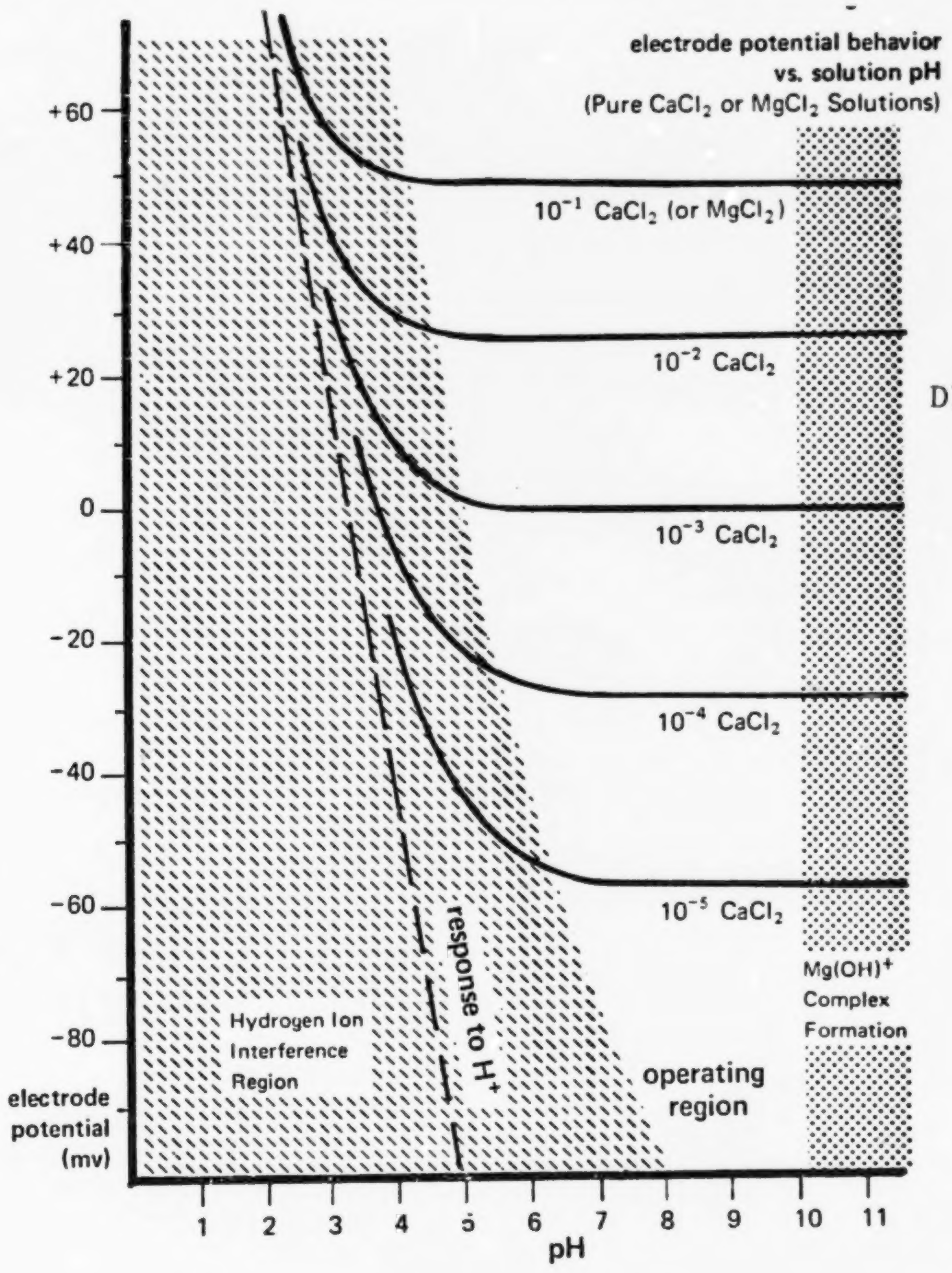

FIGURE IV-3

DIVALENT ELECTRODE pH INFLUENCE

(OR-001)

3. Experimental Procedures

The determinations necessary to calculate the missing constants would naturally be simpler if pure $CaSO_3$ and $MgSO_3$ solutions could be investigated. However, all of the preparation methods described in Gmelin are reported to always yield a certain fraction of sulfate. Therefore, possible sulfate complexes were considered. The next difficulty encountered was the fact that neither reagent grade $CaSO_3$ nor $MgSO_3$ were available commercially. Only $CaSO_3$ in a purified form was available from City Chemical Corporation, New York.

a. Dissociation Constants

The sulfite solutions were therefore made by mixing $CaCl_2$ or $MgCl_2$ solutions with solid potassium sulfite. K_2SO_3, $CaCl_2$, and $MgCl_2$ were available as reagent grade chemicals from Baker or Fisher. Since it was found that supersaturated $CaSO_3$ solutions are very stable, the measurements to determine the $CaSO_3$ dissociation constant were performed in the supersaturated region. For the analytical methods used this increased the accuracy of characterizing the aqueous system. In addition it had the advantage that the activity measurements with ion sensitive electrodes in more concentrated solutions yielded quicker response times and more stable end potentials.

The determinations were performed in a five necked, one liter, round bottom flask. At the beginning, 500 ml of $CaCl_2$ solution of known $CaCl_2$ content was added. The solution was deaerated for about one-half hour by bubbling through it nitrogen saturated with H_2O. After the deaeration, the calcium activity and the pH were measured. Then a known amount of solid K_2SO_3 was added and dissolved by stirring with a magnetic stirrer. The solution was kept under a nitrogen blanket during this procedure. The calcium activity and the pH were determined again.

For the determination of total sulfite in solution, the method described in the ASTM designation D 1339-62T was used. The solution was fixed directly in the five necked flask by adding the KI, HCl, and KIO_3 solutions. This avoided any oxidation which might have had occurred using other sampling techniques. The iodide content of the fixed solution was determined using the dead stop technique as described in the designation D 1339-62T. The determination of the sulfate content in the solution was based on the assumption that the reagent grade K_2SO_3 used was sulfate free. It was assumed that sulfate was formed by oxidation in solution which was caused by residual oxygen. The sulfate content was then calculated as the difference between the moles of K_2SO_3 added to the solution and the SO_3 content.

Another limiting case, namely that no oxidation occurred in the solution and the sulfate in solution was present as an impurity in the solid K_2SO_3, was also considered. This assumption slightly changes the total potassium and total sulfate content. This slight deviation had no influence on the calculated dissociation constant. The actual case that sulfate was present in the original K_2SO_3 and formed by oxidation lies between these limiting cases. Results obtained using the two limiting cases are given in Section IV-D-4. The constant for $MgSO_3$ was determined the same way using $MgCl_2$ instead of $CaCl_2$. The experimental results are reported in Section IV-D-4.

b. Solubility Product Constants

The next task was the determination of the solubility products. Theoretically the only values necessary for their determination are the solubilities and the dissociation constants. The literature shows no contradiction in the solubility of $MgSO_3$. The accepted value was 0.646 weight % (as $MgSO_3$) at 25°C as reported by Gmelin and measured by Hagisawa in agreement with the value found by Murasawa (GM-002). The solubility for $CaSO_3$ was quite unsure. The 1961 edition of Gmelin accepted the values of Weisberg (WE-001) and van der Linden (LI-001). Weisberg reports the solubility of $CaSO_3$ to be 43 mg/ltr at 18°C and van der Linden gives a value of 46.3 mg/ltr at 30°C. Wurz and Swoboda (WU-001) as well as J. Robart published values greater by a factor of two (RO-003). These contradictory results necessitated a redetermination of the solubility of $CaSO_3$.

Since preliminary tests showed that solutions prepared by the commercially available $CaSO_3$ and deaerated water had not reached equilibrium even after stirring for several days, it was decided to approach the equilibrium value from the unsaturated as well as from the supersaturated direction thus excluding any doubts as to whether the solutions were in equilibrium.

The first approach was achieved by adding more than the necessary amount of solid $CaSO_3$ to deaerated water and stirring the solution in a closed container for about a week. The approach from the supersaturated side was achieved in the following way. Equivalent amounts of $CaCl_2$ and K_2SO_3 were added in excess to deaerated water and the solution was seeded with $CaSO_3$ crystals. The numerical results of these tests are given in Section IV-D. Since in both approaches the commercially available $CaSO_3$ was used, X-ray diffraction was applied to determine the hydration state of the calcium sulfite present as solid.

Figure IV-4 shows the diffraction pattern in the region $2\theta = 16°-54°$. The X-ray analysis shows that the calcium sulfite contained appreciable amounts of $CaSO_4$. The hydration states of calcium sulfite is $CaSO_3 \cdot \frac{1}{2}H_2O$ and of calcium sulfate $CaSO_4 \cdot 2H_2O$. For the sulfite determination, the method described in the ASTM designation D 1339-62T was used. Total Ca^{++} was measured by potentiometric titration using the calcium sensitive electrode and EDTA as complexing agent.

In the experiment where the equilibrium was reached from the supersaturated side the total Cl^- and total K^+ are known from the way the solution was made up. In this case equivalent amounts of $CaCl_2$ and K_2SO_3 were used. The calcium and the sulfite content were determined experimentally and moles of sulfate were calculated as the difference of the total moles of calcium and the total moles of sulfite.

In the experiments where the equilibrium was reached from the unsaturated side the total calcium and total sulfite content were determined using the described techniques. Sulfate was calculated by difference between total calcium and total sulfite.

D. RESULTS OF THE EXPERIMENTAL PROGRAM

The results of the experimental program to determine or verify the unknown or uncertain chemical equilibrium constants necessary to characterize the aqueous scrubbing system are given in this section. The following determinations were made for the systems indicated:

FIGURE IV-4 - X-RAY DIFFRACTION PATTERN OF CALCIUM SULFITE

CrK$_\alpha$, full scale 2x10^4 Imp/Min

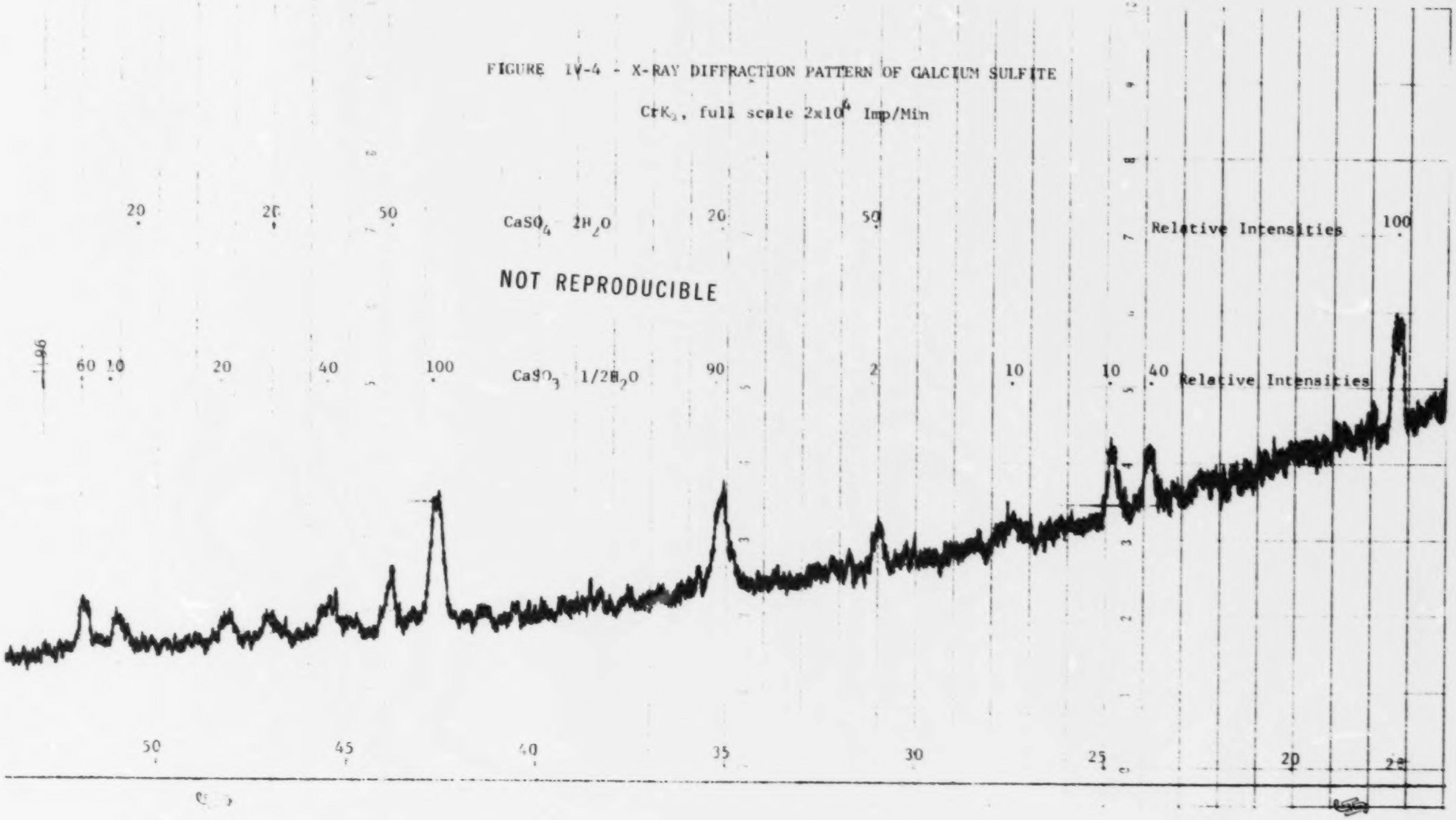

NOT REPRODUCIBLE

1. $CaSO_4$ System:	Verification of experimental procedure by redetermination of dissociation constant; resolution of conflicting values of the solubility product at 25°C.
2. $CaNO_3^+$ System:	Verification of literature dissociation constant.
3. $CaSO_3$ System:	Determination of dissociation constant and solubility product.
4. $MgSO_3$ System:	Determination of dissociation constant and calculation of solubility product.

In addition the temperature dependence of the $CaSO_3^\circ$ and $MgSO_3^\circ$ dissociation constants was calculated using the experimentally determined K_D values and the extrapolation method described in Section IV-A-2-c. The results are given and discussed below.

1. $CaSO_4$ Equilibria

The experimental procedure was checked by redetermining the dissociation constant of $CaSO_4^\circ$ and solubility product of $CaSO_4 \cdot 2H_2O$ at 25°C. The dissociation constant of $CaSO_4^\circ$ is known fairly accurately. There is some disagreement as to the value of the solubility product. The Ca^{++} activity of a solution saturated with $CaSO_4 \cdot 2H_2O$ was measured using Orion Ca^{++} and divalent ion sensitive electrodes. The electrodes were calibrated with standard $CaCl_2$ solutions. Computer calculations showed that the atmospheric partial pressure of CO_2 had negligible effect on the Ca^{++} activity of the $CaCl_2$ standard solutions. Further calculations showed that the unexpectedly high pH (~9) of the $CaSO_4$ solution was probably caused by the small amount of carbonate impurity present in the starting material. The Ca^{++} activity was unaffected by this impurity. The total Ca^{++} concentration, or solubility, was found to be 0.0154 mole/ℓ, in agreement with the value obtained by Marshall (MA-002). Since only $CaSO_4 \cdot 2H_2O$ was added to the solution, the total sulfate concentration is also 0.0154 mole/ℓ. A calculation using these two inputs and a value of 4.9×10^{-3} for the dissociation constant yielded a Ca^{++} activity nearly identical to the average value obtained using the two electrodes (5.1×10^{-3} mole/ℓ). This measurement verifies the $CaSO_4$ dissociation constant given in Table IV-2. A computer printout for the system is given in Table IV-7.

The solubility product was calculated from the computed Ca^{++} and $SO_4^{=}$ activities.

$$K_{sp} = a_{Ca^{++}} a_{SO_4^{=}} \tag{IV-57}$$

The calculated solubility product constant (2.41×10^{-5}) shows much better agreement with the values 2.4×10^{-5} and 2.5×10^{-5} given by Latimer (LA-001) and Nakayama and Resnick (NA-002) than with the values given by Marshall (MA-002). Marshall originally published a value of 4.23×10^{-5} and later (MA-004) of 3.03×10^{-5}. A value of 2.4×10^{-5} was accepted.

2. $CaNO_3^+$ Equilibria

Although the $CaNO_3^+$ ion pair is weakly associated, computer calculations showed that significant amounts of $CaNO_3^+$ can be formed at the high NO_3^- and Ca^{++} concentrations found in certain process models. The $CaNO_3^+$ dissociation constant was checked by making up solutions containing known amounts of $Ca(NO_3)_2 \cdot 4H_2O$ and measuring the Ca^{++} activity of these solutions. The measured activities agree with the computer calculated values within the

TABLE IV-7 - SATURATED $CaSO_4 \cdot 2H_2O$ SOLUTION AT 25°C

```
                          INPUT CONCENTRATIONS (MOLES/LITER)

SO4--=1.54000-02     NO3-  =0.00000          CA++ =1.54000-02     MG++ =0.00000
NA+  =0.00000        CL-   =0.00000
SO2  =0.00000
CO2  =0.00000

                               AQUEOUS SOLUTION EQUILIBRIA

        COMPONENT        CONCENTRATION          ACTIVITY          ACTIVITY COEFFICIENT
        H+                 1.041-07             8.944-08               8.589-01
        OH-                1.364-07             1.133-07               8.303-01
        SO4--              1.052-02             4.710-03               4.477-01
        HSO4-              4.880-08             4.052-08               8.303-01
        CA++               1.052-02             5.113-03               4.861-01
        CAOH+              1.652-08             1.371-08               8.303-01
        CASO4              4.881-03             4.918-03               1.007+00

          PH =         7.048           IONIC STRENGTH = 4.20742-02            RES. E.N. =  -2.119-10
```

limits obtained by assuming a ±1 mV error in the potential measurements. The results are given in Table IV-8. Therefore the value given in Table IV-2 is acceptable.

3. $CaSO_3$ Equilibria

The $CaSO_3^\circ$ dissociation constant was obtained from measurements of the Ca^{++} ion activity in a solution containing Ca^{++}, $SO_3^=$, $SO_4^=$, K^+, and Cl^- as the key species. Table IV-9 gives the total amounts of the five key species and the measured Ca^{++} ion activities for the four determinations.

K_D was determined by a trial and error procedure. A trial value of K_D and the total amounts of the five key species were input to the chemical equilibrium computer program. The computer calculated Ca^{++} activity was compared to the measured value to obtain a better approximation to K_D and the calculation process was repeated. The average relative deviation from the measured Ca^{++} activity, d, was calculated for each trial value of K_D.

$$d = \frac{1}{N} \sum_{i=1}^{N} \frac{|a_{c_i} - a_{m_i}|}{a_{m_i}} \qquad \text{(IV-58)}$$

In Equation IV-58, a_{c_i} is the calculated Ca^{++} activity, a_{m_i} is the measured Ca^{++} activity, and N is the number of measurements (four in this case). The plot of d vs. K_D has a minimum at $K_D = 4.0 \times 10^{-4}$ (Figure IV-5). This is the accepted value of K_D for $CaSO_3^\circ$. The Ca^{++} activities calculated using this value of K_D are given in Table IV-9. A typical computer output giving the species distribution is given in Table IV-10. The constants for potassium were substituted for those of sodium for these calculations.

TABLE IV-8

CALCIUM ACTIVITY IN CALCIUM NITRATE SOLUTIONS

Case	Total Calcium Concentration mole/ℓ	Measured Ca^{++} Activity	Calculated Ca^{++} Activity
1	1.585x10^{-3}	1.1 (±0.1) x10^{-3}	1.18x10^{-3}
2	2.51x10^{-3}	1.8 (±0.15) x10^{-3}	1.74x10^{-3}
3	2.55x10^{-2}	1.1 (±0.1) x 10^{-2}	1.02x10^{-2}
4	1.99x10^{-1}	4.6 (±0.3) x 10^{-2}	4.33x10^{-2}

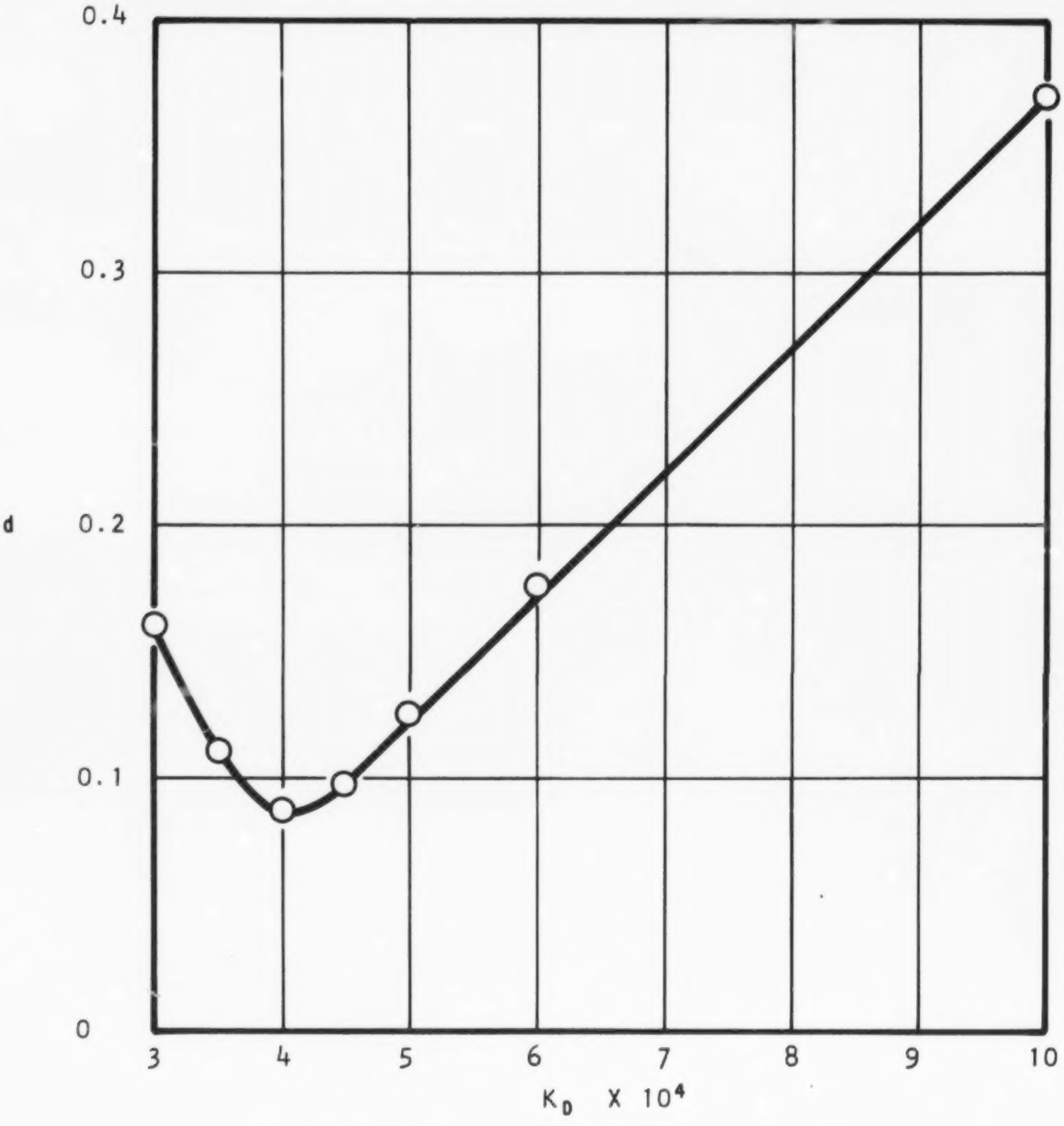

FIGURE IV-5 RELATIVE DEVIATION OF CALCULATED Ca^{++} ACTIVITY VS TRIAL DISSOCIATION CONSTANT

TABLE IV-9

RESULTS OF THE $CaSO_3^\circ$ DISSOCIATION CONSTANT DETERMINATION

	Total Concentrations (mole/ℓ)						
Case	(Ca^{++})	(SO_2)	$(SO_4^=)$	(K^+)	(Cl^-)	Measured Calcium Activity	Calculated Calcium Activity*
1	1.99×10^{-3}	1.86×10^{-3}	1.4×10^{-4}	4.00×10^{-3}	3.98×10^{-3}	6.5×10^{-4}	6.8×10^{-4}
2	3.98×10^{-3}	9.38×10^{-4}	6.4×10^{-5}	2.00×10^{-3}	7.96×10^{-3}	1.8×10^{-3}	2.1×10^{-3}
3	9.95×10^{-4}	1.90×10^{-3}	1.49×10^{-4}	4.10×10^{-3}	1.99×10^{-3}	3.1×10^{-4}	2.7×10^{-4}
4	3.98×10^{-4}	1.90×10^{-3}	1.27×10^{-4}	4.03×10^{-3}	7.96×10^{-4}	9.3×10^{-5}	9.3×10^{-5}

* Calculated using $K_D(CaSO_3^\circ) = 4.0 \times 10^{-4}$

TABLE IV-10

CHEMICAL EQUILIBRIA FOR CASE 3 OF $CaSO_3^\circ$ EQUILIBRIUM CONSTANT DETERMINATION USING K_D = $4.0x10^{-4}$

```
                          INPUT  CONCENTRATIONS  (MOLES/LITER)

SO4--=1.49000-04     NO3-  =0.00000          CA++  =9.95000-04     MG++  =0.00000
NA+  =4.09500-03     CL-   =1.99000-03
SO2  =1.89800-03
CO2  =0.00000
                              AQUEOUS SOLUTION EQUILIBRIA

          COMPONENT        CONCENTRATION          ACTIVITY         ACTIVITY COEFFICIENT
          H+                  8.745-10           8.076-10              9.235-01
          OH-                 1.368-05           1.254-05              9.171-01
          HSO3-               1.278-05           1.172-05              9.171-01
          SO3--               1.276-03           9.025-04              7.075-01
          SO4--               1.396-04           9.783-05              7.009-01
          HSO4-               8.287-12           7.601-12              9.171-01
          H2SO3               7.295-13           7.304-13              1.001+00
          CA++                3.799-04           2.705-04              7.121-01
          CAOH+               8.761-08           8.035-08              9.171-01
          CASO3               6.096-04           6.103-04              1.001+00
          CASO4               5.398-06           5.405-06              1.001+00
          NA+                 4.091-03           3.762-03              9.195-01
          NAOH                1.269-08           1.270-08              1.001+00
          NASO4-              4.013-06           3.680-06              9.171-01
          CL-                 1.990-03           1.825-03              9.169-01
PSO2 =6.00758-13   ATM.

            PH =       9.093          IONIC STRENGTH = 6.64620-03          RES. E.N. =  -2.593-05
```

The $CaSO_3 \cdot \frac{1}{2}H_2O$ solubility product was obtained from measurements in which the solid-liquid equilibrium was approached from both the supersaturated and subsaturated regions. The calcium sulfite solid used here was shown to be $CaSO_3 \cdot \frac{1}{2}H_2O$ by X-ray diffraction measurements. These measurements also showed that it contained considerable amounts of $CaSO_4 \cdot 2H_2O$. The equilibrium total amounts of the key species for the three measurements are given in Table IV-11. These values were input to the chemical equilibrium program and the equilibrium distribution of the species was calculated using the experimentally determined K_D value for $CaSO_3$ ($4.0x10^{-4}$). The solubility product was then calculated from the computed Ca^{++} and $SO_3^=$ activities.

$$K_{sp} = a_{Ca^{++}} a_{SO_3^=} \qquad (IV-59)$$

The average value obtained for K_{sp} is $8.4x10^{-8}$. The K_{sp} values obtained for each measurement and the percent deviations from the mean are given in Table IV-11.

4. $MgSO_3$ Equilibria

The dissociation constant of $MgSO_3^\circ$ was obtained in a manner analogous to that for $CaSO_3^\circ$. The total amounts of the key species and the measured Mg^{++} activities for the three measurements are given in Table IV-12. The best value of K_D is $1.2x10^{-3}$ for $MgSO_3^\circ$. The Mg^{++} activities calculated using this value of K_D are given in Table IV-12. Table IV-13 is a computer printout for Case 2 assuming sulfite oxidation occurred in solution. This was the usual assumption. Table IV-14 is a computer printout for Case 2 assuming no oxidation in solution. The difference between these two is negligible.

TABLE IV-11

RESULTS OF THE $CaSO_3 \cdot \frac{1}{2}H_2O$ SOLUBILITY PRODUCT DETERMINATION

	Total Concentrations (mole/ℓ)						
Case	(Ca^{++})	(SO_2)	$(SO_4^{=})$	(K^+)	(Cl^-)	Calculated Solubility Product	% Deviation From Mean
1	9.88×10^{-4}	5.52×10^{-4}	4.36×10^{-4}	0	0	9.13×10^{-8}	+8.7
2	1.47×10^{-3}	3.00×10^{-4}	1.17×10^{-3}	0	0	7.31×10^{-8}	-12.9
3	1.18×10^{-3}	4.11×10^{-4}	7.69×10^{-4}	2.82×10^{-3}	2.82×10^{-3}	8.75×10^{-8}	+4.2

In the cases 1 and 2 equilibrium was reached from the unsaturated side.

In case 3 equilibrium was reached from the supersaturated side.

TABLE IV-12

RESULTS OF THE $MgSO_3^\circ$ DISSOCIATION CONSTANT DETERMINATION

Case	Total Concentrations (mole/ℓ) (Mg^{++})	(SO_2)	$(SO_4^=)$	(K^+)	(Cl^-)	Measured Mg^{++} Activity	Calculated Mg^{++} Activity[1]
1	9.90×10^{-4}	1.93×10^{-3}	9.0×10^{-5}	4.03×10^{-3}	1.98×10^{-3}	4.2×10^{-4}	4.2×10^{-4}
2a[2]	9.90×10^{-4}	2.35×10^{-3}	1.84×10^{-4}	5.07×10^{-3}	1.98×10^{-3}	3.8×10^{-4}	3.8×10^{-4}
2b[3]	9.90×10^{-4}	2.35×10^{-3}	1.67×10^{-4}	5.04×10^{-3}	1.98×10^{-3}	3.8×10^{-4}	3.8×10^{-4}
3	9.90×10^{-4}	1.90×10^{-3}	1.33×10^{-4}	4.07×10^{-3}	1.98×10^{-3}	4.2×10^{-4}	4.2×10^{-4}

1. Calculated using $K_D(MgSO_3^\circ) = 1.2 \times 10^{-3}$

2. Total K and SO_4 concentrations calculated assuming oxidation occurred in solution

3. Total K and SO_4 concentrations calculated assuming no oxidation in solution.

TABLE IV-13 - CHEMICAL EQUILIBRIA FOR CASE 2 OF $MgSO_3^o$ K_o DETERMINATION USING $K_o = 1.2x10^{-3}$ AND ASSUMING SULFITE OXIDIZED IN SOLUTION

```
                              INPUT CONCENTRATIONS (MOLES/LITER)

SO4--=1.64000-04   NO3- =0.00000       CA++ =0.00000        MG++ =9.90000-04
NA+  =5.07300-03   CL-  =1.98000-03
SO2  =2.35300-03
CO2  =0.00000
                                 AQUEOUS SOLUTION EQUILIBRIA

             COMPONENT       CONCENTRATION         ACTIVITY         ACTIVITY COEFFICIENT
             H+                 8.407-10           7.689-10              9.146-01
             OH-                1.454-05           1.317-05              9.064-01
             HSO3-              1.769-05           1.603-05              9.064-01
             SO3--              1.922-03           1.297-03              6.749-01
             SO4--              1.706-04           1.137-04              6.665-01
             HSO4-              9.275-12           8.407-12              9.064-01
             H2SO3              9.501-13           9.516-13              1.002+00
             MG++               5.671-04           3.827-04              6.749-01
             MGOH+              2.140-06           1.939-06              9.064-01
             MGSO3              4.131-04           4.137-04              1.002+00
             MGSO4              7.671-06           7.683-06              1.002+00
             NA+                5.067-03           4.608-03              9.094-01
             NAOH               1.632-08           1.634-08              1.002+00
             NASO4-             5.779-06           5.238-06              9.064-01
             CL-                1.980-03           1.794-03              9.061-01
PSO2 =7.82683-13  ATM.

      PH =       9.114           IONIC STRENGTH = 8.86342-03                RES. E.N. =  -4.653-09
```

TABLE IV-14 - CHEMICAL EQUILIBRIA FOR CASE 2 OF $MgSO_3$ DETERMINATION USING $K_n = 1.2 \times 10^{-3}$ AND ASSUMING NO OXIDATION IN SOLUTION

```
                              INPUT CONCENTRATIONS (MOLES/LITER)

S04--=1.67000-04     NO3- =0.00000         CA++ =0.00000         MG++ =9.90000-04
NA+  =5.04000-03     CL-  =1.98000-03
SO2  =2.35300-03
CO2  =0.00000
                                  AQUEOUS SOLUTION EQUILIBRIA

            COMPONENT         CONCENTRATION          ACTIVITY          ACTIVITY COEFFICIENT
            H+                  8.162-10             7.466-10               9.147-01
            OH-                 1.497-05             1.357-05               9.066-01
            HSO3-               1.719-05             1.558-05               9.066-01
            SO3--               1.922-03             1.298-03               6.755-01
            SO4--               1.548-04             1.033-04               6.671-01
            HSO4-               8.181-12             7.417-12               9.066-01
            H2SO3               8.965-13             9.979-13               1.002+00
            MG++                5.670-04             3.830-04               6.755-01
            MGOH+               2.205-06             1.999-06               9.066-01
            MGSO3               4.139-04             4.145-04               1.002+00
            MGSO4               6.975-06             6.986-06               1.002+00
            NA+                 5.035-03             4.580-03               9.096-01
            NAOH                1.670-08             1.673-08               1.002+00
            NASO4-              5.217-06             4.730-06               9.066-01
            CL-                 1.980-03             1.794-03               3.063-01
PSO2 =7.33513-13  ATM.

            PH =      9.127           IONIC STRENGTH = 8.31474-03          RES. E.N. =  -3.098-08
```

The solubility product for $MgSO_3 \cdot 6H_2O$ at 25°C was obtained using the experimentally determined K_0 value and literature solubility data. Gmelin gives the solubility of $MgSO_3 \cdot 6H_2O$ as 6.18×10^{-2} mole/ℓ at 25°C (GM-002). This solubility value was input to the chemical equilibrium program as total Mg and total SO_2 along with the previously determined K_0 value. The computer Mg^{++} and $SO_3^{=}$ activities were then used to obtain $K_{sp} = 5.3 \times 10^{-5}$ for $MgSO_3 \cdot 6H_2O$.

5. Temperature Dependence of the Dissociation Constants of $CaSO_3^{\circ}$ and $MgSO_3^{\circ}$

The Fuoss equation (Section IV-A-2-c) was used to obtain the temperature dependence of K_0 for $CaSO_3^{\circ}$ and $MgSO_3^{\circ}$. The experimentally determined values of K_0 at 25°C were used in the extrapolation. The constants calculated are given in Table IV-2.

V. CHEMICAL EQUILIBRIUM COMPUTER PROGRAM

In order to perform the process simulations we have described, it was necessary to develop as a subroutine, a computer program to solve the set of equilibrium and mass balance equations for aqueous solutions. In this section we shall give the problem definition, describe the computer implementation, and discuss the results obtained with this program.

A. PROBLEM FORMULATION

The program which was developed is a subroutine written in FORTRAN V for a UNIVAC 1108 computer. While some of the more sophisticated extensions of this language have been incorporated into the program, it is felt that the conversion of the routine to any other large scale digital computer can be easily accomplished.

For the problem at hand, thirty-seven chemical species are taken to be the set of unknowns that are solutions to a set of thirty-seven nonlinear equations representing the equilibria and mass balance equations. One of these species, Cl^-, the chloride ion, does not enter into any reactions. It is included in this program because it is required in the ionic strength and electroneutrality equations. Thus $\text{total}_{Cl} = Cl^-$. The remaining set of equations are given below.

$$K_w = a_{H^+}a_{OH^-} \tag{V-1}$$

$$K_2 a_{H_2SO_3} = a_{H^+}a_{HSO_3^-} \tag{V-2}$$

$$K_3 a_{HSO_3^-} = a_{H^+}a_{SO_3^=} \tag{V-3}$$

$$K_4 a_{HSO_4^-} = a_{H^+} a_{SO_4^=} \qquad \text{(V-4)}$$

$$K_5 a_{H_2CO_3} = a_{H^+} a_{HCO_3^-} \qquad \text{(V-5)}$$

$$K_6 a_{HCO_3^-} = a_{H^+} a_{CO_3^=} \qquad \text{(V-6)}$$

$$K_7 a_{CaOH^+} = a_{Ca^{++}} a_{OH^-} \qquad \text{(V-7)}$$

$$K_8 a_{CaSO_3} = a_{Ca^{++}} a_{SO_3^=} \qquad \text{(V-8)}$$

$$K_9 a_{CaCO_3} = a_{Ca^{++}} a_{CO_3^=} \qquad \text{(V-9)}$$

$$K_{10} a_{CaHCO_3^+} = a_{Ca^{++}} a_{HCO_3^-} \qquad \text{(V-10)}$$

$$K_{11} a_{CaSO_4} = a_{Ca^{++}} a_{SO_4^=} \qquad \text{(V-11)}$$

$$K_{12} a_{CaNO_3^+} = a_{Ca^{++}} a_{NO_3^-} \qquad \text{(V-12)}$$

$$K_{sp}[CaCO_3(S)] \geq a_{Ca^{++}} a_{CO_3^=} \qquad \text{(V-13)}$$

$$K_{sp}[CaSO_4(S)] \geq a_{Ca^{++}} a_{SO_4^=} \qquad \text{(V-14)}$$

$$K_{sp}[CaSO_3(S)] \geq a_{Ca^{++}} a_{SO_3^=} \qquad \text{(V-15)}$$

$$K_{sp}[Ca(OH)_2(S)] \geq a_{Ca^{++}} a^2_{OH^-} \qquad \text{(V-16)}$$

$$K_{17} a_{MgOH^+} = a_{Mg^{++}} a_{OH^-} \qquad \text{(V-17)}$$

$$K_{18} a_{MgSO_3} = a_{Mg^{++}} a_{SO_3^=} \qquad \text{(V-18)}$$

$$K_{19} a_{MgHCO_3^+} = a_{Mg^{++}} a_{HCO_3^-} \qquad \text{(V-19)}$$

$$K_{20} a_{MgSO_4} = a_{Mg^{++}} a_{SO_4^=} \qquad \text{(V-20)}$$

$$K_{21} a_{MgCO_3} = a_{Mg^{++}} a_{CO_3^=} \quad \text{(V-21)}$$

$$K_{sp}[Mg(OH)_2(S)] \geq a_{Mg^{++}} a^2_{OH^-} \quad \text{(V-22)}$$

$$K_{sp}[MgCO_3(S)] \geq a_{Mg^{++}} a_{CO_3^=} \quad \text{(V-23)}$$

$$K_{24} a_{NaOH} = a_{Na^+} a_{OH^-} \quad \text{(V-24)}$$

$$K_{25} a_{NaCO_3^-} = a_{Na^+} a_{CO_3^=} \quad \text{(V-25)}$$

$$K_{26} a_{NaHCO_3} = a_{Na^+} a_{HCO_3^-} \quad \text{(V-26)}$$

$$K_{27} a_{NaSO_4^-} = a_{Na^+} a_{SO_4^=} \quad \text{(V-27)}$$

$$K_{28} a_{NaNO_3} = a_{Na^+} a_{NO_3^-} \quad \text{(V-28)}$$

Where: $a_i = \gamma_i M_i$ = activity of component i

γ_i = activity coefficient of component i

M_i = molarity (moles/liter) of component i

Also the material balances are included:

$$\text{Total}_{SO_2} = M_{HSO_3^-} + M_{SO_3^=} + M_{H_2SO_3} + M_{CaSO_3} + M_{CaSO_3(S)} + M_{MgSO_3} \quad \text{(V-29)}$$

$$\begin{aligned}\text{Total}_{CO_2} = {} & M_{HCO_3^-} + M_{CO_3^=} + M_{H_2CO_3} + M_{CaCO_3} + M_{CaHCO_3^+} \\ & + M_{CaCO_3(S)} + M_{MgHCO_3^+} + M_{MgCO_3} + M_{MgCO_3(S)} \\ & + M_{NaCO_3^-} + M_{NaHCO_3} \qquad (V\text{-}30)\end{aligned}$$

$$\begin{aligned}\text{Total}_{SO_4^=} = {} & M_{SO_4^=} + M_{HSO_4^-} + M_{CaSO_4} + M_{CaSO_4(S)} \\ & + M_{MgSO_4} + M_{NaSO_4^-} \qquad (V\text{-}31)\end{aligned}$$

$$\text{Total}_{NO_3^-} = M_{NO_3^-} + M_{CaNO_3^+} + M_{NaNO_3} \qquad (V\text{-}32)$$

$$\begin{aligned}\text{Total}_{Ca^{++}} = {} & M_{Ca^{++}} + M_{CaOH^+} + M_{CaSO_3} + M_{CaCO_3} \\ & + M_{CaHCO_3^+} + M_{CaSO_4} + M_{CaNO_3^+} + M_{CaCO_3(S)} \\ & + M_{CaSO_4(S)} + M_{CaSO_3(S)} + M_{Ca(OH)_2(S)} \qquad (V\text{-}33)\end{aligned}$$

$$\begin{aligned}\text{Total}_{Mg^{++}} = {} & M_{Mg^{++}} + M_{MgOH^+} + M_{MgSO_3} + M_{MgHCO_3^+} + M_{MgSO_4} \\ & + M_{MgCO_3} + M_{Mg(OH)_2(S)} + M_{MgCO_3(S)} \qquad (V\text{-}34)\end{aligned}$$

$$\begin{aligned}\text{Total}_{Na^{++}} = {} & M_{Na^+} + M_{NaOH} + M_{NaCO_3^-} + M_{NaHCO_3} \\ & + M_{NaSO_4^-} + M_{NaNO_3} \qquad (V\text{-}35)\end{aligned}$$

and finally the electroneutrality equation:

$$\begin{aligned}
&M_{H^+} + 2M_{Ca^{++}} + M_{CaOH^+} + M_{CaHCO_3^+} + M_{CaNO_3^+} + 2M_{Mg^{++}} \\
&+ M_{MgHCO_3^+} + M_{Na^+} - M_{OH^-} - M_{HSO_3^-} - 2M_{SO_3^=} - 2M_{SO_4^=} \\
&- M_{HCO_3^-} - 2M_{CO_3^=} - M_{NO_3^-} - M_{HSO_4^-} - M_{NaCO_3^-} - M_{NaSO_4^-} \\
&- M_{Cl^-} = 0 \qquad \text{(V-36)}
\end{aligned}$$

The above is the total set of thirty-six equations and thirty-six unknowns that can be solved with this program. Depending upon the input concentration values, i.e., the left hand sides of Equations V-29 to V-35, some of the species and unknowns can be omitted. This reduces the size of the matrix that must be inverted for each iteration. For example, if $\text{Total}_{NO_3^-}$ is zero, then the variables $M_{NO_3^-}$, $M_{CaNO_3^+}$, and M_{NaNO_3} can be eliminated as well as Equations V-12, V-28, and V-32. If all of the input concentrations are zero then only the trivial case involving M_{OH^-} and M_{H^+} is solved.

One of the more important problems involved in the solution of these equations was the range which the magnitude of the variables may assume in relation to one another. Large ranges create numerical problems. For this reason, the values which are computed are given by

$$x_i = \ell n\, M_i \qquad \text{(V-37)}$$

The variable x_i is the natural logarithm of the molarities. When M_i ranges between $10^{\pm 36}$, x_i will vary between ±88. The equilibrium equations are of the form

$$\ell n a_i + \ell n a_j - \ell n K_k - \ell n a_k = 0 \qquad (V\text{-}38)$$

The material balances are given by

$$\ell n\left(\text{total}_x\right) - \ell n\left(\Sigma M_i\right) = 0 \qquad (V\text{-}39)$$

and the electroneutrality equation is

$$\ell n\left[\Sigma |z_i| M_i(\text{pos.})\right] - \ell n\left[\Sigma |z_i| M_i(\text{neg.})\right] = 0 \qquad (V\text{-}40)$$

An additional advantage in expressing the equations in this form will be discussed later.

Equations V-13 to V-16, V-22 and V-23 are inequalities that allow for the precipitation or dissolution of the solid species. They are included in the set of equations in a logical fashion. Wherever conditions are such that a solid species should precipitate, then the equality holds and the corresponding equation is treated the same as the others. However, when the solution is unsaturated and there is no solid species available to dissolve, the equation is internally set to zero.

The program has provisions for solving the set of equations when the partial pressures of SO_2 and/or CO_2 are inputs. In this case Equation V-2 becomes:

$$K_2 P_{SO_2} K_{pSO_2} = a_{H^+} a_{HSO_3^-} \qquad (V\text{-}2')$$

or Equation V-5 would be

$$K_5 P_{CO_2} K_{pCO_2} = a_{H^+} a_{HCO_3^-} \qquad (V\text{-}5')$$

where: $$M_{H_2SO_3} = P_{SO_2} K_{pSO_2} / \gamma_{H_2SO_3}$$

or, $$M_{H_2CO_3} = P_{CO_2} K_{pCO_2} / \gamma_{H_2CO_3}$$

with: P_i = partial pressure of i

K_{p_i} = partial pressure constant of i

For those cases where a partial pressure is input, Total SO_2 or CO_2 becomes a variable.

The equilibrium, solubility, and partial pressure constants are computed in the program as a function of temperature. The form and origin of these computations have been given in the preceding section.

B. PROGRAM IMPLEMENTATION

Classically the solution of nonlinear equations is done by one of two iterative methods. Starting with an initial guess

$$x_i^\circ \qquad i = 1, 2, \cdots, n \tag{V-41}$$

where n is the number of equations and variables, the r+1th step is given by

$$x_i^{r+1} = x_i^r + \delta_i^r \tag{V-42}$$

δ_i is the correction term which should ultimately go to zero as x_i^r goes to x_i^* which is the solution to the set of equations.

$$f_i(x_j^*) = 0 \qquad j=1,2,\cdots,n \tag{V-43}$$

The technique by which the correction step is obtained determines the method used. The Newton - Raphson method uses an expansion of the f_i in a Taylor series, giving

$$\sum_{j=1}^{n} \left(\frac{\partial f_i}{\partial x_j}\right)^r \delta_j^r = -f_i^r \qquad \text{(V-44)}$$

The corrections, δ_j^r, are obtained here by the solution of "n" simultaneous linear equations. For the gradient or steepest descent method an error term is defined.

$$\Phi = \sum_{i=1}^{n} f_i^2 \qquad \text{(V-45)}$$

and the corrections are made in the direction of the negative gradient of Φ, that is

$$\delta_i^r = -a \frac{\partial \Phi}{\partial x_i} \qquad \text{(V-46)}$$

where

$$\frac{-\partial \Phi}{\partial x_i} = -2 \sum_{j=1}^{n} f_j \frac{\partial f_j}{\partial x_i} \qquad \text{(V-47)}$$

Letting the matrix $B = -(\partial f_i/\partial x_j)$, we can write Equations V-44 and V-46 in matrix notation

$$B\delta_i = f \qquad \text{(V-48)}$$

$$\left(\frac{1}{a} I\right) \delta_g = B^T f \qquad \text{(V-49)}$$

Where I is the identity matrix
B^T is the transpose of B

Both methods are widely used in the solution of nonlinear equations; the choice of method depends on the type of problem being solved. Mathematically, the error function Φ is a hypersurface in an n+1 dimensional space. The solution, $f_j(x_i^*) = 0$, is the point of tangency of Φ with the hyperplane of the "n" variables x_i. If the problem is such that an initial guess is always close to the point of tangency, $\Phi=0$, and the surface can be reasonably approximated by a hyperplane in this region, then the Taylor series method will yield the fastest convergence. If these conditions cannot be met, then the gradient method is usually more efficient. The gradient method suffers by being extremely slow to converge once a neighborhood close to the solution is reached.

Marquardt (MA-006) gives an algorithm that combines the best features of both methods while avoiding their most serious limitations. A modification of his algorithm is used in this program. Defining two matrices, $A = B^T B$ and $g = B^T f$, we introduce a scale factor to improve the numerical aspects of the problem. Defining scaled matrices A^* and g^*

$$A^* = \left(a_{ij}^*\right) = \left[\frac{a_{ij}}{(a_{ii})^{\frac{1}{2}}(a_{jj})^{\frac{1}{2}}}\right] \qquad \text{(V-50)}$$

and

$$g^* = \left(g_i^*\right) = \left[g_i/(a_{ii})^{\frac{1}{2}}\right] \qquad \text{(V-51)}$$

then

$$\delta_i = \delta_i^*/(a_{ii})^{\frac{1}{2}} \qquad \text{(V-52)}$$

which is the solution to the following linear equations at the $r^{\underline{th}}$ iteration

$$(A^{*r} + \lambda^r I)\delta^{*r} = g^{*r} \qquad \text{(V-53)}$$

The parameter $\lambda \geq 0$ determines how much of which method is used. If λ is equal to zero then V-53 reduces to V-48, the Newton-Raphson method. Because of the normalization, the main diagonal terms of A^* are all unity. If λ^r is not negligible compared to one, then the gradient method is included in the calculation of the corrections. The amount of gradient versus Taylor series used is, of course, dependent upon the size of λ. Marquardt's alogrithm adjusts the value of λ after each iteration so that the gradient method predominates until the region is reached where the Taylor series is adequate, then λ is made smaller until the Taylor series method takes over.

Experimentation with the value of λ indicates that the Taylor series method of convergence is almost adequate for our problem. However, the rate of convergence is increased if a little of the gradient is used initially, $\lambda = 10^{-8}$, and after the error function Φ becomes small, it is set to zero. Currently λ is set to zero when Φ is less than 10^{-7}. The applicability of the Taylor series method is felt to be due to solving for the logarithm of the molarities even though the routine handles a wide range of inputs. An additional advantage to using the logarithm of the molarities is that the partial derivatives of the equations with respect to the variables are generally of the order of magnitude of one or smaller. This aids the numerical aspects of the problem when solving the linear equations in V-53. Also, in computing the matrix B, the partial derivatives of the activity coefficients are assumed to be zero.

The program was written in FORTRAN V for the UNIVAC 1108 digital computer. Appendix D contains the subroutine operating instructions and a complete listing. Examples of runs are given throughout the text of this report.

C. OBSERVATIONS REGARDING CONVERGENCE

Several observations have been made in the exercising of this routine that seem worthy of mention at this point. The most important is the data dependency on the number of iterations required to converge to a solution. The starting point, or initial guess, is the dominant factor in the rate of convergence. Typically, the routine is started with all variables set to 10^{-3} or 10^{-5} which has been close to the average value of the computed molarities for a run. However, if the input concentrations indicate a strongly acidic or alkaline solution and the starting values are the opposite, then convergence is slow. Observation of the iteration steps has shown that the program converges slowly until the iterates cross the neutral boundary, then it proceeds rapidly. Adjusting the initial values of several key species to the proper pH range improves this rate markedly. The same observations hold when dealing with unsaturated or saturated solutions. If the input concentrations would produce solids, the rate of convergence can be increased by choosing initial values for the solid species and the converse is true for unsaturated solutions.

Using the routine to simulate titration experiments, where the output of the previous solution is the initial guess for the new one, produces extremely rapid convergences.

The accuracy of the routine is very good. The residual error in the equation solutions is always less than 10^{-7}. This of course can be made smaller with the cost of longer running times.

D. VERIFICATION

This section describes the verification of the chemical equilibrium computer program calculations by comparison with experimental data. The numerical validity of the solution can be verified by substitution into the original equations. Comparison of the results with experimental data tests the accuracy of the equilibrium constants, activity coefficients, temperature correlation, and set of reactions chosen to represent the system. This is not an absolute test since experimental data are often subject to errors. The general agreement for a number of different systems and conditions does, however, substantiate the computer calculations. Typical computer printouts for the following simulations are given in Appendix C.

1. Solubility of SO_2 in Water and in Aqueous H_2SO_4

Conrad (CO-001) measured the total SO_2 dissolved in H_2O in contact with several different partial pressures of SO_2 at 25°C. For check-out purposes the total concentration of SO_2 was input to the computer program and the SO_2 partial pressure was calculated. The results are given in Table V-1.

The solubility of SO_2 in aqueous H_2SO_4 solutions was calculated using the data of Johnstone and Leppla (JO-001). In effect, this extends the SO_2-H_2O system to higher ionic strengths and lower SO_2 partial pressures and includes the sulfate equilibria. The H_2SO_4 concentration was input as total $SO_4^=$. The calculated and experimental SO_2 partial pressures are given in Table V-1. The agreement is not as good as that for the SO_2-H_2O system. Some error was introduced in converting the reported molal concentrations to molar concentrations.

2. Ca - CO_2 - H_2O System

The input data (total Ca^{++} and total CO_2) and the experimental partial pressures of CO_2 were taken from Gmelin (GM-001). The experimental system was calcium carbonate solutions with "excess" CO_2 at 40°C. The results are given in Table V-2. There does not seem to be any trend of the deviations with P_{CO_2} or solution composition. This indicates that the experimental results may be inaccurate.

3. Ca - SO_2 - H_2O System

The experimental data (total SO_2 and total Ca^{++}) and the experimental partial pressures of SO_2 were taken from Kuzminykl and Babushkina (KU-002). The experimental system was calcium bisulfite solutions saturated with sulfite. The data were

TABLE V-1

SOLUBILITY OF SO_2 IN H_2O AND AQUEOUS H_2SO_4 AT 25°C

	EXPERIMENTAL			CALCULATED		
CASE	Total SO_2 (Mole/ℓ)	Total $SO_4^=$ (Mole/ℓ)	P_{SO_2} (atm.)	P_{SO_2} (atm.)	Ionic Strength (Mole/ℓ)	PERCENT DEVIATION
1.	0.567	0	0.393	0.393	0.098	0
2.	0.581	0	0.405	0.403	0.099	- 0.5
3.	1.08	0	0.780	0.791	0.14	+ 1.4
4.	1.31	0	0.960	0.974	0.16	+ 1.4
5.	1.92×10^{-3}	0.0876	1.30×10^{-3}	1.35×10^{-3}	0.13	+ 3.8
6.	1.58×10^{-3}	0.5072	1.30×10^{-3}	1.39×10^{-3}	0.61	+ 6.9
7.	1.58×10^{-3}	0.5072	10.22×10^{-3}	11.58×10^{-3}	0.61	+13.3
8.	11.98×10^{-3}	1.055	10.22×10^{-3}	11.93×10^{-3}	1.21	+16.7

TABLE V-2

COMPARISON OF EXPERIMENTAL AND CALCULATED P_{CO_2} FOR THE Ca-CO_2-H_2O SYSTEM

	EXPERIMENTAL			CALCULATED	
CASE	Total Ca^{++} (Mole/ℓ)	Total CO_2 (Mole/ℓ)	P_{CO_2} (atm.)	P_{CO_2} (atm.)	PERCENT DEVIATION
1.	1.43×10^{-3}	3.36×10^{-3}	0.017	0.022	+29
2.	1.75×10^{-3}	4.16×10^{-3}	0.028	0.028	+ 3.4
3.	2.84×10^{-3}	8.16×10^{-3}	0.070	0.106	+51
4.	3.25×10^{-3}	7.79×10^{-3}	0.077	0.056	-27
5.	3.84×10^{-3}	10.5×10^{-3}	0.149	0.121	-19

reported as total content of SO_2 in solution (g/100g), amount of "SO_2 combined with CaO to form sulfite," and, by difference, the excess SO_2 in solution.

The data for computer input was the total SO_2 in solution and total Ca^{++} in solution. The total Ca^{++} was taken as the molar equivalent of the "combined SO_2". Computer calculations were made at 25 and 50°C. The calculated equilibrium P_{SO_2} was compared with the experimental value. The results are summarized in Table V-3. Except for Case 2 at high P_{SO_2} the experimental and calculated results agree well. The calculated results are satisfactory for the temperature range and ionic strength range (0.7-1.3) involved. The agreement appears to be better at lower SO_2 partial pressure.

4. Mg - SO_2 - SO_4 - H_2O System

The experimental data were obtained from Pinaev (PI-001). The experimental system consisted of low partial pressures of SO_2 over magnesium bisulfite - sulfate solutions saturated with the sulfite. The comparison of experimental and calculated pH and P_{SO_2} is given in Table V-4. The agreement is not as good in this case as for most of the other simulations. The reason for this is not clear, especially in view of the good results obtained for the SO_2 - $SO_4^=$ - H_2O systems.

5. Simulation of Laboratory Experiment

The chemical equilibrium computer program was used to simulate an HEW laboratory experiment. The experiment was for SO_2 absorption by saturated $Ca(OH)_2$ solution (run 545). The experiment yielded pH and SO_2 exit concentration values as a function of time. The conditions used to simulate the experiment are given below.

TABLE V-3

COMPARISON OF EXPERIMENTAL AND CALCULATED P_{SO_2} FOR CaO-SO_2-H_2O SYSTEM

CASE	T(°C)	TOTAL SO_2 (Mole/ℓ)	TOTAL Ca^{++} (Mole/ℓ)	EXPERIMENTAL P_{SO_2} (atm.)	IONIC STRENGTH (Mole/ℓ)	CALCULATED P_{SO_2} (atm.)	PERCENT DEVIATION
1.	50	0.533	0.242	0.0985	0.72	0.104	+ 5.6
2.	50	1.03	0.455	0.420	1.36	0.287	-32
3.	25	0.569	0.262	0.0408	0.78	0.0420	+ 2.9
4.	50	0.805	0.395	0.217	1.07	0.197	- 9.2

TABLE V-4

COMPARISON OF THE EXPERIMENTAL AND CALCULATED P_{SO_2} AND pH FOR THE Mg-SO_2-SO_4-H_2O SYSTEM

		EXPERIMENTAL					CALCULATED			
CASE	T (°C)	Total Mg^{++} (Mole/ℓ)	Total SO_2 (Mole/ℓ)	Total $SO_4^=$ (Mole/ℓ)	P_{SO_2} (atm.) x10^5	pH (at30°C)	P_{SO_2} (atm.) x10^5	pH	I (Mole/ℓ).	PERCENT DEVIATION OF P_{SO_2}
1.	30	0.5387	0.1099	0.4548	3.95	5.88	0.58	5.67	0.88	- 85
2.	30	0.5471	0.1717	0.4319	5.39	5.70	2.89	5.31	0.90	- 46
7.	30	0.8500	0.3012	0.6581	8.17	4.87	12.0	4.97	1.21	+ 47
7.	50	0.9034	0.3434	0.6666	12.6	----	14.8	----	1.08	+ 17
16.	30	1.2476	0.3886	1.0229	19.7	4.02	56.4	4.46	1.54	+186

Temperature: 59°C (138°F)
$Ca(OH)_2$ Concentration: 1.26 g/ℓ (0.017 mole/ℓ)
P_{CO_2}: 0.068 atm
SO_2 Inlet Concentration: 2800 ppm

The experimental SO_2 exit concentration versus time curve was graphically integrated to give the amount of SO_2 absorbed at selected times. The trapezoidal rule was used for the latter stages of the run where the SO_2 exit concentration was changing with time. Two different values were assumed for the oxidation of sulfite to sulfate. The experiment was simulated with values of 10 and 90% for the oxidation of total SO_2 absorbed.

The simulation was started by inputting the total amount of Ca^{++} equivalent to 1.26 g/ℓ of $Ca(OH)_2$. For the next point the CO_2 partial pressure (0.068 atm) was applied to the system. Then total SO_2 and $SO_4^=$ amounts were input for the selected time increments. The outputs for each point included the concentrations and activities of the species present, the pH, and the partial pressure of SO_2 above the solution. Since precipitation and dissolution of solids is taken into account by the program, it was also possible to see if solids were present. The results obtained for pH and P_{SO_2} as a function of time are shown in Figures V-1 and V-2 with the experimental curves. In general the agreement is good. The degree of sulfite oxidation has an effect on the pH and P_{SO_2} that is especially large near the end of the run. The case with 90% SO_2 oxidation lies closer to the experimental curve. The discrepancy between the calculated and experimental results in the intermediate stages might be caused by a rate-controlled dissolution of calcium carbonate precipitated at the start of the run. In the latter stages when the solution is "clear", the agreement is good with the 90% SO_2 oxidation case. At 95 min., assuming 85% oxidation, the calculated P_{SO_2} is 2200 ppm.

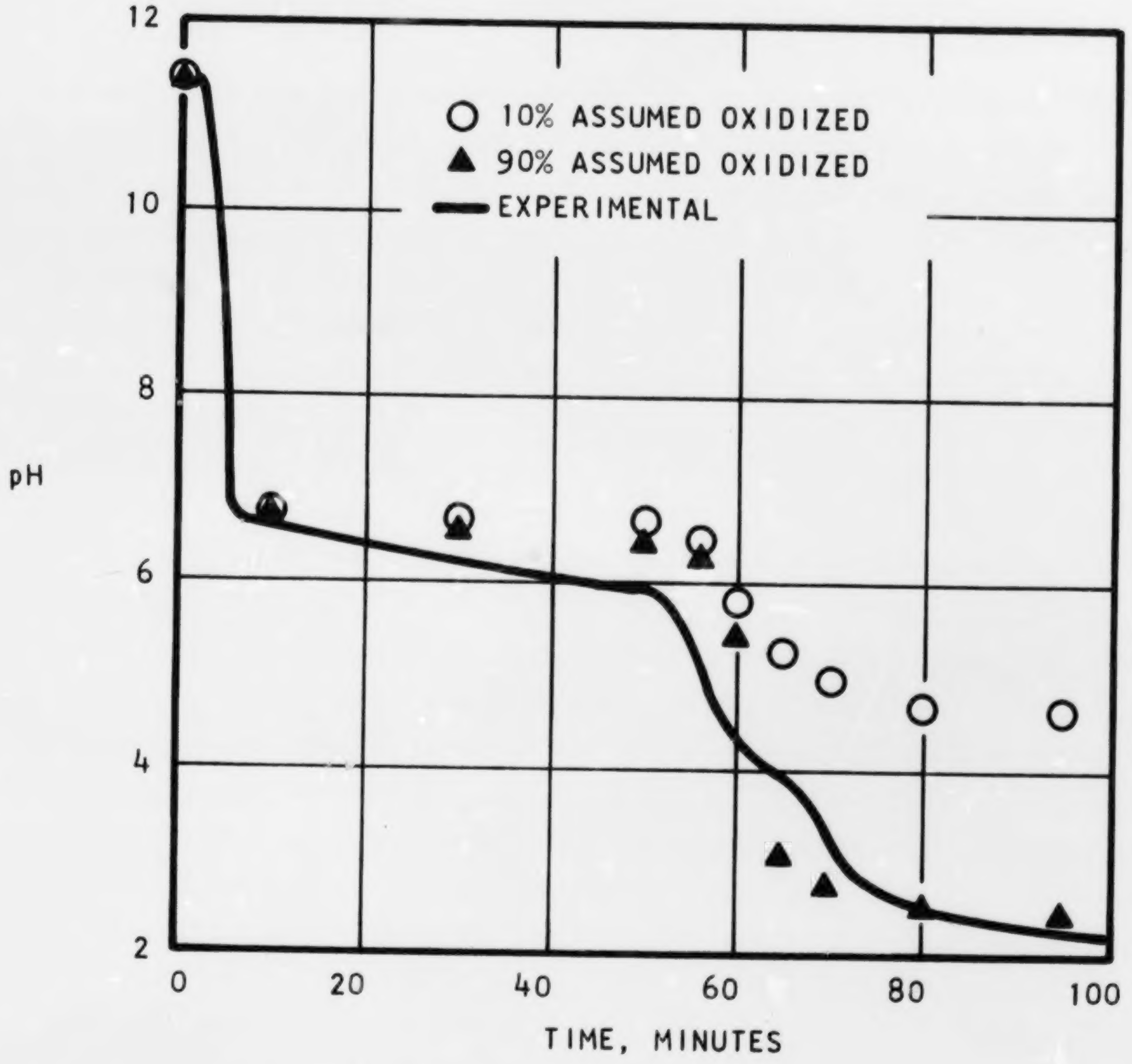

FIGURE V-1 pH CORRELATION

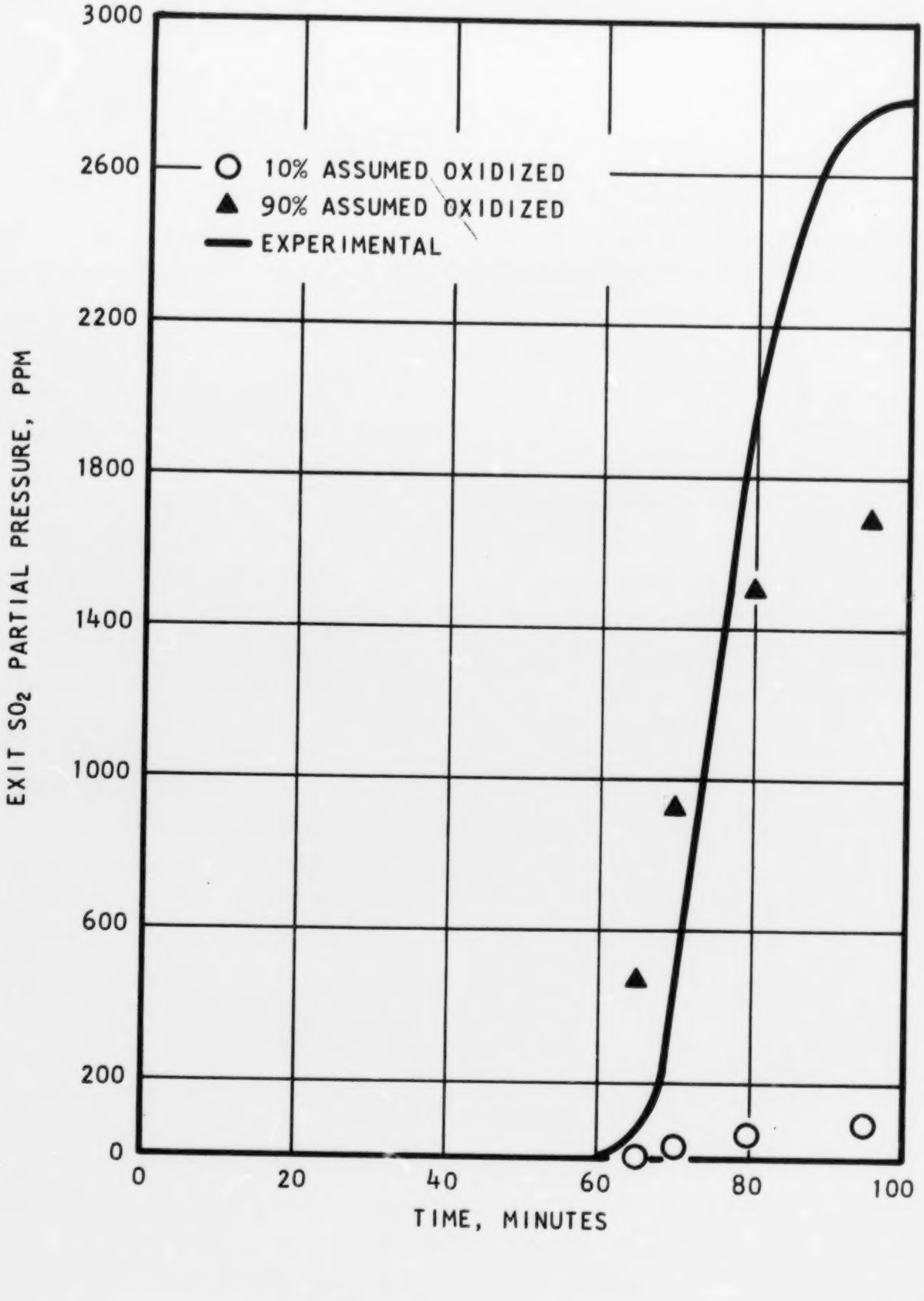

FIGURE V-2 P_{SO_2} CORRELATION

6. Sea Water Model

Garrels (GA-001) developed a chemical model of sea water involving complexes of Ca^{++}, Mg^{++}, Na^{+}, K^{+}, $SO_4^{=}$, and $CO_3^{=}$, at 25°C, pH 8.1, and an ionic strength of 0.7. Single ion activity coefficients were calculated by the mean salt method using experimental mean activity coefficients. The Garrels and Radian calculated results are given in Table V-5. Most of the variation is due to differences in calculating activity coefficients and the slight difference in pH. Garrels used pH as a known quantity. The calculated CO_2 partial pressure is in good agreement with the average atmosphere value (3×10^{-4} atm). There is also good agreement with the activities of Na^{+}(GA-001), Mg^{++}(TH-001), and Ca^{++}(TH-002) in sea water measured by ion selective electrodes. These values are also given in Table V-5. The range given for Ca^{++} and Mg^{++} is due to differences in calculated activity coefficients.

7. Other Systems

Several other systems have been studied in less depth than those given above. The agreement between calculated and Radian determined Ca^{++} activity in calcium nitrate solutions has been discussed in Section IV-D-2. The highest ionic strength used in this case was ~ 0.55 mole/ℓ.

The solubility of solids in salt solutions was briefly investigated. The experimental concentrations of the soluble species were input as usual. An excess of the species forming the solids was input in molar equivalent amounts. The solubility was then obtained by subtracting the computer calculated "concentration" of solid formed from the input concentrations of the solid forming species. For example, the solubility of $CaSO_4 \cdot 2H_2O$ in a 0.1M NaCl, 0.05 M $MgCl_2$ solution is

TABLE V-5
SEA WATER MODEL RESULTS

QUANTITY	GARRELS' RESULTS	RADIAN'S RESULTS	MEASURED RESULTS
pH	8.1	8.33	8.1-8.2
ionic strength	0.70	0.67	
$a(Ca^{++})$	$2.64x10^{-3}$	$2.27x10^{-3}$	$2.14-2.49x10^{-3}$
$a(Mg^{++})$	$1.69x10^{-2}$	$1.49x10^{-2}$	$1.39-1.73x10^{-2}$
$a(Na^{+})$	0.356	0.344	0.35
$a(CO_3^{=})$	$4.7x10^{-6}$	$1.07x10^{-5}$	
$a(HCO_3^{-})$	$9.75x10^{-4}$	$1.07x10^{-3}$	
$a(SO_4^{=})$	$1.79x10^{-3}$	$2.08x10^{-3}$	
$M(CaSO_4^{\circ})$	$8x10^{-4}$	$8.58x10^{-4}$	
$M(CaHCO_3^{+})$	$1x10^{-4}$	$5.94x10^{-5}$	
$M(CaCO_3^{\circ})$	$2x10^{-5}$	$3.43x10^{-5}$	
$M(MgSO_4^{\circ})$	$5.9x10^{-3}$	$4.86x10^{-3}$	
$M(MgHCO_3^{+})$	$5x10^{-4}$	$1.95x10^{-4}$	
$M(MgCO_3^{\circ})$	$1.5x10^{-4}$	$3.54x10^{-4}$	
$M(NaSO_4^{-})$	$5.7x10^{-3}$	$5.07x10^{-3}$	
$M(NaHCO_3)$	$5x10^{-4}$	$1.85x10^{-4}$	
P_{CO_2} (atm)	---------	$3.3x10^{-4}$	$\sim 3x10^{-4}$

a(x) - activity of x

M(x) - molarity of x (moles/ℓ)

0.0356M (OS-001). Using total Ca^{++} and $SO_4^=$ concentrations of 0.1M, the calculated solid $CaSO_4 \cdot 2H_2O$ concentration was 0.0685M. Therefore the calculated solubility is 0.0315M (Table V-6). Results are given in Table V-7. for the solubility of $Ca(OH)_2$ in a $NaNO_3$ solution at 50°C.

The essential validity of the chemical equilibrium computer program is demonstrated by the successful reproduction of experimental results over a very wide range of conditions. Figure V-3. shows a comparison of experimental and calculated partial pressures of SO_2 and CO_2 for five of the systems discussed above. In general, the agreement is excellent for the wide range of partial pressures, temperature, solution composition, and ionic strength involved.

TABLE V-6

SOLUBILITY OF $CaSO_4 - 2H_2O$ IN A $MgCl_2$, NaCl SOLUTION AT 25°C

```
                         INPUT CONCENTRATIONS (MOLES/LITER)

SO4--=1.00000-01    NO3-  =0.00000        CA++ =1.00000-01     MG++ =5.00000-02
NA+  =1.00000-01    CL-   =2.00000-01
SO2  =0.00000
CO2  =0.00000
                              AQUEOUS SOLUTION EQUILIBRIA

        COMPONENT          CONCENTRATION           ACTIVITY          ACTIVITY COEFFICIENT
        H+                   2.654-07              2.258-07               3.503-01
        OH-                  6.151-08              4.490-08               7.299-01
        SO4--                1.842-02              3.292-03               1.787-01
        HSO4-                9.790-08              7.145-08               7.299-01
        CA++                 2.687-02              7.290-03               2.713-01
        CAOH+                1.062-08              7.750-09               7.299-01
        CASO4                4.628-03              4.901-03               1.059+00
        CASO4(S)             6.850-02              6.850-02               1.000+00
        CA(OH)2(S)           1.216-37              1.216-37               1.000+00
        MG++                 4.326-02              1.228-02               2.838-01
        MGOH+                2.904-07              2.120-07               7.299-01
        MGSO4                6.739-03              7.136-03               1.059+00
        MG(OH)2(S)           2.849-33              2.849-33               1.000+00
        NA+                  9.829-02              7.220-02               7.346-01
        NAOH                 8.239-10              8.725-10               1.059+00
        NASO4-               1.712-03              1.249-03               7.299-01
        CL-                  2.000-01              1.362-01               6.810-01

   PH =        6.647           IONIC STRENGTH = 3.27167-01            RES. E.N. =    2.402-03
```

Calculated Solubility = 0.0315 mole/ℓ

Experimental Solubility = 0.0356 mole/ℓ (OS-001)

TABLE V-7

SOLUBILITY OF $Ca(OH)_2$ IN A $NaNO_3$ SOLUTION AT 50°C

```
                         INPUT CONCENTRATIONS (MOLES/LITER)

SO4-- =0.00000        NO3- =8.42000-01     CA++ =1.00000-01    MG++ =0.00000
NA+   =8.42000-01     CL-  =0.00000
SO2   =0.00000
CO2   =0.00000

                          AQUEOUS SOLUTION EQUILIBRIA

          COMPONENT        CONCENTRATION       ACTIVITY        ACTIVITY COEFFICIENT
          H+                 1.424-12          1.450-12             1.018+00
          OH-                4.996-02          3.782-02             7.571-01
          NO3-               7.759-01          3.116-01             4.016-01
          CA++               1.757-02          3.960-03             2.254-01
          CAOH+              5.515-03          4.176-03             7.571-01
          CANO3+             7.071-03          5.354-03             7.571-01
          CA(OH)2(S)         6.984-02          6.984-02             1.000+00
          NA+                7.781-01          5.518-01             7.092-01
          NAOH               4.847-03          5.618-03             1.159+00
          NANO3              5.905-02          6.844-02             1.159+00

            PH =      11.839         IONIC STRENGTH = 8.43326-01          RES. E.N. =   1.510-06
```

Calculated Solubility = 0.0302 mole/ℓ

Experimental Solubility = 0.0260 mole/kg H_2O (MA-003)

Experimental Solubility in Pure Water = 0.017 mole/kg H_2O

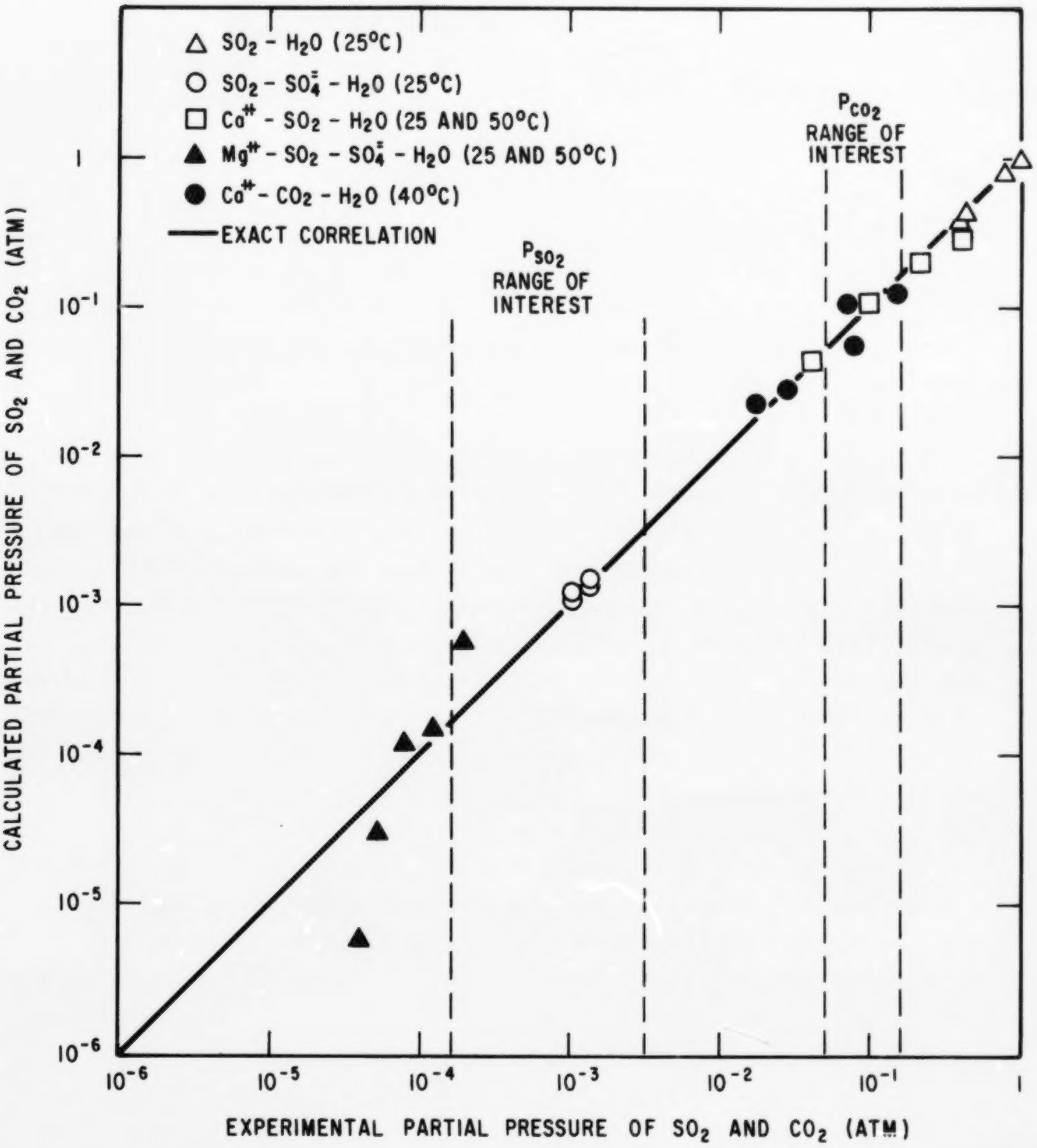

FIGURE V-3 COMPARISON OF CALCULATED AND EXPERIMENTAL PARTIAL PRESSURES OF SO_2 AND CO_2 FOR THE SYSTEMS STUDIED

VI. INHOUSE TEST PROGRAM

NAPCA is planning to conduct some inhouse tests which will simulate a venturi scrubbing unit for the limestone injection - wet scrubbing process. These tests will use the equipment designed and used for particulate removal studies. Radian has assisted in the preparation of a test program for these NAPCA inhouse studies. The details of the program design have been reported in Radian Technical Note 200-002-5 (OT-002).

There are two sections of the NAPCA apparatus that appear as if they may contribute significant information to the design of the limestone injection - wet scrubbing process. These are the venturi scrubbing section itself and the effluent hold tanks that will be used in conjunction with this wet scrubbing section. In addition to gaining some general idea as to the capability of the venturi as a gas-liquid contacting device for the wet scrubbing process, the venturi scrubbing section will be used to determine the extent of vapor-liquid and solid-liquid mass transfer in the contacting device.

The effluent hold tanks will be used to obtain information concerning the hydration and dissolution rates of calcium oxide and the precipitation rates of calcium sulfite, sulfate, and carbonate. In addition, these tests are designed to gather preliminary information on the absorption of NO_x, the possible build-up of Na^+, Cl^-, and NO_3^- ions in the system, and the reactions of the absorbed NO_x in the wet scrubbing process.

Several process simulations for the NAPCA pilot unit system have been made using Radian's current process model (based upon several process assumptions and Radian's chemical equilibrium program) so that approximate process flow rates and compositions could be determined. Results from these simulations have been presented in Section III of this report.

To accomplish the goals of this test program, Radian has devised a set of approximately 35 experiments. These experiments are conveniently divided into three types depending upon the objective of the experiments. The first set of experiments is designed to measure the extent of v-ℓ mass transfer in the scrubbing section. The second type is designed to measure the extent of s-ℓ mass transfer in the scrubbing section. The third type measures the s-ℓ mass transfer rates in the effluent hold tanks. The first two types of experiments are basically qualitative in nature, whereas in the third type a quantitative measure of the rates is expected.

VII. SUMMARY AND CONCLUSIONS

The work reported here has formed the basis of a theoretical description of the scrubbing section of the limestone injection - wet scrubbing process. For the two scrubbers of interest, the turbulent contact absorber and the marble bed, it was shown that vapor in plug flow and completely backmixed liquid should satisfactorily describe the flow patterns.

Based upon observations of NAPCA bubbler experiments, recalculated literature values, and KP&L experience, it appears that the rate-limiting step in the vapor to liquid to solid reaction chain will be a step involving the solids. The implications of this are that the vapor and liquid phases may be considered to be in equilibrium with respect to SO_2 and CO_2.

A literature search and screening procedure yielded the significant chemical reactions and chemical species. A set of mass balance and equilibrium equations were formulated to describe an aqueous system containing SO_2, CO_2, Ca^{++}, Mg^{++}, Na^+, NO_3^-, $SO_4^=$, and Cl^-. The individual species considered are given in Table IV-5.

To solve the thermodynamic equilibria equations individual ion activity coefficients were required. An extended form of the Debye-Hückel theory was used. The literature data were carefully evaluated to select the most accurate equilibrium values.

Pertinent missing thermodynamic data were determined in the Radian laboratory. The dissociation constant at 25°C for ion complexes

$$CaSO_3 \rightleftarrows Ca^{++} + SO_3^=$$

$$MgSO_3 \rightleftarrows Mg^{++} + SO_3^{=}$$

were 4.0×10^{-4} and 1.2×10^{-3} respectively (in molar units). The solubility product constants of $CaSO_3 \cdot \frac{1}{2}H_2O$ and $MgSO_3 \cdot 6H_2O$ were found to be 8.4×10^{-8} and 5.3×10^{-5} respectively at 25°C.

Several laboratory systems and full scale scrubbing processes were simulated using appropriate assumptions along with the chemical equilibrium computer program described in Section V. Comparison of calculated with experimental equilibrium and solubility data confirmed the validity and accuracy of this program. Application of the program to process simulation led to the following observations:

1. Equilibrium calculations indicate that for the TCA and marble bed scrubbers to operate in a proper hydraulic range (vapor 2500 to 3500 lbs/hr-ft^2; liquid 8-15 gpm/ft^2), a slurry scrubber feed would most likely be required. If none of the limestone contained in the flue gas stream reacts in the scrubber bed the clear liquid rate required for 90% SO_2 removal from a 3000 ppm SO_2 flue gas would be slightly above the 15 gpm/ft^2 limit dictated by scrubber design. That is, not enough basic species can be made to dissolve in the liquor, so more liquor is required than is reasonable.

If a slurry is recirculated to the scrubber, solid-liquid mass transfer becomes important to the process.

2. Calculations indicate that under typical operating conditions, the equilibrium partial pressure of SO_2 above a liquor of pH 4-4.5 is less than 300 ppm. Thus it is not necessary that the liquor leaving the scrubber be highly alkaline to achieve good SO_2 removal.

3. Theoretical considerations and process calculations show that ionic strength (amount of dissolved salts) of the scrubber liquor may be an important process parameter. Ionic strength can significantly affect solubilities of the basic species required for SO_2 removal. The form of this relationship implies the existence of an "optimum" operating ionic strength. Degree of NO_x removal, composition of reactant, and solubility of flyash components influence ionic strength, but overall conditions can be controlled by amount of liquor purged from the process.

Scaling phenomena may also be affected by ionic strength. The possibility exists that SO_2 removal could be improved and scaling reduced by judicious addition of makeup water or purge of liquor at different points in the process.

4. The $SO_3^= \rightarrow SO_4^=$ oxidation reaction has a pronounced effect on calculated values of equilibrium SO_2 partial pressure. Again, the functional form of this behavior suggests an optimum level of oxidation at least from the standpoint of SO_2 removal. Unfortunately, the oxidation rate is dominated by catalytic species and will be difficult to define.

5. The solution chemistry of the process differs significantly between high calcium limestone and dolomite reactant cases. This could be particularly important in waste disposal or liquor purge considerations since dissolved $MgSO_4$ may be present in high concentration for processes operated with dolomite. The ionic strength of the scrubber liquor (discussed in point 3) is also strongly affected by reactant composition.

A process parameter study now underway will attempt to further examine and explain these observations. Radian has also assisted the design of a NAPCA in-house test program that should indicate the approach to vapor-liquid equilibrium in the scrubbing section and provide some rate data on dissolution and precipitation rates in the hold tanks.

VIII. NOMENCLATURE

Symbol	Definition	Section No.
a	gas-liquid interfacial area per unit bed volume	II
a	center-to-center distance of ions in an ion-pair	IV
a	a scale factor	V
a_i	activity of the i^{th} species	IV,V
$\mathring{a}_i$	ion size parameter	IV
a_m's	activities of the m-species where m denotes the class of species affecting the n^{th} reaction step	II
a_{ij}	element ij of the A matrix	V
a_{ij}^*	element ij of the A^* matrix	V
A	Debye-Huckel limiting slope constant	IV
A	matrix with elements $(\partial f_j/\partial x_i)(\partial f_i/\partial x_j)$	V
A^*	scaled A matrix	V
A,B,C,D	parameters in the expression for log K as a function of temperature	IV

Symbol	Definition	Section No.
b_i	deviation parameter in extended Debye-Huckel equation	IV
B	Debye-Huckel coefficient of $\overset{\circ}{a}_i$	IV
B	matrix with elements $-(\partial f_i/\partial x_j)$	V
B^T	transpose of the B matrix	V
C	designation for clarifier	II,III
CB	flow rate and designation of the clarifier bottoms	II,III
CF	flow rate and designation of the clarifier feed	II,III
CL	flow rate and designation of the clarifier liquid	IV
D_L, D_s	dispersion coefficients of the liquid and solids, respectively	II
D^*	dielectric constant of solvent	IV
E	electromotive force of cell	II,III
E°	standard electromotive force of cell	IV
f	vector with elements f_i	V
f_i	functions for the i^{th} equation which equal zero for the solution x_i^*	V

Symbol	Definition	Section No.
f_{n1}, f_{n2}	driving force functions 1 and 2, respectively	II
F	designation for filter	II,III
F	Faraday charge	IV
FA	flow rate and designation of fly ash stream	II,III
FB	flow rate and designation of the filter bottoms	II,III
FG	flow rate and designation of the flue gas	II,III
FL	flow rate and designation of filter liquid	II
g	g-matrix with elements $(\partial f_j/\partial x_i)(f_i)$	V
g^*	scaled g-matrix	V
ΔH_T°	standard enthalpy of reaction at the temperature T	IV
I	ionic strength defined by equation (IV-19)	III,IV
I	identity matrix	V

Symbol	Definition	Section No.
k	Boltzman constant	IV
k_{Gj}	individual mass transfer coefficient for the gas film	II
k_n	rate constant for the n^{th} rate step	II
K	equilibrium constant	IV
K_{Gj}	overall mass transfer coefficient for j^{th} species and the gas-liquid interface based on gas-phase driving force	II
K_n	equilibrium constant for the n^{th} step	II,IV,V
K_w	activity product of water	V
L	liquid flow rate expressed in terms of H_2O in solution (e.g., kg H_2O per minute)	II,III
LA	flow rate and designation for the sum of the LS and FA streams	II
LS	flow rate and designation of limestone stream	II,III
m_i	molality of the i^{th} liquid species (g-moles/kg H_2O in solution)	II,III

Symbol	Definition	Section No.
M_i	molarity of the i^{th} species (g-moles/liter of solution)	IV,V
MW_i	molecular weight of the i^{th} species	III
N	Avogardo's number	IV
N_G	number of transfer units	II
P_i	partial pressure of the i^{th} species	IV,V
P	designation for process water hold tank	II,III
P	absolute pressure	II,III
r_{nk}	n^{th} step rate for the formation of the k^{th} species based upon a unit length of scrubber	II
$\bar{r}_{nk}$	n^{th} step rate averaged over the scrubber residence-time distribution	II
R	gas constant	IV
RL	flow rate and designation of recycled liquid	III
$R(t/\tau)$	normalized residence-time distribution of solids in the scrubber	II

Symbol	Definition	Section No.
S	cross-sectional area of the scrubber	II
S	designation for scrubber	II,III
SB	flow rate and designation of the scrubber bottoms	II,III
SF	flow rate and designation of scrubber feed	II,III
SG	flow rate and designation of stack gas	II,III
SR	flow rate and designation of slurry recycle	II,III
t	time	II
t_s	time required for complete reaction of solids	II
T	absolute temperature	IV
T^*	standard state absolute temperature	IV
U_i	constant in equation IV-23 for $_i$ of uncharged species	IV
ν_+,ν_-	number of cations (+) or anions (-) formed from one molecule of electrolyte	IV

Symbol	Definition	Section No.
V	molar flow rate of inert gas	II
w_ℓ	molality of solid species $\underline{\ell}$ based upon water in scrubber liquor (g-moles of solid/kg H_2O in solution)	II
WM	flow rate and designation of the water makeup	II,III
x_i	natural logarithm of the molarity of the i^{th} species	V
$\overset{\circ}{x}_i$	initial guess of x_i	V
x_i^*	value of x_i which is solution to the set of equations	V
x_i^{r+1}	value of x_i at the $r+1^{th}$ step	V
y	mole fraction of gaseous species	II
$(y_i)_j$	mole fraction of the j^{th} gaseous species at the gas-liquid interface	II
y_j	mole fraction of gaseous species $\underline{j}$.	II
y_j^*	mole fraction of j^{th} gaseous species in equilibrium with a liquid of mole fraction x or molality m.	II

Symbol	Definition	Section No.
Y_j	mole ratio of gas species j based upon inert flue gas.	II
Y_j^*	mole ratio of j^{th} gaseous species in equilibrium with a liquid of mole ratio X or molality m.	II
z_i	charge on the i^{th} ion	IV
Z	vertical distance along scrubber	II
GREEK		
γ_i	individual activity coefficient	IV,V
$\gamma_{\pm}$	mean activity coefficient	IV
δ_i^r	correction term for x_i at the r^{th} iteration step	V
ε	fundamental charge	IV
λ^r	parameter giving the amount of gradient method used in the r^{th} step	V
$\rho_{solution}$	density of solution (g/liter)	III
$\hat{\rho}$	molar density of the scrubber liquor (g-moles/liter)	II

Symbol	Definition	Section No.
τ	mean residence time of the scrubber solids	II
Φ	sum of the squared errors of f functions	V

IX. LITERATURE CITED

AR-001 Arkhipova, G. P., et al., *Russ. J. of App. Chem.*, *37*, 2275 (1964).

AU-001 Austin, J. M., and A. D. Mair, *J. Phys. Chem.*, *66*, 519 (1962).

BE-001 Bechtel Corporation, "Alkali Scrubbing Test Facility, Phase 1: Preliminary Engineering", a report to NAPCA, Public Health Service, HEW Contr. No. PH22-68-67 by Bechtel Corp., May 1969.

BE-002 Bell, R. P., and J. H. B. George, *Trans. Faraday Soc.*, *49*, 619 (1953).

BI-001 Bichowsky, F. R., *J. Am. Chem. Soc.*, *45*, 2234 (1923).

BO-002 Boynton, R. S., *Chemistry and Technology of Lime and Limestone*, Interscience Publishers, New York, 1967.

BR-001 Bransom, S. H., and G. A. R. Trollope, *AICHE Journ.*, *10*(6), 842-847 (1964).

BR-004 Brian, P. L. T., *AICHE Journ.*, *10*(1), 5 (1964).

BR-005 Brian, P. L. T., and Beaverstock, M. C., *Chem. Engr. Sci.*, *20*, 47-56 (1965).

BR-006 Brink, J. A., and C. E. Contant, *Ind. Engr. Chem.*, *50*(8), 1157-1160 (1958).

CA-001 Campbell, J., *Chem. Ed.*, *25*, 498 (1948).

CA-002 *Chem. Abstracts*, *59*, 8184g; Vasil'ev, V. P., et al, Izv. Vysshikh Uchebn. Zavedenii, Khim. i Khim. Tekhnol., *6*, 339 (1963).

CH-001 Chen, B. H., and W. J. M. Douglas, *Can. J. Chem. Engr.*, *46*, 245-9 (1968).

CH-002 Chertkov, B. A., *Khim. Prom.*, *7*, 533-36 (1962).

CH-003 Chen, B. H., and W. J. M. Douglas, *Can. J. Chem. Engr.*, *47*, 113-118 (1969).

CO-001 Conrad, F. H., and W. L. Beuschlein, *J. Am. Chem. Soc.*, *56*, 2554 (1934).

DA-001 Davies, Cecil W., *Ion Association*, Washington, D. C., Butterworth, 1962.

DA-002 Davies, C. W., and E. C. Righellato, *Trans. Faraday Soc.*, *26*, 592 (1930).

DA-003 Davies, C. W., and D. I. Stock, *Trans. Faraday Soc.*, *44*, 856 (1948).

DO-001 Douglas, H. R., et al., *Chem. Engr. Prog.*, *59*(12), 85-9 (1963).

DO-002 Douglas, W. J. M., *Chem. Engr. Prog.*, *60*(7), 66-71 (1964).

EI-001 Eigen, et. al., Z. Physik Chem., 30, 130-136 (1961).

FE-001 Feitknecht, W., P. Schindler, Pure Appl. Chem., 6, 130 (1963).

FR-001 Frear, G. L., and J. Johnston, J. Am. Chem. Soc., 51, 2082 (1929).

FU-001 Fuoss, Raymond M., J. Am. Chem. Soc., 80, 5059 (1958).

GA-001 Garrels, R. M., and M. E. Thompson, Am. J. Sci., 260, 57 (1962).

GA-002 Garrels, R. M., and M. E. Thompson, Am. J. Sci., 259, 24 (1961).

GA-003 Garrels, Robert M., and Charles L. Christ, Solutions, Minerals, and Equilibria, Harper and Row, New York, 1965.

GI-001 Gimblett, F. G. R., and C. B. Monk, Trans. Faraday Soc., 50, 965 (1954).

GJ-001 Gjaldbeck, J. K., Z. Anorg. Chem., 144, 269 (1925).

GL-003 Glasson, D. R., J. Appl. Chem. (London), 10, 38-42 (1960).

GL-004 Glasson, D. R., J. Appl. Chem. (London), 10, 42-8 (1960).

GM-001 *Gmelin Handbuch der anorg. Chemie*, 8. Auflage, Calcium, Teil B Lieferung 3, 1961.

GM-002 *Gmelin Handbuch der anorg. Chemie*, System 27 Magnesium, 8. Auflage, 1931.

GR-001 Green, C., "Installation and Initial Operation of SO_2 Removal Equipment", Paper presented at Missouri Valley Electric Assoc., Kansas City, Mo., April 16, 1969.

GR-002 Greenwood, I., *J. Biol. Chem.*, *141*, 789 (1941).

HA-001 Halla, F., *Monatsh.*, *93*, 948 (1962).

HA-002 Harned, H. S., and B. B. Owen, *The Physical Chemistry of Electrolytic Solutions*, Third Edition, Reinhold, New York, 1958.

HA-003 Harned, H. S., and F. T. Bonner, *J. Am. Chem. Soc.*, *67*, 1026 (1945).

HA-004 Harned, H. S., and S. R. Scholes, Jr., *J. Am. Chem. Soc.*, *63*, 1706 (1941).

HA-005 Harned, H. S., and Davis, *J. Am. Chem. Soc.*, *65*, 2030 (1943).

HA-006 Harris, L. S., *Chem. Engr. Prog.*, *62*(4), 55-59 (1966).

HA-007 Hamer, Walter J., Theoretical Mean Activity Coefficients of Strong Electrolytes in Aqueous Solutions from 0 to 100°C, National Standard Reference Series - National Bureau of Standards 24, 1968.

HE-001 Helgeson, H. R., J. Phys. Chem., 71, 3121 (1967).

HI-001 Himmelblau, D. M., and J. C. Wang, AICHE Journ., 10(4), 574-580 (1964).

HO-001 Hobler, Tadeusz, Mass Transfer and Absorbers, Intern. Series of Monograms in Chem. Engr., Vol. 6, Permagon Press, Oxford, 1966.

HO-002 Hostetler, P. B., J. Phys. Chem., 67, 720 (1963).

IS-001 Ishii, T., and S. Fugita, Chem. Engr. (Japan), 3(2), 236-8 (1965).

JE-001 Jenkins, I. L., and C. B. Monk, J. Am. Chem. Soc., 72, 2695 (1950).

JO-001 Johnstone, H. F., and D. W. Leppla, J. Am. Chem. Soc., 56, 2233 (1934).

JO-002 Jonakin, J., and J. F. McLaughlin, "Operating Experience with the First Full Scale System for Removal of SO_2 and Dust from Stack Gases", Paper presented at Amer. Power Conf., Chicago, Ill., April 22-24, 1969.

KL-001 Klotz, Irving M., Chemical Thermodynamics, Benjamin, New York, 417, 1964.

KO-002 Kontorovich, S. I., et. al., *Colloid Journal*, *25*, 467-71 (1963).

KO-003 Kontorovich, S. I., et. al., *J. Phy. Chem.* (USSR), *157*, 709-12 (1964).

KU-001 Kunii, D., and Levenspiel, O., *Fluidization Engineering*, John Wiley and Sons, Inc., New York, 1969.

KU-002 Kuminykh, I. N., and M. D. Babushkina, *J. Appl. Chem.* (USSR), *29*, 1607 (1956).

LA-001 Latimer, W. M., *Oxidation Potentials*, Prentice Hall, New York, 1952.

LA-002 Larson, M. A., and A. D. Randolph, *Chem. Engr. Prog. Symposium Series*, *65*(95), 1-13 (1969).

LE-002 Levenspiel, O., *Chemical Reaction Engineering*, John Wiley and Sons, Inc., New York, 1962.

LI-001 Linden, T. van der., *J. Soc. Chem. Ind.*, *36*, 96 (1917).

MA-001 Matthews, F. W., and A. O. McIntosh, *Can. J. Res.*, *26B*, 747 (1948).

MA-002 Marshall, W. L., and Ruth Slusher, *J. Phys. Chem.*, *70*, 4015 (1966).

MA-003 Marshall, W. L., and L. B. Yeatts, *J. Phys. Chem.*, *71*, 2641 (1967).

MA-004	Marshall, W. L., and L. B. Yeatts, J. Phys. Chem., 73, 81 (1969).
MA-005	Manvelyan, M. G., et. al., J. Appl. Chem. (USSR), 34, 896 (1961).
MA-006	Marguardt, D. W., JSIAM, 11, 431 (1963).
MI-002	Miller, D. M., and J. Jonakin, Electrical World, 35-36 (March 4, 1968).
MU-001	Mullins, J. W., Crystallization, Butterworths, London, 1961.
NA-001	Nair, V. S. R., and G. H. Nancollas, J. Chem. Soc., (London), 3706 (1958).
NA-002	Nakayama, F. S., and B. A. Rasnick, Anal. Chem., 39, 1022 (1967).
NI-001	Nielsen, A. E., Kinetics of Precipitation, Pergamon Press, Oxford, 1964.
NO-002	Nonhebel, G., (editor), Gas Purification Processes, George Newnes Limited, London, 1964.
OR-001	Orion Divalent Cation Electrode Model 92-32 Instruction Manual, Orion Res. Inc., Cambridge, Mass., 1967.
OS-001	Ostroff, A. G., and A. V. Metler, J. Chem. Engr. Data, 11, 346 (1966).

OT-002 Ottmers, D. M., "Test Program for the NAPCA Inhouse Venturi Scrubber", Radian Technical Note 200-002-5, 16 January 1969.

PI-001 Pinaev, V. A., *J. Appl. Chem.* (USSR), *36*, 2049 (1963).

PL-001 Plumley, A. L., Whiddon, O. D., Shutko, F. W., and Jonakin, J., "Removal of SO_2 and Dust from Stack Gases", Paper presented at Am. Power Conf., Chicago, Illinois, April 25-27, 1967.

PL-002 Plumley, A. L., Jonakin, J., Martin, J. R., and Singer, J. G., *Combustion*, *40*(1), 16-23 (1968).

PO-001 Pollock, W. A., Tomany, J. P., and Frieling, G., *Mech. Engr.*, *89*(8), 21-25 (1967).

RO-001 Robinson, R. A., and R. H. Stokes, *Electrolyte Solutions*, Second Edition, (London), 1965.

RO-002 Robinson, R. A., *J. Am. Chem. Soc.*, *59*, 84 (1937).

RO-003 Robart, J., *Bl. Assoc. Chimsites Sucrerie Distill France*, *31*, 108-11 (1913).

SE-001 Semrau, K. F., *J. Air Poll. Contr. Assoc.*, *10*(3), 200-207 (1960).

SE-002 Semrau, K. T., C. W. Marynowski, K. E. Lunde, and C. E. Lapple, *Ind. Engr. Chem.*, *50*(11), 1615-1620 (1958).

SE-004 Seel, F., H. Knorre, *Z. anorg. allg. Chem.*, *322*, 310 (1963).

SH-001 Sherwood, T. K., and Pigford, R. L., *Absorption and Extraction*, McGraw-Hill, New York, 1952.

SI-001 Sillén, L. G., *Stability Constants of Metal-Ion Complexes*, *Section I*: *Inorganic Ligands*, Special Publication No. 17, London: The Chemical Society, Burlington House, W.1, 1964.

SN-001 Snavely, E. S., and F. E. Blount, *Corrosion*, *25*, 397 (1969).

SQ-002 Squires, A. M., *Chem. Engr.* (NY), *74*(24), 133-140 (1967).

ST-001 Strauss, W., *Industrial Gas Cleaning*, Intern. Series of Monographs in Chem. Engr., Vol. 8, Pergamon Press, Oxford, 1966.

TA-001 Tartar, H. V., and H. H. Garretson, *J. Am. Chem. Soc.*, *63*, 808 (1941).

TA-002 Tahei, M. and G. F. Haines, *J. Air Poll. Contr. Assoc.*, *19*(6), 427-431 (1969).

TE-001 Tennessee Valley Authority, "Sulfur Oxide Removal from Power Plant Stack Gas: Conceptual Design and Cost Study, Use of Limestone in Wet Scrubbing Process", Prepared for NAPCA by TVA under Contract No. TV-29233A, 1969.

TE-003 Teller, A. J., Chem. Engr., 67, 111-124 (July 11, 1960).

TH-001 Thompson, Mary E., Science, 153, 866 (1966).

TH-002 Thompson, Mary E., and J. W. Ross, Jr., Science, 154, 1643 (1966).

VO-002 Volgin, B. P., et. al., Int. Chem. Engr., 8(1), 113-118 (1968).

WE-001 Weisberg, J., Bl. Soc. Chim (3), 15, 1247-50 (1896).

WU-001 Wurz, O., W. Swoboda, Textil Rundsch, 3, 201-206 (1948).

YU-001 Yui, N., Bull. Inst. Phys. Chem. Res. Tokyo, 19, 1229 (1940).

STANDARD TITLE PAGE FOR TECHNICAL REPORTS	1. Report No. CPA 22-69-138	**2. Govt. Accession No.**	3. Recipient's Catalog No.

4. Title and Subtitle
A Theoretical Description of the Limestone Injection - Wet Scrubbing Process, Vol. I

5. Report Date
June 9, 1970

6. Performing Organization Code

7. Author(s)

8. Performing Organization Rept. No.

9. Performing Organization Name and Address
Radian Corporation
8409 Research Blvd., P.O. Box 9948
Austin, Texas 78758

10. Project/Task/Work Unit No.

11. Contract/Grant No.
CPA 22-69-138

12. Sponsoring Agency Name and Address
National Air Pollution Control Administration
Bur. of Engrg. & Physical Sciences
5710 Wooster Pike
Cincinnati, Ohio 45227

13. Type of Report & Period Covered
Final
6/9/69 - 4/9/70

14. Sponsoring Agency Code

15. Supplementary Notes

16. Abstracts

17. Key Words and Document Analysis. 17a. Descriptors

17b. Identifiers/Open-Ended Terms

17c. COSATI Field/Group

18. Distribution Statement	19. Security Class (This Report) UNCLASSIFIED	21. No. of Pages
	20. Security Class (This Page) UNCLASSIFIED	22. Price

FORM CFSTI-35 (4-70)